1

POLARIMETRIC REMOTE SENSING OF GEOPHYSICAL MEDIA WITH LAYER RANDOM MEDIUM MODEL

S. V. Nghiem, M. Borgeaud, J. A. Kong, and R. T. Shin

1.1 Introduction

With advances in polarimetric radar technology, polarimetry has become important to the remote sensing of geophysical media. Fully polarimetric radar signals convey additional information regarding the

remotely sensed media and thereby provide more accurate identification and classification of terrain types in radar imagery. The encountered geophysical media are inhomogeneous and often stratified into multiple layers. To study the fully polarimetric scattering properties of the media, the layer random medium model has been developed.

In this chapter, the three-layer random medium model applied to the fully polarimetric remote sensing of geophysical media is presented. The chapter is composed of five sections. Section 1.2 considers the polarimetric scattering descriptions in terms of the scattering, covariance, and Mueller matrices. The relations between the matrix elements and the polarimetric backscattering coefficients are shown. Section 1.3 sets forth the theoretical model formulated from Maxwell's equations to derive the polarimetric scattering coefficients. This model describes the random media by means of correlation functions in conjunction with the strong permittivity fluctuation theory. Section 1.4 discusses the results for a case of sea ice with and without snow cover. Physical insights provided by the theoretical model are used to explain the behavior of the corresponding covariance matrix and the polarization signatures calculated with the Mueller matrix. Finally, the chapter is summarized in section 1.5.

1.2 Polarimetric Descriptions

To describe electromagnetic polarization properties, various methods have been devised. In 1852, Sir George Stokes [1] introduced four quantities, known as the Stokes parameters, to characterize a beam of partially polarized light. The Stokes parameters were later (1888) modified by Lord Rayleigh [2] in his treatment of "Interference of Polarized Light". As a geometrical representation, Poincaré [3] denoted polarization states with points on a sphere called the Poincaré sphere. In 1948, Mueller [4] considered the Stokes parameters as components of a vector which, due to "the effect of an optical instrument," could be transformed into another vector by a real 4×4 matrix. Expressed in two orthogonal polarimetric components, the incident and the scattered fields are related by the Jones matrix [5] or the complex scattering matrix [6,7]. To characterize the polarimetric scattering properties of random media, the covariance matrix is defined by the product of the polarimetric feature vector and its transposed complex conjugate [8]. Various forms of the Mueller matrix, or Stokes matrix, and other polari-

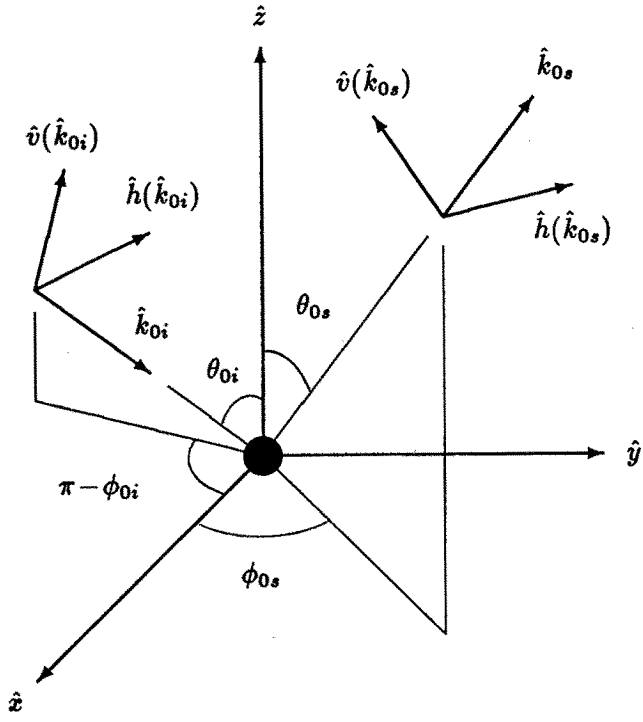

Figure 1.2.1 Coordinate systems.

metric descriptions [9-21] have been used. In the following subsections, the polarimetric descriptions used in this chapter are considered.

a. Scattering Matrix

Let an incident electric field $(\overline{E}_i)$ propagate in the direction of incident wave vector $\overline{k}_{0i}$ and illuminate the scatterer giving rise to the scattered field $(\overline{E}_s)$ propagating in the direction of scattered wave vector $\overline{k}_{0s}$ as shown in Fig. 1.2.1. Associated with the incident field, Cartesian coordinate system $(\hat{h}(k_{0zi}), \hat{v}(k_{0zi}), \hat{k}_{0i})$, connoted as the incident basis, is defined with respect to vertical direction $\hat{z}$ of the global Cartesian coordinate system $(\hat{x}, \hat{y}, \hat{z})$ as follows

$$\hat{h}(k_{0zi}) = \frac{\hat{z} \times \overline{k}_{0i}}{|\hat{z} \times \overline{k}_{0i}|}, \quad \hat{v}(k_{0zi}) = \frac{\overline{k}_{0i} \times \hat{h}(k_{0zi})}{|\overline{k}_{0i} \times \hat{h}(k_{0zi})|} \tag{1a}$$

$$\hat{k}_{0i} = \overline{k}_{0i}/|\overline{k}_{0i}| \quad \text{with} \quad \overline{k}_{0i} = k_{xi}\hat{x} + k_{yi}\hat{y} + k_{0zi}\hat{z} \tag{1b}$$

Similarly, scattered basis $(\hat{h}(k_{0zs}), \hat{v}(k_{0zs}), \hat{k}_{0s})$ is determined by

$$\hat{h}(k_{0zs}) = \frac{\hat{z} \times \overline{k}_{0s}}{|\hat{z} \times \overline{k}_{0s}|}, \quad \hat{v}(k_{0zs}) = \frac{\overline{k}_{0s} \times \hat{h}(k_{0zs})}{|\overline{k}_{0s} \times \hat{h}(k_{0zs})|} \tag{1c}$$

$$\hat{k}_{0s} = \overline{k}_{0s}/|\overline{k}_{0s}| \quad \text{with} \quad \overline{k}_{0s} = k_{xs}\hat{x} + k_{ys}\hat{y} + k_{0zs}\hat{z} \tag{1d}$$

In (1), the incident and the scattered wave vectors can be expressed in terms of the angles in Fig. 1.2.1 such that $\theta_{0s} = \theta_{0i}$ and $\phi_{0s} = \phi_{0i} + \pi$ in the backscattering direction.

Expressed in the incident basis, E_{hi} and E_{vi} are the components of $\overline{E}_i$ in directions $\hat{h}(k_{0zi})$ and $\hat{v}(k_{0zi})$, respectively. For scattered field $\overline{E}_s$, the components in the scattered basis are E_{hs} along $\hat{h}(k_{0zs})$ and E_{vs} along $\hat{v}(\hat{k}_{0zs})$. This coordinate connotation will be convenient for the subsequent derivation of the scattered field. The incident and scattered fields are then related by scattering matrix $\overline{\overline{F}}$ defined by

$$\begin{bmatrix} E_{hs} \\ E_{vs} \end{bmatrix} = \frac{e^{ikr}}{r} \overline{\overline{F}} \cdot \begin{bmatrix} E_{hi} \\ E_{vi} \end{bmatrix} = \frac{e^{ikr}}{r} \begin{bmatrix} f_{hh} & f_{hv} \\ f_{vh} & f_{vv} \end{bmatrix} \cdot \begin{bmatrix} E_{hi} \\ E_{vi} \end{bmatrix} \tag{2}$$

where factor e^{ikr}/r is the spherical wave transformation and scattering matrix element $f_{\mu\nu}$ is for scattered polarization μ and incident polarization ν with μ and ν being h or v.

In the backscattering direction, relation $f_{hv} = f_{vh}$ holds for reciprocal media when $\overline{E}_s$ is delineated in the incident basis. Note that the transformation of backscattered field $\overline{E}_s$ from the scattered basis to the incident basis results in the sign changes of f_{hh} and f_{hv}. Hereafter, only backscattering is considered.

b. Covariance Matrix

The polarimetric backscattering information pertaining to a remotely sensed geophysical terrain can be conveyed in form of polarimetric feature vector $\overline{X}$ defined with illuminated area A and the scattering matrix elements in the expression

$$\overline{X} = \lim_{\substack{r \to \infty \\ A \to \infty}} \sqrt{\frac{4\pi r^2}{A}} \frac{e^{ikr}}{r} \begin{bmatrix} f_{hh} \\ f_{hv} \\ f_{vv} \end{bmatrix} \tag{3}$$

As an ensemble average of the product between polarimetric feature vector $\overline{X}$ and its transposed complex conjugate $\overline{X}^{\dagger}$, covariance matrix $\overline{\overline{C}}$ characterizes the fully polarimetric scattering properties of the geophysical media; explicitly,

$$\overline{\overline{C}} = \left\langle \overline{X} \cdot \overline{X}^{\dagger} \right\rangle = \lim_{A \to \infty} \frac{4\pi}{A} \left\langle \begin{bmatrix} f_{hh} f_{hh}^* & f_{hh} f_{hv}^* & f_{hh} f_{vv}^* \\ f_{hv} f_{hh}^* & f_{hv} f_{hv}^* & f_{hv} f_{vv}^* \\ f_{vv} f_{hh}^* & f_{vv} f_{hv}^* & f_{vv} f_{vv}^* \end{bmatrix} \right\rangle \tag{4}$$

where the asterisk denotes the complex conjugate and the angular brackets are for the ensemble average. It is obvious from (4) that the covariance matrix is hermitian.

In the above definitions of the polarimetric feature vector and the covariance matrix, reciprocity relation $f_{hv} = f_{vh}$ has been implied for the reciprocal media under consideration. Consequently, no loss of information results from dismissing f_{vh}. It should be noted that the reciprocity relation elicits the implementation of the scattered-to-incident basis transformation.

c. Mueller Matrix

The scattering effects of geophysical terrain can also be described by the Mueller matrix which relates the Stokes vectors of the incident and the scattered fields. For the incident field, the Stokes vector is

$$\overline{I}_i = \begin{bmatrix} I_i \\ Q_i \\ U_i \\ V_i \end{bmatrix} = \begin{bmatrix} I_{hi} + I_{vi} \\ I_{hi} - I_{vi} \\ U_i \\ V_i \end{bmatrix} \tag{5}$$

where the components of $\overline{I}_i$ are defined based on the linear polarimetric components of $\overline{E}_i$ and the free-space intrinsic impedance η in the following equations

$$I_{hi} = \frac{1}{\eta} E_{hi} E_{hi}^* , \qquad I_{vi} = \frac{1}{\eta} E_{vi} E_{vi}^* \tag{6a}$$

$$U_i = \frac{2}{\eta} \mathrm{Re}\left(E_{vi} E_{hi}^*\right) , \quad V_i = \frac{2}{\eta} \mathrm{Im}\left(E_{vi} E_{hi}^*\right) \tag{6b}$$

For the field backscattered from reciprocal media, the Stokes vector

has the form

$$\bar{I}_s = \begin{bmatrix} I_s \\ Q_s \\ U_s \\ V_s \end{bmatrix} = \begin{bmatrix} I_{hs} + I_{vs} \\ I_{hs} - I_{vs} \\ U_s \\ V_s \end{bmatrix} \tag{7}$$

whose components are defined with the ensemble averages of the scattered field components as

$$I_{hs} = \frac{1}{\eta} \lim_{\substack{r\to\infty \\ A\to\infty}} \frac{4\pi r^2}{A} \langle E_{hs} E_{hs}^* \rangle \tag{8a}$$

$$I_{vs} = \frac{1}{\eta} \lim_{\substack{r\to\infty \\ A\to\infty}} \frac{4\pi r^2}{A} \langle E_{vs} E_{vs}^* \rangle \tag{8b}$$

$$U_s = \frac{2}{\eta} \lim_{\substack{r\to\infty \\ A\to\infty}} \frac{4\pi r^2}{A} \mathrm{Re} \langle E_{vs} E_{hs}^* \rangle \tag{8c}$$

$$V_s = \frac{2}{\eta} \lim_{\substack{r\to\infty \\ A\to\infty}} \frac{4\pi r^2}{A} \mathrm{Im} \langle E_{vs} E_{hs}^* \rangle \tag{8d}$$

Relating the incident to the scattered Stokes vectors, Mueller matrix $\overline{\overline{M}}$ depicts the backscattering effect by

$$\bar{I}_s = \overline{\overline{M}} \cdot \bar{I}_i = \begin{bmatrix} M_{11} & M_{12} & M_{13} & M_{14} \\ M_{21} & M_{22} & M_{23} & M_{24} \\ M_{31} & M_{32} & M_{33} & M_{34} \\ M_{41} & M_{42} & M_{43} & M_{44} \end{bmatrix} \cdot \begin{bmatrix} I_i \\ Q_i \\ U_i \\ V_i \end{bmatrix} \tag{9}$$

In the incident basis, the Mueller matrix is a 4×4 matrix composed of 16 elements which are derived from equations (2,5-9) and written in terms of the scattering matrix elements as

$$M_{11} = \lim_{A\to\infty} \frac{4\pi}{A} \frac{1}{2} \langle f_{hh} f_{hh}^* + 2 f_{hv} f_{hv}^* + f_{vv} f_{vv}^* \rangle \tag{10a}$$

$$M_{12} = \lim_{A\to\infty} \frac{4\pi}{A} \frac{1}{2} \langle f_{hh} f_{hh}^* - f_{vv} f_{vv}^* \rangle = M_{21} \tag{10b}$$

$$M_{13} = \lim_{A\to\infty} \frac{4\pi}{A} \mathrm{Re} \langle f_{hh} f_{hv}^* + f_{hv} f_{vv}^* \rangle = M_{31} \tag{10c}$$

$$M_{14} = \lim_{A\to\infty} \frac{4\pi}{A} \mathrm{Im} \langle f_{hh} f_{hv}^* + f_{hv} f_{vv}^* \rangle = -M_{41} \tag{10d}$$

$$M_{22} = \lim_{A\to\infty} \frac{4\pi}{A} \frac{1}{2} \langle f_{hh} f_{hh}^* - 2 f_{hv} f_{hv}^* + f_{vv} f_{vv}^* \rangle \tag{10e}$$

$$M_{23} = \lim_{A\to\infty} \frac{4\pi}{A}\mathrm{Re}\left\langle f_{hh}f_{hv}^* - f_{hv}f_{vv}^*\right\rangle = \quad M_{32} \tag{10f}$$

$$M_{24} = \lim_{A\to\infty} \frac{4\pi}{A}\mathrm{Im}\left\langle f_{hh}f_{hv}^* - f_{hv}f_{vv}^*\right\rangle = -M_{42} \tag{10g}$$

$$M_{33} = \lim_{A\to\infty} \frac{4\pi}{A}\mathrm{Re}\left\langle f_{hh}f_{vv}^* + f_{hv}f_{hv}^*\right\rangle \tag{10h}$$

$$M_{34} = \lim_{A\to\infty} \frac{4\pi}{A}\mathrm{Im}\left\langle f_{hh}f_{vv}^*\right\rangle = -M_{43} \tag{10i}$$

$$M_{44} = \lim_{A\to\infty} \frac{4\pi}{A}\mathrm{Re}\left\langle f_{hh}f_{vv}^* - f_{hv}f_{hv}^*\right\rangle \tag{10j}$$

For given transmit and receive antenna polarizations, the received power is proportional to a scattering coefficient defined in terms of the Mueller matrix as [12,19,22]

$$\sigma(\alpha_r,\beta_r;\alpha_i,\beta_i) = \frac{\bar{I}_r^{\mathsf{T}}\cdot\bar{\bar{T}}\cdot\bar{\bar{M}}\cdot\bar{I}_i}{2I_rI_i} \tag{11}$$

where T denotes the transpose and Mueller matrix $\bar{\bar{M}}$ is symmetrized by diagonal matrix $\bar{\bar{T}}$ whose diagonal elements are $T_{11} = T_{22} = T_{33} = -T_{44} = 1$. Stokes vector $\bar{I}_m$ in (11) depends on orientation angle α_m and ellipticity angle β_m (Fig. 1.2.2) as follows

$$\bar{I}_m = \begin{bmatrix} I_m \\ Q_m \\ U_m \\ V_m \end{bmatrix} = I_m \begin{bmatrix} 1 \\ \cos 2\alpha_m \cos 2\beta_m \\ \sin 2\alpha_m \cos 2\beta_m \\ \sin 2\beta_m \end{bmatrix} \tag{12}$$

with antenna operating mode $m = i$ for transmitting (incident) and $m = r$ for receiving. The orientation angles vary from 0° to 180° with 0° corresponding to $\hat{h}$ and 90° to $\hat{v}$ direction. The ellipticity angles range from −45° to 45° with 0° corresponding to linear, positive values to right-hand, and negative values to left-hand waves. The polarization states can be described geometrically by the Poincaré sphere with the upper hemisphere for right-hand polarizations and the lower for left-hand [23]. If the same antenna is used for both transmitting and receiving, the transmit and receive polarizations are identical and the corresponding scattering cross section is called the copolarized signature [22].

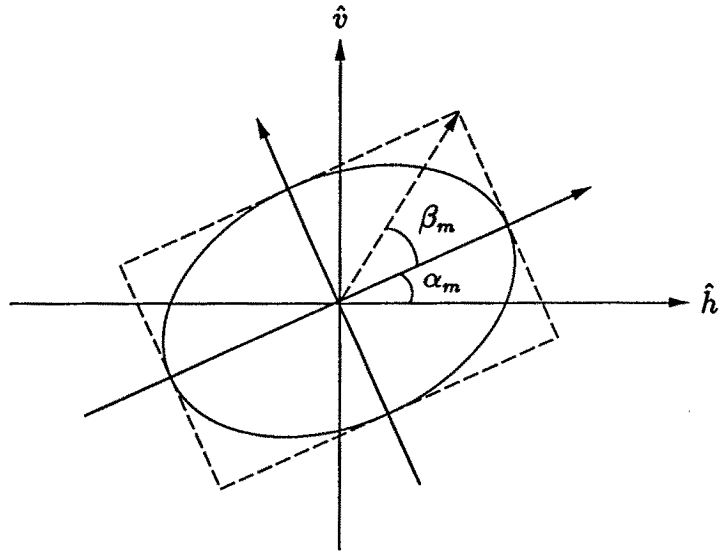

a Polarization ellipse

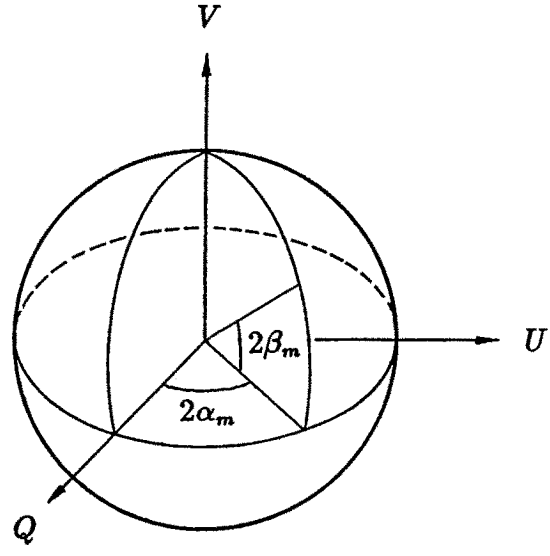

b Poincaré sphere

Figure 1.2.2 Geometrical representations of polarizations.

d. Scattering Coefficients

For polarimetric backscattering, the scattering coefficients are defined by [44]

$$\sigma_{\mu\tau\nu\kappa} = \lim_{\substack{r\to\infty \\ A\to\infty}} \frac{4\pi r^2}{A} \frac{\langle E_{\mu s} E^*_{\nu s}\rangle}{E_{\tau i}\, E^*_{\kappa i}} \tag{13}$$

where subscripts μ, ν, τ, and κ can be h or v. The components of the scattered field in (13) are obtained by measuring the h and the v returns while the incident field is transmitted exclusively with h or v polarization. From (2), this measurement procedure can be described mathematically by the following equations relating the scattered to the incident field components

$$E_{\mu s} = \frac{e^{ikr}}{r}\left(f_{\mu\tau}E_{\tau i} + f_{\mu\kappa}E_{\kappa i}\right)\big|_{E_{\kappa i}=0} = \frac{e^{ikr}}{r} f_{\mu\tau}E_{\tau i} \tag{14a}$$

$$E_{\nu s} = \frac{e^{ikr}}{r}\left(f_{\nu\tau}E_{\tau i} + f_{\nu\kappa}E_{\kappa i}\right)\big|_{E_{\tau i}=0} = \frac{e^{ikr}}{r} f_{\nu\kappa}E_{\kappa i} \tag{14b}$$

Substituting (14) in (13) renders polarimetric backscattering coefficient $\sigma_{\mu\nu\tau\kappa}$ in terms of scattering matrix components

$$\sigma_{\mu\tau\nu\kappa} = \lim_{A\to\infty} \frac{4\pi}{A}\left\langle f_{\mu\tau} f^*_{\nu\kappa}\right\rangle \tag{15}$$

By means of (15), the covariance matrix can be expressed with the backscattering coefficients as

$$\overline{\overline{C}} = \begin{bmatrix} \sigma_{hhhh} & \sigma_{hhhv} & \sigma_{hhvv} \\ \sigma^*_{hhhv} & \sigma_{hvhv} & \sigma_{hvvv} \\ \sigma^*_{hhvv} & \sigma^*_{hvvv} & \sigma_{vvvv} \end{bmatrix} \tag{16}$$

in which diagonal element σ_{hhhh}, σ_{hvhv}, and σ_{vvvv} are conventional backscattering coefficient σ_{hh}, σ_{hv}, and σ_{vv}, respectively. Normalized to $\sigma = \sigma_{hhhh}$, the covariance matrix can be formed as

$$\overline{\overline{C}} = \sigma \begin{bmatrix} 1 & \beta\sqrt{e} & \rho\sqrt{\gamma} \\ \beta^*\sqrt{e} & e & \xi\sqrt{\gamma e} \\ \rho^*\sqrt{\gamma} & \xi^*\sqrt{\gamma e} & \gamma \end{bmatrix} \tag{17}$$

where intensity ratio γ and e and correlation coefficient ρ, β, and ξ are

$$\gamma = \frac{\sigma_{vvvv}}{\sigma}, \quad e = \frac{\sigma_{hvhv}}{\sigma} \tag{18a}$$

$$\rho = \frac{\sigma_{hhvv}}{\sigma\sqrt{\gamma}}, \quad \beta = \frac{\sigma_{hhhv}}{\sigma\sqrt{e}}, \quad \xi = \frac{\sigma_{hvvv}}{\sigma\sqrt{\gamma e}} \tag{18b}$$

In terms of the polarimetric backscattering coefficients, the Mueller matrix elements can also be written as

$$M_{11} = \frac{1}{2}(\sigma_{hhhh} + 2\sigma_{hvhv} + \sigma_{vvvv}) \tag{19a}$$

$$M_{12} = \frac{1}{2}(\sigma_{hhhh} - \sigma_{vvvv}) = M_{21} \tag{19b}$$

$$M_{13} = \mathrm{Re}(\sigma_{hhhv} + \sigma_{hvvv}) = M_{31} \tag{19c}$$

$$M_{14} = \mathrm{Im}(\sigma_{hhhv} + \sigma_{hvvv}) = -M_{41} \tag{19d}$$

$$M_{22} = \frac{1}{2}(\sigma_{hhhh} - 2\sigma_{hvhv} + \sigma_{vvvv}) \tag{19e}$$

$$M_{23} = \mathrm{Re}(\sigma_{hhhv} - \sigma_{hvvv}) = M_{32} \tag{19f}$$

$$M_{24} = \mathrm{Im}(\sigma_{hhhv} - \sigma_{hvvv}) = -M_{42} \tag{19g}$$

$$M_{33} = \mathrm{Re}(\sigma_{hhvv}) + \sigma_{hvhv} \tag{19h}$$

$$M_{34} = \mathrm{Im}(\sigma_{hhvv}) = -M_{43} \tag{19i}$$

$$M_{44} = \mathrm{Re}(\sigma_{hhvv}) - \sigma_{hvhv} \tag{19j}$$

The use of the reciprocity relation for the media under consideration has been implied in the expressions for the covariance and the Mueller matrices. As seen from (16) and (19), both matrices are fully expressible with the complete set of polarimetric backscattering coefficients containing 9 independent parameters and therefore convey the same information regarding the terrain scattering properties. In the next section, the polarimetric backscattering coefficients will be derived with the scattered field in the scattered basis for reciprocal geophysical media with a three-layer configuration. Then, the scattered-to-incident basis transformation is applied to calculate the covariance and the Mueller matrices.

1.3 Random Medium Model

Random medium models have been used to account for the scattering due to embedded inhomogeneities in geophysical media [7,23-45]. For active and passive remote sensing, terrain media have been modeled with a two-layer anisotropic configuration [37,38]. When the permittivity fluctuations of the random media are strong, the singularity of the dyadic Green's function in the renormalization method has to be properly accounted for [40]. In this case, the scattering coefficients can be calculated under the distorted Born approximation [39-41]. For fully polarimetric remote sensing, two-layer isotropic and anisotropic random medium models have been used to derive the covariance and Mueller matrices and applied to investigate the backscattering from bare terrain fields such as sea ice and vegetation [43,44].

Presented in the following subsections is the three-layer anisotropic random medium model which can account for fully polarimetric backscattering from geophysical media under the effects of precipitation such as sea ice under snow or vegetation under fog. The model configuration (Fig. 1.3.1) has four different regions separated by three interfaces. The covering layer is modeled as an isotropic random medium. The middle layer is described as an anisotropic random medium due to the preferred alignment of the nonspherical scatterers. The underlying layer is considered as a homogeneous half space. The scattering effects of the random media are characterized by three-dimensional correlation functions with variances and correlation lengths corresponding to the fluctuation strengths and the physical geometries of the scatterers, respectively. The strong fluctuation theory is used to calculate the effective permittivities and the distorted Born approximation is then applied to obtain the complete set of polarimetric backscattering coefficients.

a. Formulation

The scattering configuration is depicted in Fig. 1.3.1. Region 0 is air with real permittivity ϵ_0. Region 1 is a scattering medium with isotropic scatterers randomly embedded such as snow or fog whose electrical property can be characterized by inhomogeneous permittivity $\epsilon_1(\overline{r})$. Region 2 contains nonspherical scatterers constituting an anisotropic random medium such as sea ice or vegetation which has spatially dependent permittivity $\epsilon_2(\overline{r})$. Region 3 is the underlying half space with homogeneous permittivity ϵ_3. The three regions are as-

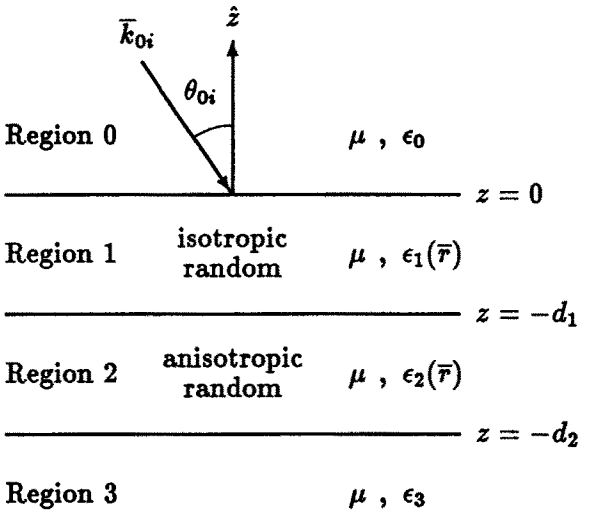

Figure 1.3.1 Scattering configuration.

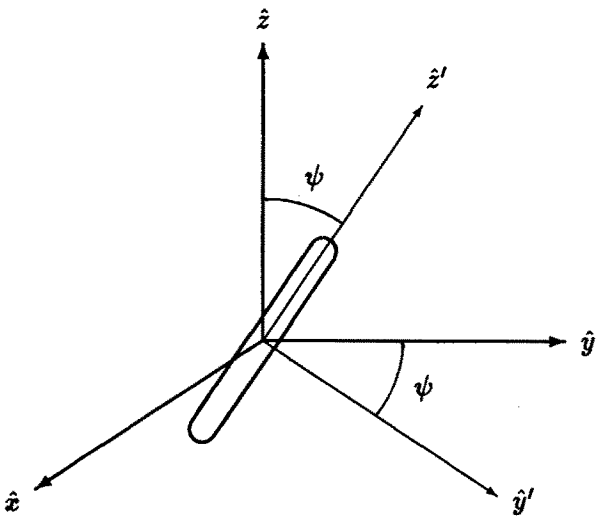

Figure 1.3.2 Geometry of scatterer in region 2.

sumed to have identical permeability μ. The infinite planar interfaces at location $z = -d_1$ and $z = -d_2$ in Cartesian coordinate system $(\hat{x}, \hat{y}, \hat{z})$ are shown in Fig. 1.3.1. Due to the preferred alignment of the nonspherical scatterers, the medium in region 2 is considered as effectively uniaxial with optic axis z' tilted off the z-axis by angle ψ in the yz-plane as illustrated in Fig. 1.3.2.

In the phasor notation defined with $e^{-i\omega t}$ [23], time-harmonic total field $\overline{E}_0(\overline{r}), \overline{E}_1(\overline{r})$, and $\overline{E}_2(\overline{r})$, respectively in region 0, 1, and 2, satisfy the following wave equations

$$\nabla \times \nabla \times \overline{E}_0(\overline{r}) - k_0^2 \overline{E}_0(\overline{r}) = 0 \tag{20}$$

$$\nabla \times \nabla \times \overline{E}_1(\overline{r}) - k_0^2 \frac{\epsilon_1(\overline{r})}{\epsilon_0} \overline{E}_1(\overline{r}) = 0 \tag{21}$$

$$\nabla \times \nabla \times \overline{E}_2(\overline{r}) - k_0^2 \frac{\epsilon_2(\overline{r})}{\epsilon_0} \overline{E}_2(\overline{r}) = 0 \tag{22}$$

where the wave number is $k_0 = \omega\sqrt{\mu\epsilon_0}$ and ω is the angular frequency. In the remote sensing of geophysical media, strong permittivity fluctuations are often encountered. The strong fluctuation theory [40] is therefore necessitated in the calculations of the random-medium effective permittivities. Deterministic permittivity $\overline{\overline{\epsilon}}_{g1} = \epsilon_{g1}\overline{\overline{I}}$, where $\overline{\overline{I}}$ is the unit dyadic, and $\overline{\overline{\epsilon}}_{g2}$ are introduced in both sides of (21) and (22), respectively, and the following vectors for $m = 1$ and $m = 2$

$$k_0^2 \overline{\overline{Q}}_m(\overline{r}) \cdot \overline{E}_m(\overline{r}) = k_0^2 \left[\frac{\epsilon_m(\overline{r})\overline{\overline{I}} - \overline{\overline{\epsilon}}_{gm}}{\epsilon_0} \right] \cdot \overline{E}_m(\overline{r}) \tag{23}$$

are treated as the effective sources so that wave equation (9) and (10) for the scattering random media become

$$\nabla \times \nabla \times \overline{E}_m(\overline{r}) - k_0^2 \frac{\overline{\overline{\epsilon}}_{gm}}{\epsilon_0} \cdot \overline{E}_m(\overline{r}) = k_0^2 \overline{\overline{Q}}_m(\overline{r}) \cdot \overline{E}_m(\overline{r}) \tag{24}$$

The permittivities in $\overline{\overline{\epsilon}}_{g1}$ and $\overline{\overline{\epsilon}}_{g2}$ are determined by the elimination of secular terms [40]. Physically, $\overline{\overline{\epsilon}}_{g1}$ and $\overline{\overline{\epsilon}}_{g2}$ are the effective permittivity tensors in the very low frequency limit where the scattering loss is negligible compared to the absorption loss [24].

In form of an integral equation, the total field in region $m = 0, 1, 2$ is the superposition of the mean field and the scattered field; explicitly,

$$\overline{E}_m(\overline{r}) = \overline{E}_m^{(0)}(\overline{r}) + k_0^2 \sum_{n=1}^{2} \int_{V_n} d\overline{r}_n \, \overline{\overline{G}}_{mn}(\overline{r}, \overline{r}_n) \cdot \overline{\overline{Q}}_n(\overline{r}_n) \cdot \overline{E}_n(\overline{r}_n) \tag{25}$$

Mean field $\overline{E}_m^{(0)}(\overline{r})$ is the solution to the homogeneous wave equations where the effective sources vanish in the absence of the scatterers.

As a particular solution to the inhomogeneous wave equations in the presence of the scatterers in region $n = 1,2$ occupying volume V_n, the scattered field in (25) is the integrals of the products between the effective source and dyadic Green's functions $\overline{\overline{G}}_{mn}(\bar{r},\bar{r}_n)$ defined by

$$\nabla \times \nabla \times \overline{\overline{G}}_{mn}(\bar{r},\bar{r}_n) - k_0^2 \frac{\overline{\overline{\epsilon}}_{gm}}{\epsilon_0} \cdot \overline{\overline{G}}_{mn}(\bar{r},\bar{r}_n) = \delta(\bar{r}-\bar{r}_n)\overline{\overline{I}} \qquad (26)$$

where first subscript m in $\overline{\overline{G}}_{mn}(\bar{r},\bar{r}_n)$ denotes the observation region containing observation point $\bar{r}$, second subscript n stands for source region $n = 1,2$ containing source point $\bar{r}_n$, and $\delta(\bar{r}-\bar{r}_n)$ is the Dirac delta function. When $m \neq n$ signifying observation point $\bar{r}$ is outside source region n within which $\bar{r}_n$ is restricted, the Dirac delta function in the right-hand side of (26) vanishes. It is also obvious from (26) that an observation point in a scattering region can coincide with a source point in the same region $(m = n = 1,2)$ thus giving rise to the singularity of dyadic Green's function $\overline{\overline{G}}_{nn}(\bar{r},\bar{r}_n)$ which can be decomposed into a principal value part and a Dirac delta part

$$\overline{\overline{G}}_{nn}(\bar{r},\bar{r}_n) = PV\overline{\overline{G}}_{nn}(\bar{r},\bar{r}_n) - \delta(\bar{r}-\bar{r}_n)k_0^{-2}\overline{\overline{S}}_n\,, \quad n = 1,2 \qquad (27)$$

Dyadic coefficient $\overline{\overline{S}}_n$ is conformed with the shape of the source exclusion volume and determined by the condition of secular-term elimination [40]. With the decomposed Green's function of (27), the singular part in the integrand on the right-hand side of (25) for $m = n$ can be extracted and then combined with total field $\overline{E}_n(\bar{r})$ on the left-hand side to form external field $\overline{F}_n(\bar{r})$ in scattering region $n = 1,2$

$$\overline{F}_n(\bar{r}) = \left[\overline{\overline{I}} + \overline{\overline{S}}_n \cdot \overline{\overline{Q}}_n(\bar{r})\right] \cdot \overline{E}_n(\bar{r}) \qquad (28)$$

In terms of external field $\overline{F}_n(\bar{r})$, the vector source of (23) can be redefined by introducing scatterer $\overline{\overline{\xi}}_n(\bar{r})$ such that

$$k_0^2\overline{\overline{\xi}}_n(\bar{r}) \cdot \overline{F}_n(\bar{r}) = k_0^2\overline{\overline{Q}}_n(\bar{r}) \cdot \overline{E}_n(\bar{r}) \qquad (29)$$

It follows from (29) that scatterer $\overline{\overline{\xi}}_n(\bar{r})$ for the isotropic $(n = 1)$ and the anisotropic $(n = 2)$ random media are

$$\overline{\overline{\xi}}_n(\bar{r}) = \overline{\overline{Q}}_n(\bar{r}) \cdot \left[\overline{\overline{I}} + \overline{\overline{S}}_n \cdot \overline{\overline{Q}}_n(\bar{r})\right]^{-1} \qquad (30)$$

By applying the distorted Born approximation [35, 39-41] to (25) with the new definition of the sources in (29), the total field observed in region 0 is

$$\overline{E}_0(\overline{r}) = \overline{E}_0^{(0)}(\overline{r}) + k_0^2 \sum_{n=1}^{2} \int_{V_n} d\overline{r}_n \langle \overline{\overline{G}}_{0n}(\overline{r}, \overline{r}_n) \rangle \cdot \overline{\overline{\xi}}_n(\overline{r}_n) \cdot \langle \overline{F}_n(\overline{r}_n) \rangle \quad (31)$$

where isotropic effective permittivity $\overline{\overline{\epsilon}}_{eff1} = \epsilon_{eff1}\overline{\overline{I}}$ for region 1 and uniaxial permittivity $\overline{\overline{\epsilon}}_{eff2}$ for region 2 are used to calculate the mean dyadic Green's functions and the mean fields. The polarimetric scattering coefficients can then be obtained with the following correlation of the scattered field in (31)

$$\langle \overline{E}_{0s}(\overline{r}) \cdot \overline{E}_{0s}^*(\overline{r}) \rangle = \sum_{n=1}^{2} \sum_{i,j,k,l,m}^{x,y,z} k_0^4 \int_{V_n} d\overline{r}_n \int_{V_n} d\overline{r}_n^o \, C_{\xi njklm}(\overline{r}_n, \overline{r}_n^o)$$
$$\cdot [\langle G_{0nij}(\overline{r}, \overline{r}_n) \rangle \langle F_{nk}(\overline{r}_n) \rangle] \cdot [\langle G_{0nil}(\overline{r}, \overline{r}_n^o) \rangle \langle F_{nm}(\overline{r}_n^o) \rangle]^* \quad (32)$$

For random media $n = 1$ and $n = 2$, $C_{\xi njklm}(\overline{r}_n, \overline{r}_n^o)$ in (32) is the $jklm$ element of fourth-rank correlation tensor $\overline{\overline{C}}_{\xi n}(\overline{r}_n, \overline{r}_n^o)$ defined as

$$C_{\xi njklm}(\overline{r}_n, \overline{r}_n^o) = \langle \xi_{njk}(\overline{r}_n) \xi_{nlm}^*(\overline{r}_n^o) \rangle \quad (33)$$

With specified correlation functions, the polarimetric scattering coefficients can thus be obtained after the effective permittivities of the random media are calculated as shown in the next subsection.

b. Effective Permittivities

The strong permittivity fluctuation theory [40] is used to derive the effective permittivities of the random media. The singularities of the dyadic Green's functions in the bilocal approximated Dyson's equations are accounted for and the low-frequency approximation is applied to obtain the results for the isotropic and the anisotropic random media. The derivations are done in the frequency domain with the Fourier-transform method. The isotropic random medium is characterized with a correlation function of spherical form and the anisotropic random medium is described with a correlation function of spheroidal form. When the spheroidal form is reduced to spherical, the anisotropic result is confirmed with the isotropic case. Following is the summary

of the effective permittivity calculations first for the isotropic and then for the anisotropic random media.

Consider an isotropic random medium composed of a host medium with permittivity ϵ_{b1} and randomly embedded scatterers with permittivity ϵ_{s1} and total fractional volume f_{s1} where subscript 1 is used for the isotropic random medium in accordance to the notation in Fig. 1.3.1. By introducing auxiliary permittivity $\overline{\overline{\epsilon}}_{g1}$ into the wave equation as in (24), dyadic Green's function $\overline{\overline{G}}_{g1}(\bar{r}, \bar{r}_1)$ satisfies the inhomogeneous differential equation of the form (26). Subscripts $g1$ is used here to indicate that $\overline{\overline{G}}_{g1}(\bar{r}, \bar{r}_1)$ corresponds to a medium with permittivity ϵ_{g1}. To account for the singularity, $\overline{\overline{G}}_{g1}(\bar{r}, \bar{r}_1) = \overline{\overline{G}}_{g1}(\bar{r} - \bar{r}_1)$ is decomposed as in (27) with $\overline{\overline{S}}_1 = S_1 \overline{\overline{I}}$ for the Dirac delta part. By using the following definition for the Fourier transform

$$\overline{\overline{G}}_{g1}(\bar{r}) \equiv \frac{1}{8\pi^3} \int_{-\infty}^{\infty} d\bar{k}\, \overline{\overline{G}}_{g1}(\bar{k})\, e^{i\bar{k}\cdot\bar{r}} \tag{34}$$

the dyadic Green's function in the frequency domain is found to be

$$\overline{\overline{G}}_{g1}(\bar{k}) = \frac{\overline{\overline{I}}}{D(k)} - \frac{\bar{k}\,\bar{k}}{k_{g1}^2 D(k)} \quad \text{with} \quad \begin{cases} D(k) = k^2 - k_{g1}^2 \\ k_{g1}^2 = \omega^2 \mu \epsilon_{g1} \end{cases} \tag{35}$$

Under the bilocal and the low-frequency approximations [40], the effective permittivity of the isotropic random medium is composed of a quasi-static part (ϵ_{g1}) and a correction part

$$\overline{\overline{\epsilon}}_{eff1} = \epsilon_{g1} \overline{\overline{I}} + \epsilon_0 \left[\overline{\overline{I}} - \overline{\overline{\xi}}^{(0)}_{eff1} \cdot \overline{\overline{S}}_1 \right]^{-1} \cdot \overline{\overline{\xi}}^{(0)}_{eff1} \tag{36}$$

The correction part in (36) physically accounts for the modification in the wave speed and attenuation due to the scattering effect of the scatterers. For $j, m = x, y, z$, the jm element of $\overline{\overline{\xi}}^{(0)}_{eff1}$ is related to the Green's function (35) in the following manner

$$[\overline{\overline{\xi}}^{(0)}_{eff1}]_{jm} = \sum_{k,l}^{x,y,z} \Gamma^{(0)}_{\xi 1 jklm} \left\{ k_0^2 \int_{-\infty}^{\infty} d\bar{k}\, [\overline{\overline{G}}_{g1}(\bar{k})]_{kl} \Phi_{\xi 1}(\bar{k}) + [\overline{\overline{S}}_1]_{kl} \right\} \tag{37}$$

To arrive at (37), the correlation function has been defined as

$$\Gamma_{\xi 1 jklm}(\bar{r}_1, \bar{r}_1^{\circ}) = \langle \xi_{1jk}(\bar{r}_1) \xi_{1lm}(\bar{r}_1^{\circ}) \rangle \tag{38a}$$

and the random medium has been assumed to be statistically homogeneous so that (38a) can be written as

$$\Gamma_{\xi 1jklm}(\bar{r}_1, \bar{r}_1^o) = \Gamma_{\xi 1jklm}(\bar{r}_1 - \bar{r}_1^o) \equiv \Gamma^{(0)}_{\xi 1jklm} R_{\xi 1}(\bar{r}_1 - \bar{r}_1^o) \qquad (38b)$$

where $R_{\xi 1}(\bar{r} = \bar{r}_1 - \bar{r}_1^o)$ is the normalized correlation function such that $R_{\xi 1}(0)$ is equal to 1. In (37), $\Phi_{\xi 1}(\bar{k})$ is the Fourier transform of the normalized correlation function $R_{\xi 1}(\bar{r})$ defined as

$$\Phi_{\xi 1}(\bar{k}) \equiv \frac{1}{8\pi^3} \int_{-\infty}^{\infty} d\bar{r}\; R_{\xi 1}(\bar{r})\; e^{i\bar{k}\cdot\bar{r}} \qquad (39)$$

In the isotropic random medium, $\bar{\bar{\xi}}_1(\bar{r}_1)$ is a scalar multiple of the unit dyadic $\bar{\bar{I}}$ and non-zero coefficient $\Gamma^{(0)}_{\xi 1jklm}$ are

$$\Gamma^{(0)}_{\xi 1jklm} = \langle \xi_{1jk}(\bar{r}_1)\xi_{1lm}(\bar{r}_1)\rangle \equiv \delta_{\xi 1}\ , \quad \begin{cases} k=j,\ l=m \\ j,m=x,y,z \end{cases} \qquad (40)$$

For a spherically symmetric correlation function, it is seen from (36-40) that the effective permittivity of the isotropic random medium is independent of direction and expressed as a scalar multiple of $\bar{\bar{I}}$

$$\bar{\bar{\epsilon}}_{eff1} = \epsilon_{eff1}\bar{\bar{I}} = \left[\epsilon_{g1} + \frac{\epsilon_0 \delta_{\xi 1}\,(I_0 + S_1)}{1 - \delta_{\xi 1}\,(I_0 + S_1)\,S_1}\right]\bar{\bar{I}} \qquad (41)$$

where I_0 is the integral of the product between a diagonal element of the dyadic Green's function and the correlation function in the frequency domain

$$I_0 = k_0^2 \int_0^{\infty} d\bar{k}\; [\bar{\bar{G}}_{g1}(\bar{k})]_{jj} \Phi_{\xi 1}(\bar{k}) \qquad (42)$$

Due to the isotropy of the medium, any diagonal element ($jj = xx$, yy, or zz) of the dyadic Green's function (35) can be used in (42) to yield an identical result for I_0. For an isotropic random medium characterized by an exponential correlation function of spherical form with correlation length ℓ_1, $R_{\xi 1}(\bar{r})$ is expressed as

$$R_{\xi 1}(\bar{r}) = \exp\left(-\frac{r}{\ell_1}\right) \qquad (43a)$$

whose Fourier transform is obtained by carrying out the integration (39) in the spherical coordinates to yield

$$\Phi_{\xi 1}(\bar{k}) = \frac{\ell_1^3}{\pi^2(1+k^2\ell_1^2)^2} \tag{43b}$$

With the use of (43b), the integration (42) is then carried out analytically by a change of variables into the spherical coordinates. The result for I_0 is

$$I_0 = \frac{\epsilon_0}{3\epsilon_{g1}}\left[-\frac{3\vartheta^2+1}{(\vartheta+1)^2} + i\frac{4\vartheta\sqrt{\vartheta}}{(\vartheta+1)^2}\right]_{\vartheta = k_{g1}^2\ell_1^2} \tag{44}$$

Coefficient S_1, which conforms with the shape of the source exclusion volume, can be determined by requiring the cancelation of the frequency dependent terms in (37) so that the secular term is eliminated. For the isotropic case, S_1 is thereby obtained

$$S_1 = -\lim_{\omega\to 0} I_0 = \frac{\epsilon_0}{3\epsilon_{g1}} \tag{45}$$

The elimination of the secular term also imposes the condition of zero-mean on the scatterer tensor

$$\left\langle \bar{\bar{\xi}}_1(\bar{r}) \right\rangle = 0 \tag{46}$$

Condition (46) and (45) together with definition (30) and (23) for $n=1$ determine auxiliary permittivity $\bar{\bar{\epsilon}}_{g1}$ with the relation

$$\left(\frac{\epsilon_{b1}-\epsilon_{g1}}{\epsilon_{b1}+2\epsilon_{g1}}\right)(1-f_{s1}) + \left(\frac{\epsilon_{s1}-\epsilon_{g1}}{\epsilon_{s1}+2\epsilon_{g1}}\right) f_{s1} = 0 \tag{47}$$

When the value of ϵ_{g1} is obtained, variance $\delta_{\xi 1}$ is found from (40)

$$\delta_{\xi 1} = 9\frac{\epsilon_{g1}^2}{\epsilon_0^2}\left[\left(\frac{\epsilon_{b1}-\epsilon_{g1}}{\epsilon_{b1}+2\epsilon_{g1}}\right)^2(1-f_{s1}) + \left(\frac{\epsilon_{s1}-\epsilon_{g1}}{\epsilon_{s1}+2\epsilon_{g1}}\right)^2 f_{s1}\right] \tag{48}$$

In summary of the isotropic case, the isotropic effective permittivity is calculated with (41) where ϵ_{g1}, $\delta_{\xi 1}$, I_0, and S_1 are given by (47), (48), (44), and (45), respectively.

Consider now an anisotropic random medium composed of a host medium with permittivity ϵ_{b2} and embedded nonspherical scatterers with permittivity ϵ_{s2} and total fractional volume f_{s2}. The scatterers with a preferred alignment direction and an azimuthal symmetry effectively give rise to the uniaxial anisotropy of the random medium whose optic axis is the z' axis in Cartesian coordinate system $(\hat{x}', \hat{y}', \hat{z}')$ illustrated in Fig. 1.3.2. The principle for deriving the anisotropic effective permittivity is the same as in the previous paragraph; however, the anisotropy of the medium needs be accounted for. In this case, an appropriate form of auxiliary permittivity $\overline{\overline{\epsilon}}_{g2}$ is

$$\overline{\overline{\epsilon}}_{g2} = \begin{bmatrix} \epsilon_{g2\rho'} & 0 & 0 \\ 0 & \epsilon_{g2\rho'} & 0 \\ 0 & 0 & \epsilon_{g2z'} \end{bmatrix} \tag{49}$$

Equation (49) is expressed in the primed coordinate system shown in Fig. 1.3.2. This coordinate system is used to calculate the effective permittivity of the anisotropic random medium and a rotation transformation with tilt angle ψ is then applied to transform the result into unprime Cartesian coordinate system $(\hat{x}, \hat{y}, \hat{z})$. Corresponding dyadic Green's function $\overline{\overline{G}}_{g2}(\overline{r}')$ is decomposed as in (27) with the Dirac delta part having uniaxial dyadic coefficient

$$\overline{\overline{S}}_2 = \begin{bmatrix} S_{2\rho'} & 0 & 0 \\ 0 & S_{2\rho'} & 0 \\ 0 & 0 & S_{2z'} \end{bmatrix} \tag{50}$$

According to the Fourier transform definition (34) where the subscript 1 is replaced by 2 and $\overline{r}$ and $\overline{k}$ are respectively changed to $\overline{r}'$ and $\overline{k}'$, dyadic Green's function $\overline{\overline{G}}_{g2}(\overline{r}')$ has frequency-domain version $\overline{\overline{G}}_{g2}(\overline{k}')$ written as

$$\overline{\overline{G}}_{g2}(\overline{k}') = \frac{1}{(k_x'^2 + k_y'^2) D_o(\overline{k}')} \begin{bmatrix} k_y'^2 & -k_x' k_y' & 0 \\ -k_x' k_y' & k_x'^2 & 0 \\ 0 & 0 & 0 \end{bmatrix} +$$

$$\frac{1}{(k_x'^2 + k_y'^2) D_e(\overline{k}')} \begin{bmatrix} k_x'^2 & k_x' k_y' & 0 \\ k_x' k_y' & k_y'^2 & 0 \\ 0 & 0 & \frac{k_{g2\rho'}^2}{k_{g2z'}^2}(k_x'^2 + k_y'^2) \end{bmatrix} - \frac{\overline{k}' \overline{k}'}{k_{g2z'}^2 D_e(\overline{k}')} \tag{51}$$

where $D_o(\overline{k}')$, $D_e(\overline{k}')$, $k^2_{g2\rho'}$, and $k^2_{g2z'}$ are defined as follows

$$D_o(\overline{k}') = k_x'^2 + k_y'^2 + k_z'^2 - k^2_{g2\rho'} \tag{52a}$$

$$D_e(\overline{k}') = k_z'^2 + \frac{k^2_{g2\rho'}}{k^2_{g2z'}}(k_x'^2 + k_y'^2 - k^2_{g2z'}) \tag{52b}$$

$$k^2_{g2\rho'} = \omega^2\mu_0\epsilon_{g2\rho'}, \quad k^2_{g2z'} = \omega^2\mu_0\epsilon_{g2z'} \tag{52c}$$

Similar to (36), the effective permittivity of the anisotropic random medium is composed of a quasi-static part and a scattering-effect part

$$\overline{\overline{\epsilon}}_{eff2}(\hat{r}') = \overline{\overline{\epsilon}}_{g2} + \epsilon_0\left[\overline{\overline{I}} - \overline{\overline{\xi}}^{(0)}_{eff2}\cdot\overline{\overline{S}}_2\right]^{-1}\cdot\overline{\overline{\xi}}^{(0)}_{eff2} \tag{53}$$

where $\hat{r}'$ indicates the primed coordinate system and the jm element of effective scatterer $\overline{\overline{\xi}}^{(0)}_{eff2}$ under the low-frequency approximation is of the form (37) with subscript 1 changed to 2 and $j, m = x', y', z'$

$$[\overline{\overline{\xi}}^{(0)}_{eff2}]_{jm} = \sum_{k,l}^{x',y',z'} \Gamma^{(0)}_{\xi 2jklm}\left\{k_0^2\int_{-\infty}^{\infty} d\overline{k}'\,[\overline{\overline{G}}_{g2}(\overline{k}')]_{kl}\Phi_{\xi 2}(\overline{k}') + [\overline{\overline{S}}_2]_{kl}\right\} \tag{54}$$

The statically homogeneous anisotropic random medium is described with fourth-rank correlation tensor $\overline{\overline{\Gamma}}_{\xi 2}(\overline{r}_2', \overline{r}_2^{o\prime}) = \left\langle \overline{\overline{\xi}}_2(\overline{r}_2')\overline{\overline{\xi}}_2(\overline{r}_2^{o\prime})\right\rangle$ where $\overline{\overline{\xi}}_2(\overline{r}_2')$ is a diagonal tensor in the primed coordinates; thus, the non-zero elements of $\overline{\overline{\Gamma}}_{\xi 2}(\overline{r}_2', \overline{r}_2^{o\prime}) = \overline{\overline{\Gamma}}_{\xi 2}(\overline{r}_2' - \overline{r}_2^{o\prime})$ are

$$\Gamma_{\xi 2jklm}(\overline{r}') = \delta_{\xi 2\rho'}R_{\xi 2}(\overline{r}'), \quad jklm = \begin{cases} x'x'x'x', & x'x'y'y' \\ y'y'x'x', & y'y'y'y' \end{cases} \tag{55a}$$

$$\Gamma_{\xi 2jklm}(\overline{r}') = \delta_{\xi 2z'}R_{\xi 2}(\overline{r}'), \quad jklm = z'z'z'z' \tag{55b}$$

$$\Gamma_{\xi 2jklm}(\overline{r}') = \delta_{\xi 2c'}R_{\xi 2}(\overline{r}'), \quad jklm = \begin{cases} x'x'z'z', & y'y'z'z' \\ z'z'x'x', & z'z'y'y' \end{cases} \tag{55c}$$

where $\overline{r}' = \overline{r}_2' - \overline{r}_2^{o\prime}$ and $\Gamma_{\xi 2jklm}(\overline{r}')$ has normalizing variance $\Gamma_{\xi 2jklm}(\overline{r}' = 0) = \langle \xi_{2jk}(\overline{r}_2')\xi_{1lm}(\overline{r}_2')\rangle \equiv \Gamma^{(0)}_{\xi 2jklm}$ which can takes on the value of $\delta_{\xi 2\rho'}$, $\delta_{\xi 2z'}$, or $\delta_{\xi 2c'}$ such that $R_{\xi 2}(0) = 1$. For an azimuthally symmetric correlation function, it is observed from (49-55) that $\overline{\overline{\epsilon}}_{eff2}(\hat{r}')$ is uniaxial and expressed with the permittivity tensor

$$\overline{\overline{\epsilon}}_{eff2}(\hat{r}') = \begin{bmatrix} \epsilon_{eff2\rho'} & 0 & 0 \\ 0 & \epsilon_{eff2\rho'} & 0 \\ 0 & 0 & \epsilon_{eff2z'} \end{bmatrix} \tag{56a}$$

$$\epsilon_{eff2\rho'} = \epsilon_{g2\rho'} + \frac{\epsilon_0 \delta_{\xi 2\rho'}(I_{\rho'} + S_{2\rho'})}{1 - \delta_{\xi 2\rho'}(I_{\rho'} + S_{2\rho'})S_{2\rho'}}$$
$$\epsilon_{eff2z'} = \epsilon_{g2z'} + \frac{\epsilon_0 \delta_{\xi 2z'}(I_{z'} + S_{2z'})}{1 - \delta_{\xi 2z'}(I_{z'} + S_{2z'})S_{2z'}} \tag{56b}$$

where $I_{z'}$ and $I_{\rho'}$ are the integrals in the frequency domain of the products between the corresponding diagonal element of the dyadic Green's function and normalized correlation function $\Phi_{\xi 2}(\overline{k}')$ defined as in (39) with the subscript 1 changed to 2 and $\overline{k}$ and $\overline{r}$ to $\overline{k}'$ and $\overline{r}'$. In the cylindrical coordinates, integral $I_{z'}$ and $I_{\rho'}$ are

$$I_{z'} = k_0^2 \int_0^{2\pi} d\phi' \int_0^{\infty} dk'_\rho k'_\rho \int_{-\infty}^{\infty} dk'_z (-k_{g2z'}^{-2}) \cdot \left[\frac{k_z'^2 - k_{g2\rho'}^2}{k_z'^2 + k_\rho'^2 (\epsilon_{g2\rho'}/\epsilon_{g2z'}) - k_{g2\rho'}^2} \right] \Phi_{\xi 2}(\overline{k}') \tag{57a}$$

$$I_{\rho'} = k_0^2 \int_0^{2\pi} d\phi' \int_0^{\infty} dk'_\rho k'_\rho \int_{-\infty}^{\infty} dk'_z \cdot \left[\frac{\sin^2\phi'}{k_z'^2 + k_\rho'^2 - k_{g2\rho'}^2} + \frac{(k_\rho'^{-2} - k_z'^{-2}) k_\rho'^2 \cos^2\phi'}{k_z'^2 + k_\rho'^2 (\epsilon_{g2\rho'}/\epsilon_{g2z'}) - k_{g2\rho'}^2} \right] \Phi_{\xi 2}(\overline{k}') \tag{57b}$$

For an anisotropic random medium characterized by an exponential correlation function of spheroidal form with correlation length $\ell_{2\rho'}$ and $\ell_{2z'}$, $R_{\xi 2}(\overline{r}')$ is expressed as

$$R_{\xi 2}(\overline{r}') = \exp\left(-\sqrt{\frac{x'^2 + y'^2}{\ell_{2\rho'}^2} + \frac{z'^2}{\ell_{2z'}^2}} \right) \tag{58a}$$

whose Fourier transform is obtained by carrying out the Fourier integration in the cylindrical coordinates or by applying the scaling theorem on (43b) to yield

$$\Phi_{\xi 2}(\overline{k}') = \frac{\ell_{2\rho'}^2 \ell_{2z'}}{\pi^2 (1 + k_\rho'^2 \ell_{2\rho'}^2 + k_z'^2 \ell_{2z'}^2)^2} \tag{58b}$$

With the use of (58b), the integrations in (57) can then be carried out analytically by effectuating the integrations over ϕ', using contour

integration technique for the integrations over k'_z, and then performing the integrations over k'_ρ. The result for $I_{z'}$ is determined as follows

$$I_{z'} = -\frac{2\epsilon_0}{\epsilon_{g2z'}}(\mathcal{I}_s + \mathcal{I}_d) \tag{59a}$$

$$\mathcal{I}_s = -\frac{\alpha\gamma_\ell^2\sqrt{\alpha\gamma_\ell^2}}{2a^2}\left[\frac{\sqrt{-\zeta}}{\vartheta_e} + \frac{\vartheta_e+\zeta}{\vartheta_e\sqrt{\vartheta_e}}\left(\frac{\pi}{2} - \tan^{-1}\frac{\sqrt{-\zeta}}{\sqrt{\vartheta_e}}\right)\right] \tag{59b}$$

$$\mathcal{I}_d = \frac{\alpha\gamma_\ell^2}{2a^2}\left[\frac{1+a\nu_{gz}^2}{\vartheta_o} + \frac{\vartheta_o(a+2)-(b+a\nu_{gz}^2)}{\vartheta_o\sqrt{\vartheta_o}}\left(\frac{\pi}{2} - \tan^{-1}\frac{1}{\sqrt{\vartheta_o}}\right)\right] \tag{59c}$$

$$a = \alpha\gamma_\ell^2 - 1, \quad \alpha = \frac{\epsilon_{g2z'}}{\epsilon_{g2\rho'}}, \quad \gamma_\ell = \frac{\ell_{2\rho'}}{\ell_{2z'}}, \quad \nu_{gz'}^2 = k_{g2\rho'}^2\ell_{2z'}^2 \tag{59d}$$

$$\zeta = \alpha\gamma_\ell^2\nu_{gz'}^2, \quad b = \frac{\alpha\gamma_\ell^2+\zeta}{a}, \quad \vartheta_o = b-1, \quad \vartheta_e = b+\zeta \tag{59e}$$

Integral $I_{\rho'}$ involves additional terms in the dyadic Green's function and the result is found to be

$$I_{\rho'} = \nu_{0\rho'}^2(\mathcal{I}_1^o - \mathcal{I}_2^o - \mathcal{I}_3^o) + \alpha\nu_{0\rho'}^2\left[(\mathcal{I}_1^e - \mathcal{I}_2^e - \mathcal{I}_3^e) + \frac{1}{\zeta}(\mathcal{I}_s + \mathcal{I}_d - \frac{1}{2})\right] \tag{60a}$$

$$\mathcal{I}_1^e = \frac{\alpha\gamma_\ell^2\sqrt{\alpha\gamma_\ell^2}}{2a^2\vartheta_e}\left[-\frac{\sqrt{-\zeta}}{b} + \frac{1}{\sqrt{\vartheta_e}}\left(\frac{\pi}{2} - \tan^{-1}\frac{\sqrt{-\zeta}}{\sqrt{\vartheta_e}}\right)\right] \tag{60b}$$

$$\mathcal{I}_2^e = \frac{1}{2a\vartheta_o}\left[1 - \frac{1}{\sqrt{\vartheta_o}}\left(\frac{\pi}{2} - \tan^{-1}\frac{1}{\sqrt{\vartheta_o}}\right)\right] \tag{60c}$$

$$\mathcal{I}_3^e = \frac{\alpha\gamma_\ell^2}{2a^2\vartheta_o}\left[-\frac{1}{b} + \frac{1}{\sqrt{\vartheta_o}}\left(\frac{\pi}{2} - \tan^{-1}\frac{1}{\sqrt{\vartheta_o}}\right)\right] \tag{60d}$$

$$\mathcal{I}_{1,2,3}^o = \mathcal{I}_{1,2,3}^e(\alpha = 1), \quad \nu_{0\rho'} = k_0\ell_{2\rho'} \tag{60e}$$

Diagonal element $S_{g2\rho'}$ and $S_{g2z'}$ of dyadic coefficient $\overline{\overline{S}}_2$ in the singular part of the Green's function for the anisotropic medium are obtained by requiring the cancelation of the frequency dependent terms

in (54) to eliminate the secular terms. Derived from (54), (59), and (60), coefficient $S_{g2\rho'}$ and $S_{g2z'}$ are

$$S_{2\rho'} = -\lim_{\omega\to 0} I_{\rho'} = \frac{\epsilon_0}{2\epsilon_{g2\rho'}a\sqrt{a}}\left[(1+a)\tan^{-1}\sqrt{a}-\sqrt{a}\right] \quad (61a)$$

$$S_{2z'} = -\lim_{\omega\to 0} I_{z'} = \frac{\epsilon_0(1+a)}{\epsilon_{g2z'}a\sqrt{a}}\left[\sqrt{a}-\tan^{-1}\sqrt{a}\right] \quad (61b)$$

Similar to (46), the zero-mean condition is imposed on scatterer $\bar{\bar{\xi}}_2(\bar{r})$ for the elimination of the secular terms. This condition together with (61) and definition (30) and (23) for $n = 2$ in the primed coordinate system determine auxiliary permittivity $\bar{\bar{\epsilon}}_{g2}$ in the following manner

$$\frac{(\epsilon_{b2}-\epsilon_{g2\rho'})(1-f_{s2})}{\epsilon_0+S_{2\rho'}(\epsilon_{b2}-\epsilon_{g2\rho'})}+\frac{(\epsilon_{s2}-\epsilon_{g2\rho'})f_{s2}}{\epsilon_0+S_{2\rho'}(\epsilon_{s2}-\epsilon_{g2\rho'})}=0 \quad (62a)$$

$$\frac{(\epsilon_{b2}-\epsilon_{g2z'})(1-f_{s2})}{\epsilon_0+S_{2z'}(\epsilon_{b2}-\epsilon_{g2z'})}+\frac{(\epsilon_{s2}-\epsilon_{g2z'})f_{s2}}{\epsilon_0+S_{2z'}(\epsilon_{s2}-\epsilon_{g2z'})}=0 \quad (62b)$$

Numerical values of $\epsilon_{g2\rho'}$, $\epsilon_{g2z'}$, $S_{2\rho'}$, and $S_{2z'}$ are obtained by solving (61) and (62) iteratively. A suggested scheme for the iteration is to initially assign $\epsilon_{g2\rho'} = \epsilon_{g2z'} = \epsilon_{b2}$ then use (61) to find $S_{2\rho'}$ and $S_{2z'}$ which are subsequently employed to recalculate $\epsilon_{g2\rho'}$ and $\epsilon_{g2z'}$ with (62) rearranged as

$$\epsilon_{g2\rho'} = \epsilon_{b2}+\frac{f_{s2}(\epsilon_{s2}-\epsilon_{g2\rho'})}{(1-f_{s2})}\frac{\epsilon_0+S_{2\rho'}(\epsilon_{b2}-\epsilon_{g2\rho'})}{\epsilon_0+S_{2\rho'}(\epsilon_{s2}-\epsilon_{g2\rho'})} \quad (63a)$$

$$\epsilon_{g2z'} = \epsilon_{b2}+\frac{f_{s2}(\epsilon_{s2}-\epsilon_{g2z'})}{(1-f_{s2})}\frac{\epsilon_0+S_{2z'}(\epsilon_{b2}-\epsilon_{g2z'})}{\epsilon_0+S_{2z'}(\epsilon_{s2}-\epsilon_{g2z'})} \quad (63b)$$

The iteration is repeated until a required accuracy is achieved. Equation (63) indicates that small fractional volume f_{s2} leads to a fast conversion rate for the iterative solution and explains why the background permittivity has been chosen as the initial value for the auxiliary permittivities. After $\epsilon_{g2\rho'}$, $\epsilon_{g2z'}$, $S_{2\rho'}$, and $S_{2z'}$ are computed, variance $\delta_{\xi 2\rho'}$, $\delta_{\xi 2z'}$, and $\delta_{\xi 2c'}$ are found from (55)

$$\delta_{\xi 2\rho'} = \left[\frac{\epsilon_{b2}-\epsilon_{g2\rho'}}{\epsilon_0+S_{2\rho'}(\epsilon_{b2}-\epsilon_{g2\rho'})}\right]^2(1-f_{s2})+\left[\frac{\epsilon_{s2}-\epsilon_{g2\rho'}}{\epsilon_0+S_{2\rho'}(\epsilon_{s2}-\epsilon_{g2\rho'})}\right]^2 f_{s2} \quad (64a)$$

$$\delta_{\xi 2z'} = \left[\frac{\epsilon_{b2}-\epsilon_{g2z'}}{\epsilon_0+S_{2z'}(\epsilon_{b2}-\epsilon_{g2z'})}\right]^2(1-f_{s2})+\left[\frac{\epsilon_{s2}-\epsilon_{g2z'}}{\epsilon_0+S_{2z'}(\epsilon_{s2}-\epsilon_{g2z'})}\right]^2 f_{s2} \quad (64b)$$

In summary of the anisotropic case, the anisotropic effective permittivity tensor is calculated in the primed coordinate system of Fig. 1.3.2 with (56) where $\epsilon_{g2\rho'}$, $\epsilon_{g2z'}$, $S_{2\rho'}$, and $S_{2z'}$ are obtained by iterating (63) and (61) and then $\delta_{\xi 2\rho'}$, $\delta_{\xi 2z'}$, $\delta_{\xi 2c'}$, $I_{\rho'}$, and $I_{z'}$ are determined by (64a-c), (60), and (59), respectively. To transform the result into the unprimed coordinate system, the following operation is applied

$$\bar{\bar{\epsilon}}_{eff2} = \bar{\bar{T}}_\psi \cdot \bar{\bar{\epsilon}}_{eff2}(\hat{r}') \cdot \bar{\bar{T}}_\psi^{-1} \quad \text{with} \quad \bar{\bar{T}}_\psi = \begin{bmatrix} 1 & 0 & 0 \\ 0 & \cos\psi & \sin\psi \\ 0 & -\sin\psi & \cos\psi \end{bmatrix} \tag{65}$$

where $\bar{\bar{T}}_\psi$ is the transformation matrix which rotates a vector by angle ψ from the primed coordinates to the unprimed coordinates. After the rotation, the anisotropic effective permittivity, which is a symmetric tensor in the $(\hat{x}, \hat{y}, \hat{z})$ system, is related to tilt angle ψ by

$$\bar{\bar{\epsilon}}_{eff2} = \begin{bmatrix} \epsilon_{eff2xx} & 0 & 0 \\ 0 & \epsilon_{eff2yy} & \epsilon_{eff2yz} \\ 0 & \epsilon_{eff2zy} & \epsilon_{eff2zz} \end{bmatrix} \tag{66a}$$

$$\begin{aligned} \epsilon_{eff2xx} &= \epsilon_{eff2\rho'} \ , \quad \epsilon_{eff2yz} = \epsilon_{eff2zy} \\ \epsilon_{eff2yz} &= (\epsilon_{eff2z'} - \epsilon_{eff2\rho'}) \cos\psi \sin\psi \\ \epsilon_{eff2yy} &= \epsilon_{eff2\rho'} \cos^2\psi + \epsilon_{eff2z'} \sin^2\psi \\ \epsilon_{eff2zz} &= \epsilon_{eff2\rho'} \sin^2\psi + \epsilon_{eff2z'} \cos^2\psi \end{aligned} \tag{66b}$$

In this subsection, the effective permittivities of the isotropic and anisotropic random media have been derived. It is necessary to note that the principal branch cut of square root $\sqrt{w}$ for complex number w has been chosen such that $-\pi < \arg w \leq \pi$ where $\arg w$ denotes the argument of w. Also, inverse tangent $\tan^{-1} w$ for complex number w is determined by

$$\tan^{-1} w = \frac{1}{2i} \ln w_a \quad \text{with} \quad w_a = \frac{1 + iw}{1 - iw} \tag{67}$$

where $\ln w_a$ is the natural logarithm of w_a on the principal Riemann sheet $|w_a| > 0$ and $-\pi < \arg w_a < \pi$.

Auxiliary permittivity ϵ_{g1} of the isotropic random medium as obtained is the same as the Polder and van Santern mixing formula [41];

thus, auxiliary permittivity ϵ_{g2} of the anisotropic random medium obtained in a similar manner can be considered as a more generalized version. Related to the auxiliary permittivity and the shape of the exclusion volume, the dyadic coefficient of the Dirac delta part in the Green's function is also derivable with a surface integration over a limiting equicorrelation surface and proved to satisfy the following condition [42]

$$2\frac{\epsilon_{g\rho}}{\epsilon_0}S_\rho + \frac{\epsilon_{gz}}{\epsilon_0}S_z = 1 \tag{68}$$

where $\epsilon_{g\rho} = \epsilon_{gz} = \epsilon_{g1}$ and $S_\rho = S_z = S_1$ for the isotropic case or $\epsilon_{g\rho} = \epsilon_{g2\rho'}$, $\epsilon_{gz} = \epsilon_{g2z'}$, $S_\rho = S_{2\rho'}$, and $S_z = S_{2z'}$ for the anisotropic case.

As mentioned earlier, the anisotropic effective permittivity becomes isotropic when the spheroidal correlation function is reduced to spherical. This is the case when $\ell_{2\rho'}$ approaches $\ell_{2z'}$ and it is trivial to show that

$$\lim_{\ell_{2\rho'}\to\ell_{2z'}} S_{2\rho'} = \lim_{\ell_{2\rho'}\to\ell_{2z'}} S_{2z'} \tag{69a}$$

$$\lim_{\ell_{2\rho'}\to\ell_{2z'}} \epsilon_{g2\rho'} = \lim_{\ell_{2\rho'}\to\ell_{2z'}} \epsilon_{g2z'} \tag{69b}$$

The limit (69a) has the form of (45) and consequently the variances in (64) have the same limit of the form (48) since $\epsilon_{g2\rho'}$ and $\epsilon_{g2z'}$ approach to the same limit as indicated in (69b). To prove that $I_{\rho'}$ and $I_{z'}$ have the same expression of the form (44) as $\ell_{2\rho'} \to \ell_{2z'}$, attention must be given to the afore chosen branch cuts. For instance, $\sqrt{-\zeta}$ is $-i\sqrt{\zeta}$ instead of $i\sqrt{\zeta}$; this is because $w = -\zeta \to -k^2_{g2\rho'}\ell^2_{2z'}$ as $\ell_{2\rho'} \to \ell_{2z'}$ and w is thus in the third quadrant of the complex w plane so that $\sqrt{w}$ is consequently in the fourth quadrant due to the chosen branch cut of the square root. The value of $\sqrt{-\zeta}$ so obtained is identical to $-i\sqrt{\zeta}$ and not to $i\sqrt{\zeta}$. The proof is then straight forward.

In deriving the effective permittivities, the low-frequency and the bilocal approximations have been used. The low-frequency approximation is valid when $k_{g1}\ell_1 \ll 1$ for the isotropic case or $k_{g2\rho'}\ell_{2\rho'} \ll 1$ and $k_{g2\rho'}\ell_{2z'} \ll 1$ for the anisotropic case. This approximation results in the ignorance of the spatial dispersive characteristics of the inhomogeneous media. In this case, the bilocal approximation further requires that $|[\bar{\bar{\xi}}^{(0)}_{effn}]_{jm}| \ll 1$ with $n = 1$ for the isotropic or $n = 2$ for the anisotropic case. This condition allows more simplification on

the permittivity results (41) and (56) where the denominators can be approximated to be unity.

When the low-frequency condition is removed, the spatial dispersion of the random media is manifested in the dependence of the effective scatterers on wave vector $\overline{k}$ as

$$[\overline{\overline{\xi}}_{effn}(\overline{k})]_{jm} = \sum_{k,l}^{x',y',z'} \Gamma^{(0)}_{\xi njklm} \left\{ \frac{k_0^2}{2} \int_{-\infty}^{\infty} d\overline{k}' \, [\overline{\overline{G}}_{gn}(\overline{k}')]_{kl} \right.$$
$$\left. \cdot \left[\Phi_{\xi n}(\overline{k}' - \overline{k}) + \Phi_{\xi n}(\overline{k}' + \overline{k}) \right] + [\overline{\overline{S}}_n]_{kl} \right\} \qquad (70)$$

The effective permittivities are still calculated with (36) or (53) with the effective scatterer (70) replacing the low-frequency version. In this case, the bilocal approximation is valid when $|[\overline{\overline{\xi}}_{effn}(\overline{k})]_{jm}| \ll 1$. From (36), (53), and (70), it is observed that the effective permittivities are even functions of wave vector $\overline{k}$ and can be expressed with symmetric tensors. The random media under consideration are therefore reciprocal as physically expected. Besides the above approximation, the use of the Fourier transform in this subsection implies that the media are unbounded in the calculations of the effective permittivities. In the next subsection, the effective permittivities is used to obtain the dyadic Green's function of the layer random medium which accounts for the multiple reflections, refractions, and transmissions at the medium interfaces.

c. Dyadic Green's Functions

In this subsection, the mean dyadic Green's Functions (DGFs), needed in the calculation of the scattered field correlation (32), is presented for the three-layer configuration. Rather than directly calculating $\langle \overline{\overline{G}}_{0n}(\overline{r}, \overline{r}_s) \rangle$ for observation point $\overline{r}$ in region 0 and source point $\overline{r}_s$ in region n, $\langle \overline{\overline{G}}_{n0}(\overline{r}, \overline{r}_s) \rangle$ are obtained for the source in region 0 and the observation in region n and the needed DGFs are then deduced from the symmetric relation [46]

$$\langle \overline{\overline{G}}_{mn}(\overline{r}, \overline{r}_s) \rangle = \langle \overline{\overline{G}}^{\top}_{nm}(\overline{r}_s, \overline{r}) \rangle \qquad (71)$$

In this method [23,24,36], vector wave equations are first written for the DGFs subjected to the appropriate boundary conditions at the interfaces and radiation conditions at infinite distances above and below

the interfaces. Next, the Cartesian coordinate systems corresponding to upgoing and downgoing waves in the layers are shown. The DGFs can then be solved in terms of transmission and reflection coefficients for the upgoing and downgoing waves. This procedure for obtaining the DGFs are detailed in the subsequent paragraphs.

Consider the source in region 0 at $\bar{r}_s$ above interface $z = 0$. The DGFs observed in region $n = 0, 1, 2, 3$ are governed by vector wave equations as follows

$$\nabla \times \nabla \times \langle \overline{\overline{G}}_{00}(\bar{r}, \bar{r}_s) \rangle - k_0^2 \cdot \langle \overline{\overline{G}}_{00}(\bar{r}, \bar{r}_s) \rangle = \delta(\bar{r} - \bar{r}_s) \overline{\overline{I}}, \quad z \geq 0 \tag{72a}$$

$$\nabla \times \nabla \times \langle \overline{\overline{G}}_{10}(\bar{r}, \bar{r}_s) \rangle - k_0^2 \frac{\epsilon_{eff1}}{\epsilon_0} \cdot \langle \overline{\overline{G}}_{10}(\bar{r}, \bar{r}_s) \rangle = 0, \quad 0 \geq z \geq -d_1 \tag{72b}$$

$$\nabla \times \nabla \times \langle \overline{\overline{G}}_{20}(\bar{r}, \bar{r}_s) \rangle - k_0^2 \frac{\overline{\overline{\epsilon}}_{eff2}}{\epsilon_0} \cdot \langle \overline{\overline{G}}_{20}(\bar{r}, \bar{r}_s) \rangle = 0, \quad -d_1 \geq z \geq -d_2 \tag{72c}$$

$$\nabla \times \nabla \times \langle \overline{\overline{G}}_{30}(\bar{r}, \bar{r}_s) \rangle - k_0^2 \frac{\epsilon_3}{\epsilon_0} \cdot \langle \overline{\overline{G}}_{30}(\bar{r}, \bar{r}_s) \rangle = 0, \quad -d_2 \geq z \tag{72d}$$

The boundary conditions call for the continuity of $\hat{z} \times \langle \overline{\overline{G}}_{n0} \rangle$ and $\hat{z} \times \nabla \times \langle \overline{\overline{G}}_{n0} \rangle$ at the interfaces where the tangential electric and magnetic fields are continuous, respectively. The boundary conditions can be written explicitly as

$$\left.\begin{aligned} \hat{z} \times \langle \overline{\overline{G}}_{00}(\bar{r}, \bar{r}_s) \rangle &= \hat{z} \times \langle \overline{\overline{G}}_{10}(\bar{r}, \bar{r}_s) \rangle \\ \hat{z} \times \nabla \times \langle \overline{\overline{G}}_{00}(\bar{r}, \bar{r}_s) \rangle &= \hat{z} \times \nabla \times \langle \overline{\overline{G}}_{10}(\bar{r}, \bar{r}_s) \rangle \end{aligned}\right\} \text{ at } z = 0 \tag{73a}$$

$$\left.\begin{aligned} \hat{z} \times \langle \overline{\overline{G}}_{10}(\bar{r}, \bar{r}_s) \rangle &= \hat{z} \times \langle \overline{\overline{G}}_{20}(\bar{r}, \bar{r}_s) \rangle \\ \hat{z} \times \nabla \times \langle \overline{\overline{G}}_{10}(\bar{r}, \bar{r}_s) \rangle &= \hat{z} \times \nabla \times \langle \overline{\overline{G}}_{20}(\bar{r}, \bar{r}_s) \rangle \end{aligned}\right\} \text{ at } z = -d_1 \tag{73b}$$

$$\left.\begin{aligned} \hat{z} \times \langle \overline{\overline{G}}_{20}(\bar{r}, \bar{r}_s) \rangle &= \hat{z} \times \langle \overline{\overline{G}}_{30}(\bar{r}, \bar{r}_s) \rangle \\ \hat{z} \times \nabla \times \langle \overline{\overline{G}}_{20}(\bar{r}, \bar{r}_s) \rangle &= \hat{z} \times \nabla \times \langle \overline{\overline{G}}_{30}(\bar{r}, \bar{r}_s) \rangle \end{aligned}\right\} \text{ at } z = -d_2 \tag{73c}$$

To express the solutions for the DGFs physically in terms upgoing of and downgoing waves, Cartesian coordinate systems are defined to coincide with directions of electromagnetic fields and Poynting vectors. In the same manner as (1), coordinate system $(\hat{h}(k_{nz}^w), \hat{v}(k_{nz}^w), \hat{k}_n^w)$, corresponding to upgoing $(w = u)$ and downgoing $(w = d)$ waves in the isotropic media $(n = 0, 1, 3)$, are determined by

$$\hat{h}(k_{nz}^w) = \frac{\hat{z} \times \bar{k}_n^w}{|\hat{z} \times \bar{k}_n^w|}, \quad \hat{v}(k_{nz}^w) = \frac{\bar{k}_n^w \times \hat{h}(k_{nz}^w)}{|\bar{k}_n^w \times \hat{h}(k_{nz}^w)|} \tag{74a}$$

$$\hat{k}_n^w = \overline{k}_n^w / |\overline{k}_n^w| \quad \text{with} \quad \overline{k}_n^w = k_x\hat{x} + k_y\hat{y} + k_{nz}^w\hat{z} \tag{74b}$$

where the z components of the wave vectors are related as follows

$$k_{nz}^u = -k_{nz}^d = k_{nz} = \sqrt{k_n^2 - k_x^2 - k_y^2}, \quad \text{with} \quad k_n^2 = \begin{cases} \omega^2\mu\epsilon_n, & n = 0, 3 \\ \omega^2\mu\epsilon_{eff1}, & n = 1 \end{cases} \tag{75}$$

For the effective anisotropic medium ($n = 2$) with optic axis $\hat{z}'$, the ordinary and extraordinary waves propagating in the upgoing and downgoing directions call for four different coordinate systems. Corresponding to the ordinary waves, coordinate system $(\hat{o}(k_{2z}^w), \hat{e}(k_{2z}^w), \hat{k}_2^w)$ are defined by

$$\hat{o}(k_{2z}^w) = \frac{\hat{z}' \times \overline{k}_2^w}{|\hat{z}' \times \overline{k}_2^w|}, \quad \hat{e}(k_{2z}^w) = \frac{\overline{k}_2^w \times \hat{o}(k_{2z}^w)}{|\overline{k}_2^w \times \hat{o}(k_{2z}^w)|} \tag{76a}$$

$$\hat{k}_2^w = \overline{k}_2^w / |\overline{k}_2^w| \quad \text{with} \quad \overline{k}_2^w = k_x\hat{x} + k_y\hat{y} + k_{2z}^w\hat{z} \tag{76b}$$

where the z components of the ordinary upgoing ($w = ou$) and the ordinary downgoing ($w = od$) wave vectors are

$$k_{2z}^{ou} = -k_{2z}^{od} = k_{2z}^o = \sqrt{k_2^2 - k_\rho^2} \quad \text{with} \quad k_2^2 = \omega^2\mu\epsilon_{eff2xx} \tag{77}$$

Corresponding to the extraordinary waves in the anisotropic medium, coordinate system $(\hat{o}(k_{2z}^w), \hat{e}(k_{2z}^w), \hat{s}_2^w)$ are defined by

$$\hat{o}(k_{2z}^w) = \frac{\hat{z}' \times \overline{k}_2^w}{|\hat{z}' \times \overline{k}_2^w|}, \quad \hat{e}(k_{2z}^w) = \frac{\overline{s}_2^w \times \hat{o}(k_{2z}^w)}{|\overline{s}_2^w \times \hat{o}(k_{2z}^w)|}, \quad \hat{s}_2^w = \overline{s}_2^w / |\overline{s}_2^w| \tag{78}$$

where the extraordinary upgoing ($w = eu$) and the extraordinary downgoing ($w = ed$) wave vectors are determined by

$$\overline{k}_2^w = k_x\hat{x} + k_y\hat{y} + k_{2z}^w\hat{z} \quad \text{with} \quad w = eu, ed \tag{79a}$$

$$k_{2z}^{eu} = -\frac{\epsilon_{eff2yz}}{\epsilon_{eff2zz}}k_y + \frac{1}{\epsilon_{eff2zz}} \cdot \sqrt{k_2^2\epsilon_{eff2z'}\epsilon_{eff2zz} - k_x^2\epsilon_{eff2\rho'}\epsilon_{eff2zz} - k_y^2\epsilon_{eff2\rho'}\epsilon_{eff2z'}} \tag{79b}$$

$$k_{2z}^{ed} = -\frac{\epsilon_{eff2yz}}{\epsilon_{eff2zz}}k_y - \frac{1}{\epsilon_{eff2zz}} \cdot \sqrt{k_2^2\epsilon_{eff2z'}\epsilon_{eff2zz} - k_x^2\epsilon_{eff2\rho'}\epsilon_{eff2zz} - k_y^2\epsilon_{eff2\rho'}\epsilon_{eff2z'}} \tag{79c}$$

and unit ray vector $\hat{s}_2^w$ [23] of the extraordinary waves are parallel to

$$\overline{s}_2^w = \overline{\overline{\epsilon}}_{eff2} \cdot \overline{k}_2^w = \epsilon_{eff2xx} k_x \hat{x} + (\epsilon_{eff2yy} k_y + \epsilon_{eff2yz} k_{2z}^w)\, \hat{y} + (\epsilon_{eff2zy} k_y + \epsilon_{eff2zz} k_{2z}^w)\, \hat{z}\ , \quad \text{with} \quad w = eu, ed \tag{80}$$

The above definitions of the unit vectors are physically descriptive. Unit vector $\hat{h}$ is parallel to TE, $\hat{v}$ to TM, $\hat{o}$ to ordinary, and $\hat{e}$ to extraordinary wave polarizations. For wave vector $\overline{k}_n^w$, all the lateral components are set identical to $\overline{k}_\rho = \hat{x}k_x + \hat{y}k_y$ in accordance to the phase matching condition and the z components are calculated from dispersion relations. Poynting vectors are all in the directions of wave vectors except for extraordinary waves whose Poynting vectors are in the directions of $\overline{s}_2^w$ given by (80).

With the defined unit vectors, solutions for the DGFs have the following forms expressed in terms of upgoing and downgoing waves as

$$\begin{aligned}
\langle \overline{\overline{G}}_{00}(\overline{r}, \overline{r}_s) \rangle = {} & \frac{i}{8\pi^2} \int_{-\infty}^{\infty} dk_x \int_{-\infty}^{\infty} dk_y \frac{e^{-i\overline{k}_0^d \cdot \overline{r}_s}}{k_{0z}} \\
& \Big\{ \hat{h}(k_{0z}^d) e^{i\overline{k}_0^d \cdot \overline{r}} \hat{h}(k_{0z}^d) \\
& + \left[R_{hh}(\overline{k}_\rho) \hat{h}(k_{0z}^u) e^{i\overline{k}_0^u \cdot \overline{r}} + R_{hv}(\overline{k}_\rho) \hat{v}(k_{0z}^u) e^{i\overline{k}_0^u \cdot \overline{r}} \right] \hat{h}(k_{0z}^d) \\
& + \hat{v}(k_{0z}^d) e^{i\overline{k}_0^d \cdot \overline{r}} \hat{v}(k_{0z}^d) \\
& + \left[R_{vh}(\overline{k}_\rho) \hat{h}(k_{0z}^u) e^{i\overline{k}_0^u \cdot \overline{r}} + R_{vv}(\overline{k}_\rho) \hat{v}(k_{0z}^u) e^{i\overline{k}_0^u \cdot \overline{r}} \right] \hat{v}(k_{0z}^d) \Big\} \\
& \qquad\qquad z_s > z \geq 0
\end{aligned} \tag{81a}$$

$$\begin{aligned}
\langle \overline{\overline{G}}_{10}(\overline{r}, \overline{r}_s) \rangle = {} & \frac{i}{8\pi^2} \int_{-\infty}^{\infty} dk_x \int_{-\infty}^{\infty} dk_y \frac{e^{-i\overline{k}_0^d \cdot \overline{r}_s}}{k_{0z}} \\
& \Big\{ \left[D_{1hh}(\overline{k}_\rho) \hat{h}(k_{1z}^d) e^{i\overline{k}_1^d \cdot \overline{r}} + D_{1hv}(\overline{k}_\rho) \hat{v}(k_{1z}^d) e^{i\overline{k}_1^d \cdot \overline{r}} \right] \hat{h}(k_{0z}^d) \\
& + \left[U_{1hh}(\overline{k}_\rho) \hat{h}(k_{1z}^u) e^{i\overline{k}_1^u \cdot \overline{r}} + U_{1hv}(\overline{k}_\rho) \hat{v}(k_{1z}^u) e^{i\overline{k}_1^u \cdot \overline{r}} \right] \hat{h}(k_{0z}^d) \\
& + \left[D_{1vh}(\overline{k}_\rho) \hat{h}(k_{1z}^d) e^{i\overline{k}_1^d \cdot \overline{r}} + D_{1vv}(\overline{k}_\rho) \hat{v}(k_{1z}^d) e^{i\overline{k}_1^d \cdot \overline{r}} \right] \hat{v}(k_{0z}^d)
\end{aligned}$$

$$+\left[U_{1vh}(\overline{k}_\rho)\hat{h}(k_{1z}^u)e^{i\overline{k}_1^u\cdot\overline{r}}+U_{1vv}(\overline{k}_\rho)\hat{v}(k_{1z}^u)e^{i\overline{k}_1^u\cdot\overline{r}}\right]\hat{v}(k_{0z}^d)\Big\}$$

$$0\geq z\geq -d_1 \qquad (81b)$$

$$\langle\overline{\overline{G}}_{20}(\overline{r},\overline{r}_s)\rangle=\frac{i}{8\pi^2}\int_{-\infty}^{\infty}dk_x\int_{-\infty}^{\infty}dk_y\frac{e^{-i\overline{k}_0^d\cdot\overline{r}_s}}{k_{0z}}$$

$$\Big\{\left[D_{2ho}(\overline{k}_\rho)\hat{o}(k_{2z}^{od})e^{i\overline{k}_2^{od}\cdot\overline{r}}+D_{2he}(\overline{k}_\rho)\hat{e}(k_{2z}^{ed})e^{i\overline{k}_2^{ed}\cdot\overline{r}}\right]\hat{h}(k_{0z}^d)$$

$$+\left[U_{2ho}(\overline{k}_\rho)\hat{o}(k_{2z}^{ou})e^{i\overline{k}_2^{ou}\cdot\overline{r}}+U_{2he}(\overline{k}_\rho)\hat{e}(k_{2z}^{eu})e^{i\overline{k}_2^{eu}\cdot\overline{r}}\right]\hat{h}(k_{0z}^d)$$

$$+\left[D_{2vo}(\overline{k}_\rho)\hat{o}(k_{2z}^{od})e^{i\overline{k}_2^{od}\cdot\overline{r}}+D_{2ve}(\overline{k}_\rho)\hat{e}(k_{2z}^{ed})e^{i\overline{k}_2^{ed}\cdot\overline{r}}\right]\hat{v}(k_{0z}^d)$$

$$+\left[U_{2vo}(\overline{k}_\rho)\hat{o}(k_{2z}^{ou})e^{i\overline{k}_2^{ou}\cdot\overline{r}}+U_{2ve}(\overline{k}_\rho)\hat{e}(k_{2z}^{eu})e^{i\overline{k}_2^{eu}\cdot\overline{r}}\right]\hat{v}(k_{0z}^d)\Big\}$$

$$-d_1\geq z\geq -d_2 \qquad (81c)$$

$$\langle\overline{\overline{G}}_{30}(\overline{r},\overline{r}_s)\rangle=\frac{i}{8\pi^2}\int_{-\infty}^{\infty}dk_x\int_{-\infty}^{\infty}dk_y\frac{e^{-i\overline{k}_0^d\cdot\overline{r}_s}}{k_{0z}}$$

$$\Big\{\left[T_{hh}(\overline{k}_\rho)\hat{h}(k_{3z}^d)e^{i\overline{k}_3^d\cdot\overline{r}}+T_{hv}(\overline{k}_\rho)\hat{v}(k_{3z}^d)e^{i\overline{k}_3^d\cdot\overline{r}}\right]\hat{h}(k_{0z}^d)$$

$$+\left[T_{vh}(\overline{k}_\rho)\hat{h}(k_{3z}^d)e^{i\overline{k}_3^d\cdot\overline{r}}+T_{vv}(\overline{k}_\rho)\hat{v}(k_{3z}^d)e^{i\overline{k}_3^d\cdot\overline{r}}\right]\hat{v}(k_{0z}^d)\Big\}$$

$$-d_2\geq z \qquad (81d)$$

DGF coefficient R's, U's, D's, and T's can be calculated directly from the boundary conditions in (73). To facilitate the calculation and the interpretation, the matrix method [23] is used to express the DGF coefficients in terms of Fresnel reflection and transmission coefficients. These expressions are determined by considering amplitude vector $\overline{A}_n$ of upgoing waves and $\overline{B}_n$ of downgoing waves in region $n=0,1,2,3$. In this method, amplitude vectors of waves propagating away and toward each interface as shown in Fig. 1.3.3 are related with matrix equations

$$\begin{bmatrix}\overline{A}_0\\ \overline{B}_1\end{bmatrix}=\begin{bmatrix}\overline{\overline{R}}_{01} & \overline{\overline{T}}_{10}\\ \overline{\overline{T}}_{01} & \overline{\overline{R}}_{10}\end{bmatrix}\cdot\begin{bmatrix}\overline{B}_0\\ \overline{A}_1\end{bmatrix} \qquad (82a)$$

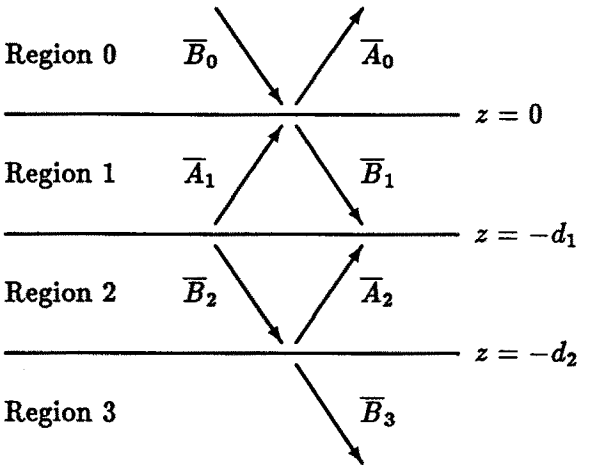

Figure 1.3.3 Amplitude vector $\overline{A}_n$ are for upgoing waves, $\overline{B}_n$ are for downgoing waves, and the arrows represent the propagation directions.

$$\begin{bmatrix} \overline{A}_1 \\ \overline{B}_2 \end{bmatrix} = \begin{bmatrix} \overline{\overline{R}}_{12} & \overline{\overline{T}}_{21} \\ \overline{\overline{T}}_{12} & \overline{\overline{R}}_{21} \end{bmatrix} \cdot \begin{bmatrix} \overline{B}_1 \\ \overline{A}_2 \end{bmatrix} \tag{82b}$$

$$\begin{bmatrix} \overline{A}_2 \\ \overline{B}_3 \end{bmatrix} = \begin{bmatrix} \overline{\overline{R}}_{23} \\ \overline{\overline{T}}_{23} \end{bmatrix} \cdot \overline{B}_2 \tag{82c}$$

Observed from (81), the amplitude vectors are also connected to incident amplitude vector $\overline{B}_0$ by

$$\overline{A}_0 \equiv \overline{\overline{R}}_0 \cdot \overline{B}_0 = \begin{bmatrix} R_{hh}(\overline{k}_\rho) & R_{vh}(\overline{k}_\rho) \\ R_{hv}(\overline{k}_\rho) & R_{vv}(\overline{k}_\rho) \end{bmatrix} \cdot \overline{B}_0 \tag{83a}$$

$$\overline{B}_1 \equiv \overline{\overline{D}}_1 \cdot \overline{B}_0 = \begin{bmatrix} D_{1hh}(\overline{k}_\rho) & D_{1vh}(\overline{k}_\rho) \\ D_{1hv}(\overline{k}_\rho) & D_{1vv}(\overline{k}_\rho) \end{bmatrix} \cdot \overline{B}_0 \tag{83b}$$

$$\overline{A}_1 \equiv \overline{\overline{U}}_1 \cdot \overline{B}_0 = \begin{bmatrix} U_{1hh}(\overline{k}_\rho) & U_{1vh}(\overline{k}_\rho) \\ U_{1hv}(\overline{k}_\rho) & U_{1vv}(\overline{k}_\rho) \end{bmatrix} \cdot \overline{B}_0 \tag{83c}$$

$$\overline{B}_2 \equiv \overline{\overline{D}}_2 \cdot \overline{B}_0 = \begin{bmatrix} D_{2ho}(\overline{k}_\rho) & D_{2vo}(\overline{k}_\rho) \\ D_{2he}(\overline{k}_\rho) & D_{2ve}(\overline{k}_\rho) \end{bmatrix} \cdot \overline{B}_0 \tag{83d}$$

$$\overline{A}_2 \equiv \overline{\overline{U}}_2 \cdot \overline{B}_0 = \begin{bmatrix} U_{2ho}(\overline{k}_\rho) & U_{2vo}(\overline{k}_\rho) \\ U_{2he}(\overline{k}_\rho) & U_{2ve}(\overline{k}_\rho) \end{bmatrix} \cdot \overline{B}_0 \tag{83e}$$

$$\overline{B}_3 \equiv \overline{\overline{T}}_3 \cdot \overline{B}_0 = \begin{bmatrix} T_{hh}(\overline{k}_\rho) & T_{vh}(\overline{k}_\rho) \\ T_{hv}(\overline{k}_\rho) & T_{vv}(\overline{k}_\rho) \end{bmatrix} \cdot \overline{B}_0 \tag{83f}$$

Equation system (82) is readily solved for the downgoing and upgoing amplitude vectors in terms of $\overline{B}_0$ and the results are then compared to (83) to obtain the following DGF coefficient matrices

$$\overline{\overline{R}}_0 = \overline{\overline{R}}_{01} + \overline{\overline{T}}_{10} \cdot \left(\overline{\overline{R}}_{12} + \overline{\overline{T}}_{21} \cdot \overline{\overline{R}}_{23} \cdot \overline{\overline{\Gamma}} \cdot \overline{\overline{T}}_{12}\right) \cdot \overline{\overline{D}}_1 \tag{84a}$$

$$\overline{\overline{D}}_1 = \left[\overline{\overline{I}} - \overline{\overline{R}}_{10} \cdot \left(\overline{\overline{R}}_{12} + \overline{\overline{T}}_{21} \cdot \overline{\overline{R}}_{23} \cdot \overline{\overline{\Gamma}} \cdot \overline{\overline{T}}_{12}\right)\right]^{-1} \cdot \overline{\overline{T}}_{01} \tag{84b}$$

$$\overline{\overline{U}}_1 = \left[\overline{\overline{R}}_{12} + \overline{\overline{T}}_{21} \cdot \overline{\overline{R}}_{23} \cdot \overline{\overline{\Gamma}} \cdot \overline{\overline{T}}_{12}\right] \cdot \overline{\overline{D}}_1 \tag{84c}$$

$$\overline{\overline{D}}_2 = \overline{\overline{\Gamma}} \cdot \overline{\overline{T}}_{12} \cdot \overline{\overline{D}}_1 \tag{84d}$$

$$\overline{\overline{U}}_2 = \overline{\overline{R}}_{23} \cdot \overline{\overline{\Gamma}} \cdot \overline{\overline{T}}_{12} \cdot \overline{\overline{D}}_1 \tag{84e}$$

$$\overline{\overline{T}}_3 = \overline{\overline{T}}_{23} \cdot \overline{\overline{\Gamma}} \cdot \overline{\overline{T}}_{12} \cdot \overline{\overline{D}}_1 \tag{84f}$$

where $\overline{\overline{\Gamma}} = (\overline{\overline{I}} - \overline{\overline{R}}_{21} \cdot \overline{\overline{R}}_{23})^{-1}$ and the reflection and transmission matrices are

$$\overline{\overline{R}}_{01} = \begin{bmatrix} R_{01hh} & 0 \\ 0 & R_{01vv} \end{bmatrix}, \quad \overline{\overline{R}}_{10} = \begin{bmatrix} R_{10hh} & 0 \\ 0 & R_{10vv} \end{bmatrix} \tag{85a}$$

$$\overline{\overline{T}}_{01} = \begin{bmatrix} T_{01hh} & 0 \\ 0 & T_{01vv} \end{bmatrix}, \quad \overline{\overline{T}}_{10} = \begin{bmatrix} T_{10hh} & 0 \\ 0 & T_{10vv} \end{bmatrix} \tag{85b}$$

$$\overline{\overline{R}}_{12} = \begin{bmatrix} e^{i2k_{1z}^u d_1} R_{12hh} & e^{i2k_{1z}^u d_1} R_{12vh} \\ e^{i2k_{1z}^u d_1} R_{12hv} & e^{i2k_{1z}^u d_1} R_{12vv} \end{bmatrix} \tag{85c}$$

$$\overline{\overline{R}}_{21} = \begin{bmatrix} e^{i(k_{2z}^{od} - k_{2z}^{ou}) d_1} R_{21oo} & e^{i(k_{2z}^{od} - k_{2z}^{eu}) d_1} R_{21eo} \\ e^{i(k_{2z}^{ed} - k_{2z}^{ou}) d_1} R_{21oe} & e^{i(k_{2z}^{ed} - k_{2z}^{eu}) d_1} R_{21ee} \end{bmatrix} \tag{85d}$$

$$\overline{\overline{T}}_{12} = \begin{bmatrix} e^{i(k_{2z}^{od} - k_{1z}^{d}) d_1} T_{12ho} & e^{i(k_{2z}^{od} - k_{1z}^{d}) d_1} T_{12vo} \\ e^{i(k_{2z}^{ed} - k_{1z}^{d}) d_1} T_{12he} & e^{i(k_{2z}^{ed} - k_{1z}^{d}) d_1} T_{12ve} \end{bmatrix} \tag{85e}$$

$$\overline{\overline{T}}_{21} = \begin{bmatrix} e^{i(k_{1z}^{u} - k_{2z}^{ou}) d_1} T_{21oh} & e^{i(k_{1z}^{u} - k_{2z}^{eu}) d_1} T_{21eh} \\ e^{i(k_{1z}^{u} - k_{2z}^{ou}) d_1} T_{21ov} & e^{i(k_{1z}^{u} - k_{2z}^{eu}) d_1} T_{21ev} \end{bmatrix} \tag{85f}$$

$$\overline{\overline{R}}_{23} = \begin{bmatrix} e^{i(k_{2z}^{ou} - k_{2z}^{od}) d_2} R_{23oo} & e^{i(k_{2z}^{ou} - k_{2z}^{ed}) d_2} R_{23eo} \\ e^{i(k_{2z}^{eu} - k_{2z}^{od}) d_2} R_{23oe} & e^{i(k_{2z}^{eu} - k_{2z}^{ed}) d_2} R_{23ee} \end{bmatrix} \tag{85g}$$

$$\overline{\overline{T}}_{23} = \begin{bmatrix} e^{i(k_{3z}^{d} - k_{2z}^{od}) d_2} T_{23oh} & e^{i(k_{3z}^{d} - k_{2z}^{ed}) d_2} T_{23eh} \\ e^{i(k_{3z}^{d} - k_{2z}^{od}) d_2} T_{23ov} & e^{i(k_{3z}^{d} - k_{2z}^{ed}) d_2} T_{23ev} \end{bmatrix} \tag{85h}$$

in which the exponents carry phase factors due to the locations of the interfaces and Fresnel reflection and transmission coefficient R's and T's are given in appendix A. The above results vividly describe the physical processes of wave interaction in the layer media. For instance, amplitude vector $\overline{B}_2$ of downgoing waves in region 2 is spelled out from (83d) and (84d) as

$$\overline{B}_2 = \overline{\overline{\Gamma}} \cdot \overline{\overline{T}}_{12} \cdot \overline{\overline{D}}_1 \cdot \overline{B}_0 \tag{86}$$

which can be interpreted as the incident wave $\overline{B}_0$ from region 0 propagates down into region 1 $(\overline{\overline{D}}_1 \cdot \overline{B}_0)$, transmits through the interface between region 1 and region 2 $(\overline{\overline{T}}_{12} \cdot \overline{\overline{D}}_1 \cdot \overline{B}_0)$, and multiply reflects between the interfaces of region 2 $(\overline{\overline{\Gamma}} \cdot \overline{\overline{T}}_{12} \cdot \overline{\overline{D}}_1 \cdot \overline{B}_0)$. This completes the derivation of the DGFs corresponding to the source in region 0 in integral form (81).

For latter calculations of the scattering coefficients involving the effective sources in the scattering regions $(n = 1, 2)$, dyadic Green's function $\langle \overline{\overline{G}}_{01}(\overline{r}, \overline{r}_s) \rangle$ and $\langle \overline{\overline{G}}_{02}(\overline{r}, \overline{r}_s) \rangle$ need be obtained by applying the symmetry relation (71) requiring the transposition of the corresponding DGFs in the last paragraph and the sign changes of k_x and k_y respectively to $-k_x$ and $-k_y$. After the integrations are carried out with the two-dimensional saddle point method [9,23], the results for the DGFs in the radiation field are

$$\langle \overline{\overline{G}}_{0n}(\overline{r}, \overline{r}_s) \rangle = \frac{e^{ik_0 r}}{4\pi r} e^{-i\overline{k}_\rho \cdot \overline{\rho}_s} \overline{\overline{g}}_n(\overline{k}_\rho, z_s) , \quad n = 1, 2 \tag{87}$$

where $\overline{\rho}_s = \hat{x} x_s + \hat{y} y_s$ and dyadic coefficient $\overline{\overline{g}}_n(\overline{k}_\rho, z_s)$ are defined as

$$\begin{aligned}
&\overline{\overline{g}}_1(\overline{k}_\rho, z_s) \equiv \\
&+ \hat{h}(k_{0z}^u)\left[D_{1hh}(-\overline{k}_\rho)\hat{h}(k_{1z}^u)e^{-ik_{1z}^u z_s} - D_{1hv}(-\overline{k}_\rho)\hat{v}(k_{1z}^u)e^{-ik_{1z}^u z_s}\right] \\
&+ \hat{h}(k_{0z}^u)\left[U_{1hh}(-\overline{k}_\rho)\hat{h}(k_{1z}^d)e^{-ik_{1z}^d z_s} - U_{1hv}(-\overline{k}_\rho)\hat{v}(k_{1z}^d)e^{-ik_{1z}^d z_s}\right] \\
&- \hat{v}(k_{0z}^u)\left[D_{1vh}(-\overline{k}_\rho)\hat{h}(k_{1z}^u)e^{-ik_{1z}^u z_s} - D_{1vv}(-\overline{k}_\rho)\hat{v}(k_{1z}^u)e^{-ik_{1z}^u z_s}\right] \\
&- \hat{v}(k_{0z}^u)\left[U_{1vh}(-\overline{k}_\rho)\hat{h}(k_{1z}^d)e^{-ik_{1z}^d z_s} - U_{1vv}(-\overline{k}_\rho)\hat{v}(k_{1z}^d)e^{-ik_{1z}^d z_s}\right]
\end{aligned} \tag{88a}$$

$$\bar{\bar{g}}_2(\bar{k}_\rho, z_s) \equiv$$

$$+ \hat{h}(k_{0z}^u)\left[D_{2ho}(-\bar{k}_\rho)\hat{o}(k_{2z}^{ou})e^{-ik_{2z}^{ou}z_s} - D_{2he}(-\bar{k}_\rho)\hat{e}(k_{2z}^{eu})e^{-ik_{2z}^{eu}z_s}\right]$$

$$+ \hat{h}(k_{0z}^u)\left[U_{2ho}(-\bar{k}_\rho)\hat{o}(k_{2z}^{od})e^{-ik_{2z}^{od}z_s} - U_{2he}(-\bar{k}_\rho)\hat{e}(k_{2z}^{ed})e^{-ik_{2z}^{ed}z_s}\right]$$

$$- \hat{v}(k_{0z}^u)\left[D_{2vo}(-\bar{k}_\rho)\hat{o}(k_{2z}^{ou})e^{-ik_{2z}^{ou}z_s} - D_{2ve}(-\bar{k}_\rho)\hat{e}(k_{2z}^{eu})e^{-ik_{2z}^{eu}z_s}\right]$$

$$- \hat{v}(k_{0z}^u)\left[U_{2vo}(-\bar{k}_\rho)\hat{o}(k_{2z}^{od})e^{-ik_{2z}^{od}z_s} - U_{2ve}(-\bar{k}_\rho)\hat{e}(k_{2z}^{ed})e^{-ik_{2z}^{ed}z_s}\right] \quad (88b)$$

In summary, the DGFs are obtained in (88) where all the coefficients are determined by (83-85) and appendix A. With the available DGFs, the scattering coefficients are derived in the next subsection.

d. Scattering Coefficients

The polarimetric backscattering coefficients are defined by (13) based on ensemble averages of scattered fields. As indicated in (32), the averages are calculated with spatial integrations over products of the DGFs, the mean fields, and the correlation functions. The DGFs have been obtained; next shown are the mean field and the correlation functions. The integrations are then carried out to derive the scattering coefficients.

The mean external fields in the scattering regions ($n = 1, 2$) can be approximated as the corresponding homogeneous solutions to the wave equations

$$\nabla \times \nabla \times \langle \overline{F}_n(\bar{r}) \rangle - k_0^2 \frac{\bar{\bar{\epsilon}}_{effn}}{\epsilon_0} \langle \overline{F}_n(\bar{r}) \rangle = 0 \ , \quad n = 1, 2 \qquad (89)$$

which are solved subjected to the boundary conditions at interface $z = 0, -d_1, -d_2$. For incident field $\overline{E}_{0i} = [\hat{h}(k_{0zi})E_{hi} + \hat{v}(k_{0zi})E_{vi}]e^{i\bar{k}_{0i}\cdot\bar{r}}$, the mean fields can be written as

$$\langle \overline{F}_n(\bar{r}) \rangle = e^{\bar{k}_{\rho i}\cdot\bar{\rho}} \overline{P}_n(\bar{k}_{\rho i}, z) \ , \quad n = 1, 2 \qquad (90)$$

where subscript i indicates the incident wave, $\bar{\rho} = \hat{x}x + \hat{y}y$ is the lateral space, $\bar{k}_{\rho i} = \hat{x}k_{xi} + \hat{y}k_{yi} = k_0(\hat{x}\sin\theta_{0i}\cos\phi_{0i} + \hat{y}\sin\theta_{0i}\sin\phi_{0i})$ is the lateral component of incident wave vector $\bar{k}_{0i}$, and polarization vector $\overline{P}_n(\bar{k}_{\rho i}, z)$ are determined by

$$\overline{P}_1(\overline{k}_{\rho i}, z) \equiv$$
$$+ E_{hi}\left[D_{1hh}(\overline{k}_{\rho i})\hat{h}(k^d_{1zi})e^{ik^d_{1zi}z} + D_{1hv}(\overline{k}_{\rho i})\hat{v}(k^d_{1zi})e^{ik^d_{1zi}z}\right]$$
$$+ E_{hi}\left[U_{1hh}(\overline{k}_{\rho i})\hat{h}(k^u_{1zi})e^{ik^u_{1zi}z} + U_{1hv}(\overline{k}_{\rho i})\hat{v}(k^u_{1zi})e^{ik^u_{1zi}z}\right]$$
$$+ E_{vi}\left[D_{1vh}(\overline{k}_{\rho i})\hat{h}(k^d_{1zi})e^{ik^d_{1zi}z} + D_{1vv}(\overline{k}_{\rho i})\hat{v}(k^d_{1zi})e^{ik^d_{1zi}z}\right]$$
$$+ E_{vi}\left[U_{1vh}(\overline{k}_{\rho i})\hat{h}(k^u_{1zi})e^{ik^u_{1zi}z} + U_{1vv}(\overline{k}_{\rho i})\hat{v}(k^u_{1zi})e^{ik^u_{1zi}z}\right] \quad (91a)$$

$$\overline{P}_2(\overline{k}_{\rho i}, z) \equiv$$
$$+ E_{hi}\left[D_{2ho}(\overline{k}_{\rho i})\hat{o}(k^{od}_{2zi})e^{ik^{od}_{2zi}z} + D_{2he}(\overline{k}_{\rho i})\hat{e}(k^{ed}_{2zi})e^{ik^{ed}_{2zi}z}\right]$$
$$+ E_{hi}\left[U_{2ho}(\overline{k}_{\rho i})\hat{o}(k^{ou}_{2zi})e^{ik^{ou}_{2zi}z} + U_{2he}(\overline{k}_{\rho i})\hat{e}(k^{eu}_{2zi})e^{ik^{eu}_{2zi}z}\right]$$
$$+ E_{vi}\left[D_{2vo}(\overline{k}_{\rho i})\hat{o}(k^{od}_{2zi})e^{ik^{od}_{2zi}z} + D_{2ve}(\overline{k}_{\rho i})\hat{e}(k^{ed}_{2zi})e^{ik^{ed}_{2zi}z}\right]$$
$$+ E_{vi}\left[U_{2vo}(\overline{k}_{\rho i})\hat{o}(k^{ou}_{2zi})e^{ik^{ou}_{2zi}z} + U_{2ve}(\overline{k}_{\rho i})\hat{e}(k^{eu}_{2zi})e^{ik^{eu}_{2zi}z}\right] \quad (91b)$$

with z components of the wave vectors defined in the same manner as (75), (77), and (79b,c) by changing k^w_{nz}, k_x, and k_y respectively to k^w_{nzi}, k_{xi}, and k_{yi}.

The correlation functions are defined by (33) in the spatial domain. To facilitate the integration of (32), Fourier transforms of the correlation functions are introduced for the statistically homogeneous scattering media under consideration

$$C_{\xi njklm}(\overline{r}_n, \overline{r}^o_n) = \int_{-\infty}^{\infty} d\overline{\beta}\Phi_{njklm}(\overline{\beta})e^{-i\overline{\beta}\cdot(\overline{r}_n - \overline{r}^o_n)}, \quad n = 1, 2 \quad (92)$$

For the isotropic random medium ($n = 1$), the non-zero elements of spectral density $\Phi_{1jklm}(\overline{\beta})$ are simply

$$\Phi_1(\overline{\beta}) = \Phi_{1jjmm}(\overline{\beta}) = \delta_1\Phi_{\xi 1}(\overline{\beta}) \quad (93)$$

where $\Phi_{\xi 1}(\overline{\beta})$ is defined as in (39) and functionally given by (43b) in conformity with the correlation function used to find the isotropic effective permittivity. For a two-constituent medium, variance δ_1 is

$$\delta_1 = 9\left|\frac{\epsilon_{g1}}{\epsilon_0}\right|^2\left[\left|\frac{\epsilon_{b1} - \epsilon_{g1}}{\epsilon_{b1} + 2\epsilon_{g1}}\right|^2(1 - f_{s1}) + \left|\frac{\epsilon_{s1} - \epsilon_{g1}}{\epsilon_{s1} + 2\epsilon_{g1}}\right|^2 f_{s1}\right] \quad (94)$$

For the anisotropic random medium ($n = 2$), the correlation functions (92) specified in the untilted coordinate system $(\hat{x}, \hat{y}, \hat{z})$ are derived by applying the rotation transformation $\overline{\overline{T}}_\psi$ on scatterer $\overline{\overline{\xi}}_2(\overline{r}_2')$ in the tilted coordinate system $(\hat{x}', \hat{y}', \hat{z}')$ so that

$$\overline{\overline{\xi}}_2(\overline{r}_2) = \overline{\overline{T}}_\psi \cdot \overline{\overline{\xi}}_2(\overline{r}_2') \cdot \overline{\overline{T}}_\psi^{-1} = \begin{bmatrix} \xi_{2xx}(\overline{r}_2) & 0 & 0 \\ 0 & \xi_{2yy}(\overline{r}_2) & \xi_{2yz}(\overline{r}_2) \\ 0 & \xi_{2zy}(\overline{r}_2) & \xi_{2zz}(\overline{r}_2) \end{bmatrix} \tag{95}$$

where the elements of $\overline{\overline{\xi}}_2(\overline{r}_2)$ have the form of (66b) with ϵ_{eff2} replaced by ξ_2. The scatterer elements in the untilted coordinates are then used in (33) to find the anisotropic correlation functions whose spectral densities can be obtained from the following spectral densities defined in the tilted coordinates as

$$\Phi_{2\rho'}(\overline{\beta}') = \Phi_{2x'x'x'x'}(\overline{\beta}') = \delta_{2\rho'}\Phi_{\xi 2}(\overline{\beta}') \tag{96a}$$

$$\Phi_{2z'}(\overline{\beta}') = \Phi_{2z'z'z'z'}(\overline{\beta}') = \delta_{2z'}\Phi_{\xi 2}(\overline{\beta}') \tag{96b}$$

$$\Phi_{2c'}(\overline{\beta}') = \Phi_{2x'x'z'z'}(\overline{\beta}') = \delta_{2c'}\Phi_{\xi 2}(\overline{\beta}') \tag{96c}$$

where $\Phi_{\xi 2}(\overline{\beta}')$ is functionally determined by (58b) in conformity with the correlation function used to calculate the anisotropic effective permittivity. For the two-constituent anisotropic random medium, the variances in (96) are

$$\delta_{2\rho'} = \left|\frac{\epsilon_{b2} - \epsilon_{g2\rho'}}{\epsilon_0 + S_{2\rho'}(\epsilon_{b2} - \epsilon_{g2\rho'})}\right|^2 (1 - f_{s2}) + \left|\frac{\epsilon_{s2} - \epsilon_{g2\rho'}}{\epsilon_0 + S_{2\rho'}(\epsilon_{s2} - \epsilon_{g2\rho'})}\right|^2 f_{s2} \tag{97a}$$

$$\delta_{2z'} = \left|\frac{\epsilon_{b2} - \epsilon_{g2z'}}{\epsilon_0 + S_{2z'}(\epsilon_{b2} - \epsilon_{g2z'})}\right|^2 (1 - f_{s2}) + \left|\frac{\epsilon_{s2} - \epsilon_{g2z'}}{\epsilon_0 + S_{2z'}(\epsilon_{s2} - \epsilon_{g2z'})}\right|^2 f_{s2} \tag{97b}$$

$$\begin{aligned} \delta_{2c'} = {} & \left[\frac{\epsilon_{b2} - \epsilon_{g2\rho'}}{\epsilon_0 + S_{2\rho'}(\epsilon_{b2} - \epsilon_{g2\rho'})}\right]\left[\frac{\epsilon_{b2} - \epsilon_{g2z'}}{\epsilon_0 + S_{2z'}(\epsilon_{b2} - \epsilon_{g2z'})}\right]^* (1 - f_{s2}) \\ & + \left[\frac{\epsilon_{s2} - \epsilon_{g2\rho'}}{\epsilon_0 + S_{2\rho'}(\epsilon_{s2} - \epsilon_{g2\rho'})}\right]\left[\frac{\epsilon_{s2} - \epsilon_{g2z'}}{\epsilon_0 + S_{2z'}(\epsilon_{s2} - \epsilon_{g2z'})}\right]^* f_{s2} \end{aligned} \tag{97c}$$

Due to the invariant property of the Fourier transform under the rotation transformation, spectral density $\Phi_{2jklm}(\overline{\beta})$ in the untilted coordinates can functionally be related to those given in (96) with

$$\Phi_{\xi 2}(\overline{\beta}) = \Phi_{\xi 2}(\beta_x' = \beta_x, \beta_y' = \beta_y \cos\psi - \beta_z \sin\psi, \beta_z' = \beta_y \sin\psi + \beta_z \cos\psi) \tag{98}$$

In the untilted coordinates, the rotation transformation together with the above invariant property give the anisotropic spectral densities

$$\Phi_{2jklm}(\overline{\beta}) = \delta_{2jklm}\Phi_{\xi 2}(\overline{\beta}) \tag{99}$$

where non-zero variance δ_{2jklm} are dependent on the tilt angle ψ as

$$\delta_{2xxxx} = \delta_{2\rho'} \tag{100a}$$

$$\delta_{2xxyy} = \delta^*_{2yyxx} = \delta_{2\rho'}\cos^2\psi + \delta_{2c'}\sin^2\psi \tag{100b}$$

$$\delta_{2xxyz} = \delta_{2xxzy} = \delta^*_{2yzxx} = \delta^*_{2zyxx} = (\delta_{2c'} - \delta_{2\rho'})\sin\psi\cos\psi \tag{100c}$$

$$\delta_{2xxzz} = \delta^*_{2zzxx} = \delta_{2\rho'}\sin^2\psi + \delta_{2c'}\cos^2\psi \tag{100d}$$

$$\delta_{2yyyy} = \delta_{2\rho'}\cos^4\psi + \delta_{2z'}\sin^4\psi + (\delta_{2c'} + \delta^*_{2c'})\sin^2\psi\cos^2\psi \tag{100e}$$

$$\begin{aligned}\delta_{2yyyz} &= \delta_{2yyzy} = \delta^*_{2yzyy} = \delta^*_{2zyyy} \\ &= (\delta_{2c'} - \delta_{2\rho'})\cos^3\psi\sin\psi + (\delta_{2z'} - \delta^*_{2c'})\sin^3\psi\cos\psi\end{aligned} \tag{100f}$$

$$\begin{aligned}\delta_{2yyzz} &= \delta^*_{2zzyy} \\ &= (\delta_{2\rho'} + \delta_{2z'})\sin^2\psi\cos^2\psi + \delta_{2c'}\cos^4\psi + \delta^*_{2c'}\sin^4\psi\end{aligned} \tag{100g}$$

$$\begin{aligned}\delta_{2yzyz} &= \delta_{2yzzy} = \delta_{2zyyz} = \delta_{2zyzy} \\ &= (\delta_{2\rho'} + \delta_{2z'} - \delta_{2c'} - \delta^*_{2c'})\sin^2\psi\cos^2\psi\end{aligned} \tag{100h}$$

$$\begin{aligned}\delta_{2yzzz} &= \delta_{2zyzz} = \delta^*_{2zzyz} = \delta^*_{2zzzy} \\ &= (\delta^*_{2c'} - \delta_{2\rho'})\sin^3\psi\cos\psi + (\delta_{2z'} - \delta_{2c'})\cos^3\psi\sin\psi\end{aligned} \tag{100i}$$

$$\delta_{2zzzz} = \delta_{2\rho'}\sin^4\psi + \delta_{2z'}\cos^4\psi + (\delta_{2c'} + \delta^*_{2c'})\sin^2\psi\cos^2\psi \tag{100j}$$

The correlation of the scattered field can now be found by substituting into (32) the dyadic Green's functions (87), the means fields (90), and the correlation functions (92). To enable the calculation of the scattering coefficients according to (13), correlations of the scattered field components are actualized in the manner of (14)

$$\langle E_{\mu s}(\overline{r})E^*_{\nu s}(\overline{r})\rangle = \frac{E_{\tau i}E^*_{\kappa i}}{(4\pi r)^2}$$

$$\left\{k_0^4\int_{-\infty}^{\infty} d\overline{\beta}_\rho \int d\overline{\rho}_1 \int d\overline{\rho}_1^o\; e^{i(\overline{k}_{\rho i} - \overline{k}_\rho - \overline{\beta}_\rho)\cdot\overline{\rho}_1} e^{-i(\overline{k}_{\rho i} - \overline{k}_\rho - \overline{\beta}_\rho)\cdot\overline{\rho}_1^o}\right.$$

$$\left.\sum_{j,m}^{x,y,z}\int_{-\infty}^{\infty} d\beta_z \int_{-d_1}^{0} dz_1 \int_{-d_1}^{0} dz_1^o\; \Phi_1(\overline{\beta}) e^{-i\beta_z(z_1 - z_1^o)}\right.$$

$$\cdot g_{1\mu j}(\overline{k}_\rho, z_1)\mathcal{F}_{1\tau j}(\overline{k}_{\rho i}, z_1)g^*_{1\nu m}(\overline{k}_\rho, z_1^o)\mathcal{F}^*_{1\kappa m}(\overline{k}_{\rho i}, z_1^o)$$

$$+ k_0^4 \int_{-\infty}^{\infty} d\overline{\beta}_\rho \int d\overline{\rho}_2 \int d\overline{\rho}_2^o \, e^{i(\overline{k}_{\rho i}-\overline{k}_\rho-\overline{\beta}_\rho)\cdot\overline{\rho}_2} e^{-i(\overline{k}_{\rho i}-\overline{k}_\rho-\overline{\beta}_\rho)\cdot\overline{\rho}_2^o}$$

$$\sum_{j,k,l,m}^{x,y,z} \int_{-\infty}^{\infty} d\beta_z \int_{-d_2}^{-d_1} dz_2 \int_{-d_1}^{-d_1} dz_2^o \; \Phi_{2jklm}(\overline{\beta}) e^{-i\beta_z(z_2-z_2^o)}$$

$$\cdot g_{2\mu j}(\overline{k}_\rho, z_2)\mathcal{F}_{2\tau k}(\overline{k}_{\rho i}, z_2)g^*_{2\nu l}(\overline{k}_\rho, z_2^o)\mathcal{F}^*_{2\kappa m}(\overline{k}_{\rho i}, z_2^o)\Big\} \tag{101}$$

where $\overline{\beta} = \overline{\beta}_\rho + \hat{z}\beta_z$, $\overline{\beta}_\rho = \hat{x}\beta_x + \hat{y}\beta_y$, subscript μ, ν, τ, and κ can be h or v, and DGF element $g_{n\mu j}(\overline{k}_\rho, z_n)$ and normalized mean field component $\mathcal{F}_{n\tau j}(\overline{k}_\rho, z_n)$ for $n = 1, 2$ and $\hat{j} = \hat{x}, \hat{y}, \hat{z}$ are defined as

$$g_{n\mu j}(\overline{k}_\rho, z_n) = \left[\hat{\mu}(k_{0z}^u) \cdot \overline{\overline{g}}_n(\overline{k}_\rho, z_n)\right] \cdot \hat{j} \tag{102a}$$

$$\mathcal{F}_{n\tau j}(\overline{k}_{\rho i}, z_n) = E_{\tau i}^{-1}\langle \overline{F}_n(\overline{r}_n)\rangle \cdot \hat{j}\,|_{E_{\nu i}=0} \tag{102b}$$

The integrations in (101) are carried out with the procedure in [37]: the integrals over $\overline{\rho}_n$ give Dirac delta function $4\pi^2\delta(\overline{k}_{\rho i} - \overline{k}_\rho - \overline{\beta}_\rho)$, the integrals over $\overline{\beta}_\rho$ then effectuate $\overline{\beta}_\rho = \overline{k}_{\rho i} - \overline{k}_\rho$, and the integrals over $\overline{\rho}_n^o$ form illuminated area A. Then (101) becomes

$$\langle E_{\mu s}(\overline{r})E^*_{\nu s}(\overline{r})\rangle = E_{\tau i}E^*_{\kappa i}\frac{k_0^4 A}{4r^2}$$

$$\Big\{ \sum_{j,m}^{x,y,z} \int_{-\infty}^{\infty} d\beta_z \int_{-d_1}^{0} dz_1 \int_{-d_1}^{0} dz_1^o \; \Phi_1(\overline{\beta}_\rho = \overline{k}_{\rho i} - \overline{k}_\rho, \beta_z) e^{-i\beta_z(z_1-z_1^o)}$$

$$\cdot g_{1\mu j}(\overline{k}_\rho, z_1)\mathcal{F}_{1\tau j}(\overline{k}_{\rho i}, z_1)g^*_{1\nu m}(\overline{k}_\rho, z_1^o)\mathcal{F}^*_{1\kappa m}(\overline{k}_{\rho i}, z_1^o)$$

$$+ \sum_{j,k,l,m}^{x,y,z} \int_{-\infty}^{\infty} d\beta_z \int_{-d_2}^{-d_1} dz_2 \int_{-d_2}^{-d_1} dz_2^o \; \Phi_{2jklm}(\overline{\beta}_\rho = \overline{k}_{\rho i} - \overline{k}_\rho, \beta_z) e^{-i\beta_z(z_2-z_2^o)}$$

$$\cdot g_{2\mu j}(\overline{k}_\rho, z_2)\mathcal{F}_{2\tau k}(\overline{k}_{\rho i}, z_2)g^*_{2\nu l}(\overline{k}_\rho, z_2^o)\mathcal{F}^*_{2\kappa m}(\overline{k}_{\rho i}, z_2^o)\Big\} \tag{103}$$

It is observed from the forms of g's and $\mathcal{F}$'s that all the polarization vectors and coefficient D's and U's can be taken out of the integrations

in (103). Retained inside the integrations are the spectral densities and the exponential terms which account for the upgoing and downgoing propagation of the mean fields and the scattered fields. Furthermore, $\phi_{0s} = \phi_{0i} + \pi$ and $\theta_{0s} = \theta_{0i}$ in the backscattering direction so that $\overline{k}_\rho = -\overline{k}_{\rho i}$ and $k_{nz}^w = k_{nzi}^w$ for wave type $w = u, d$ in region $n = 1$ or $w = ou, od, eo, ed$ in region $n = 2$. Also note that the z components of the upgoing and the downgoing wave vectors in region 1 differ only by a minus sign. Consequently, the following integrals are defined to simplify the calculation

$$\mathcal{I}_1^{abcd} \equiv \int_{-\infty}^{\infty} d\beta_z \Phi_1(2\overline{k}_{\rho i}, \beta_z) \int_{-d_1}^{0} dz_1 e^{-i(\beta_z - \kappa_{ab})z_1} \int_{-d_1}^{0} dz_1^o e^{i(\beta_z - \kappa_{cd})z_1^o} \quad (104a)$$

$$\text{with} : \begin{cases} \kappa_{ab} = (a+b)k_{1z} \; ; & a, b = -1, 1 \\ \kappa_{cd} = (c+d)k_{1z}^* \; ; & c, d = -1, 1 \end{cases} \quad (104b)$$

$$\mathcal{I}_{2jklm}^{pqrs} \equiv \int_{-\infty}^{\infty} d\beta_z \Phi_{2jklm}(2\overline{k}_{\rho i}, \beta_z) \int_{-d_2}^{-d_1} dz_2 e^{-i(\beta_z - \kappa_{pq})z_2} \int_{-d_2}^{-d_1} dz_2^o e^{i(\beta_z - \kappa_{rs})z_2^o} \quad (105a)$$

$$\text{with} : \begin{cases} \kappa_{pq} = -k_{2zi}^p + k_{2zi}^q \; ; & p, q = ou, od, eu, ed \\ \kappa_{rs} = -k_{2zi}^{r*} + k_{2zi}^{s*} \; ; & r, s = ou, od, eu, ed \end{cases} \quad (105b)$$

For the isotropic random medium, integral $\mathcal{I}_1^{abcd}$ involves 16 quantities since a, b, c, and d each has two possibilities of -1 and 1. The integrations over vertical space z_1 and z_1^o are readily carried out and the integration over β_z is performed with the residue theorem in the contour integration method. From appendix D, the result for $\mathcal{I}_1^{abcd}$ is

$$\mathcal{I}_1^{abcd} = i\frac{2\delta_1}{\pi \ell_1} \left[\frac{e^{-i(\kappa_{ab} - \kappa_{cd})d_1}}{(\kappa_{ab} - \kappa_1)^2(\kappa_{ab} - \kappa_1^*)^2(\kappa_{ab} - \kappa_{cd})} + \frac{1}{(\kappa_{cd} - \kappa_1)^2(\kappa_{cd} - \kappa_1^*)^2(\kappa_{cd} - \kappa_{ab})} - \mathcal{P}_1(\kappa_1) - \mathcal{Q}_1(\kappa_1^*) \right] \quad (106a)$$

where $\kappa_1 = i\ell^{-1}\sqrt{1 + 4k_{\rho i}^2 \ell_1^2}$ and quantities $\mathcal{P}_1(\kappa_1)$ and $\mathcal{Q}_1(\kappa_1^*)$ are

$$\mathcal{P}_1(\kappa_1) = \frac{id_1 e^{i(\kappa_1 - \kappa_{ab})d_1}}{(2\kappa_1)^2(\kappa_1 - \kappa_{ab})(\kappa_1 - \kappa_{cd})} + \frac{1 - e^{i(\kappa_1 - \kappa_{ab})d_1} + e^{-i(\kappa_{ab} - \kappa_{cd})d_1}}{(2\kappa_1)^2(\kappa_1 - \kappa_{ab})(\kappa_1 - \kappa_{cd})}$$

$$\cdot \left[\frac{1}{\kappa_1}+\frac{1}{\kappa_1-\kappa_{ab}}+\frac{1}{\kappa_1-\kappa_{cd}}\right] \tag{106b}$$

$$\mathcal{Q}_1(\kappa_1^*)=\frac{id_1e^{-i(\kappa_1^*-\kappa_{cd})d_1}}{(2\kappa_1^*)^2(\kappa_1^*-\kappa_{ab})(\kappa_1^*-\kappa_{cd})} + \frac{e^{-i(\kappa_1^*-\kappa_{cd})d_1}}{(2\kappa_1^*)^2(\kappa_1^*-\kappa_{ab})(\kappa_1^*-\kappa_{cd})} \cdot \left[\frac{1}{\kappa_1^*}+\frac{1}{\kappa_1^*-\kappa_{ab}}+\frac{1}{\kappa_1^*-\kappa_{cd}}\right] \tag{106c}$$

For the anisotropic random medium, integral $\mathcal{I}_{2jklm}^{pqrs}$ involves 256 quantities since p, q, r, and s each has four possibilities of ou, od, eu, and ed. As in the isotropic case, the integrations over vertical space z_2 and z_2^o are readily carried out and the integration over β_z is performed with the residue theorem in the contour integration method. From appendix D, the result for $\mathcal{I}_{2jklm}^{pqrs}$ is

$$\mathcal{I}_{2jklm}^{pqrs}=i\frac{2\delta_{2jklm}\ell_{2\rho'}^2\ell_{2z'}}{\pi\mathcal{L}_2^4}\left[\frac{e^{-i(\kappa_{ps}-\kappa_{rs})d_2}}{(\kappa_{pq}-\kappa_2)^2(\kappa_{pq}-\kappa_2^*)^2(\kappa_{pq}-\kappa_{rs})} + \frac{e^{i(\kappa_{rs}-\kappa_{ps})d_1}}{(\kappa_{rs}-\kappa_2)^2(\kappa_{rs}-\kappa_2^*)^2(\kappa_{rs}-\kappa_{pq})}-\mathcal{P}_2(\kappa_2)-\mathcal{Q}_2(\kappa_2^*)\right] \tag{107a}$$

where square of length $\mathcal{L}_2$ is $\mathcal{L}_2^2=\ell_{2\rho'}^2\sin^2\psi+\ell_{2z'}^2\cos^2\psi$, pole κ_2 is $\kappa_2=\mathcal{L}_2^{-2}\left[-k_{yi}(\ell_{2z'}^2-\ell_{2\rho'}^2)\sin(2\psi)+i\sqrt{(1+4k_{xi}^2\ell_{2\rho'}^2)\mathcal{L}_2^2+4k_{yi}^2\ell_{2\rho'}^2\ell_{2z'}^2}\right]$, and quantities $\mathcal{P}_2(\kappa_2)$ and $\mathcal{Q}_2(\kappa_2^*)$ are determined as follows

$$\mathcal{P}_2(\kappa_2)=\frac{i(d_2-d_1)e^{-i(\kappa_2-\kappa_{rs})d_1}e^{i(\kappa_2-\kappa_{ps})d_2}}{(2i\mathrm{Im}\kappa_2)^2(\kappa_2-\kappa_{pq})(\kappa_2-\kappa_{rs})} + \left[\frac{e^{-i(\kappa_{ps}-\kappa_{rs})d_1}+e^{-i(\kappa_{ps}-\kappa_{rs})d_2}}{(2i\mathrm{Im}\kappa_2)^2(\kappa_2-\kappa_{pq})(\kappa_2-\kappa_{rs})} - \frac{e^{-i(\kappa_2-\kappa_{rs})d_1}e^{i(\kappa_2-\kappa_{ps})d_2}}{(2i\mathrm{Im}\kappa_2)^2(\kappa_2-\kappa_{pq})(\kappa_2-\kappa_{rs})}\right] \cdot \left[\frac{1}{i\mathrm{Im}\kappa_2}+\frac{1}{\kappa_2-\kappa_{pq}}+\frac{1}{\kappa_2-\kappa_{rs}}\right] \tag{107b}$$

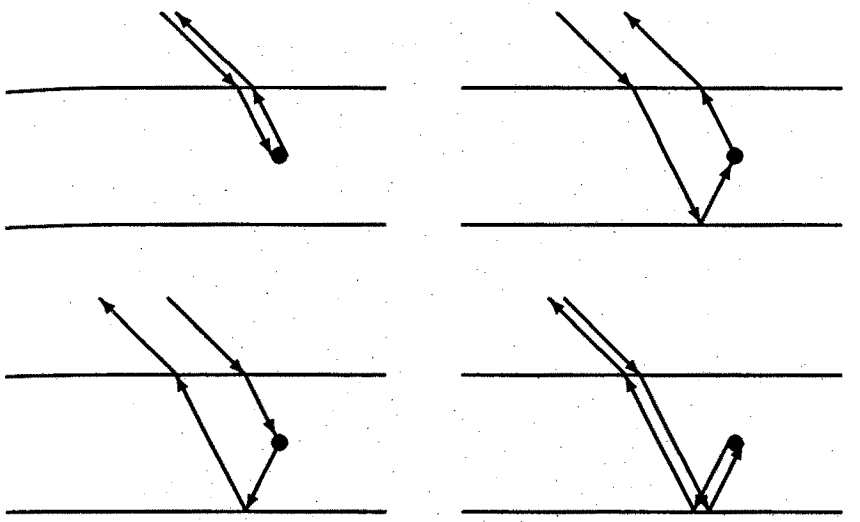

Figure 1.3.4 Wave scattering processes.

$$Q_2(\kappa_2^*) = \frac{i(d_2-d_1)e^{i(\kappa_2^*-\kappa_{pq})d_1}e^{-i(\kappa_2^*-\kappa_{rs})d_2}}{(2i\mathrm{Im}\kappa_2^*)^2(\kappa_2^*-\kappa_{pq})(\kappa_2^*-\kappa_{rs})} + \frac{e^{i(\kappa_2^*-\kappa_{pq})d_1}e^{-i(\kappa_2^*-\kappa_{rs})d_2}}{(2i\mathrm{Im}\kappa_2^*)^2(\kappa_2^*-\kappa_{pq})(\kappa_2^*-\kappa_{rs})} \cdot \left[\frac{1}{i\mathrm{Im}\kappa_2^*} + \frac{1}{\kappa_2^*-\kappa_{pq}} + \frac{1}{\kappa_2^*-\kappa_{rs}}\right] \tag{107c}$$

The polarimetric backscattering coefficients are now obtained by applying results (106) and (107) to (103) and then making use of definition (13). From the observation on the forms of the DGF and mean field coefficients, the scattering coefficients can be expressed conveniently as

$$\sigma_{\mu\tau\nu\kappa} = \pi k_0^4 \sum_{a,b,c,d}^{-1,1} \Psi_{1\mu\tau}^{ab}\Psi_{1\nu\kappa}^{cd*}\mathcal{I}_1^{abcd} + \pi k_0^4 \sum_{p,q,r,s}^{ou,od\ eu,ed} \sum_{j,k,l,m}^{x,y,z} \Psi_{2\mu\tau,jk}^{pq}\Psi_{2\nu\kappa,lm}^{rs*}\mathcal{I}_{2jklm}^{pqrs} \tag{108}$$

where all coefficient Ψ's are given in appendix B and C. The scattering coefficients obtained in (108) is for the scattered field expressed in

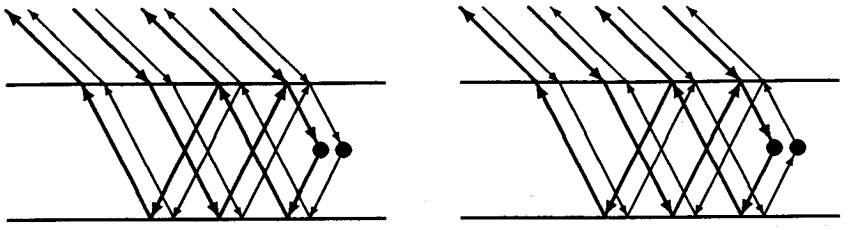

a Same directions b Opposite directions

Figure 1.3.5 Correlations of waves multiply interacting with the boundaries. Thin arrows represent complex conjugates of thick-arrow terms.

the scattered basis. To change to the incident basis, simply take the negative of $\sigma_{hrv\kappa}$ and $\sigma_{vrh\kappa}$. As calculated, the scattering coefficients are composed of 16 terms from the isotropic random medium and 256 terms from the anisotropic random medium. For the isotropic random medium, a scattered field can be an upgoing or a downgoing wave which is excited by an upgoing or a downgoing mean field as depicted in Fig. 1.3.4. Therefore, there are 4 possibilities for the total scattered field and its correlation thus consists of 16 terms. For the anisotropic random medium, a scattered field can be an upgoing or a downgoing wave excited by an upgoing or a downgoing mean field and each wave type can be ordinary or extraordinary. Therefore, there are 16 possibilities for the total scattered field and thus its correlation consists of 256 terms. Furthermore, all multiple interactions between the waves and the boundaries are accounted for and all correlations of waves with same and different propagation directions are included. For instances, Fig. 1.3.5a represents a correlation of waves multiply interacting with the boundaries and propagating in the same directions and Fig. 1.3.5b illustrates a correlation of waves propagating in opposite directions.

In this section, the random medium model is formulated and the polarimetric backscattering coefficients are obtained under the distorted Born approximation with the strong permittivity fluctuation theory. In the next section, the model is applied to study the polarimetric backscattering properties from layer random media. Consideration is also given to the polarization signatures of the media and their relations to the corresponding covariance matrices are explained.

1.4 Results and Discussion

a. Two-layer Configuration

For geophysical media with a two-layer configuration, the three-layer model is applied with the top scattering layer removed by setting its thickness and variances to zero. The reduced model is used to investigate the polarimetric backscattering directly from an uncovered anisotropic random medium such as sea ice. Consider an electromagnetic wave of 9 GHz incident on a random medium composed of an ice background with permittivity $\epsilon_{2b} = (3.15 + i0.002)\epsilon_0$ and a 3.0%-volume fraction of vertically oriented ($\psi = 0$) brine inclusions with permittivity $\epsilon_{2s} = (38 + i41)\epsilon_0$ and correlation length $\ell_{2\rho'} = 0.5$ mm and $\ell_{2z'} = 1.5$ mm for which the strong fluctuation theory (SFT) gives the variances of $\delta_{2\rho'} = 1.48$, $\delta_{2z'} = 14.9$, and $\delta_{2c'} = 4.57 - i1.08$ and the uniaxial effective permittivity tensor with $\epsilon_{2\rho'} = (3.37 + i0.034)\epsilon_0$ and $\epsilon_{2z'} = (3.85 + i0.374)\epsilon_0$ as shown in Fig. 1.4.1. The thickness of the random medium is 1.7 m and the permittivity of the underlying sea water is $\epsilon_3 = (45.0 + i40.0)\epsilon_0$. To point out the anisotropy effect on the polarimetric backscattering, a comparison is made with an isotropic random medium with the same parameters except $\ell_{2\rho'} = \ell_{2z'} = 0.5$ mm for which the SFT yields $\delta_{2\rho'} = \delta_{2z'} = \delta_{2c'} = 2.53$ and $\epsilon_{2r'} = \epsilon_{2z'} = (3.43 + i0.047)\epsilon_0$. For both the untilted anisotropic and the isotropic random media, cross term σ_{hv}, σ_{hhhv}, and σ_{hvvv} are zero under the first-order distorted Born approximation rendering the covariance matrix of the form

$$\overline{\overline{C}} = \begin{bmatrix} \sigma_{hh} & 0 & \sigma_{hhvv} \\ 0 & 0 & 0 \\ \sigma^*_{hhvv} & 0 & \sigma_{vv} \end{bmatrix} \quad \text{or} \quad \overline{\overline{C}} = \sigma \begin{bmatrix} 1 & 0 & \rho\sqrt{\gamma} \\ 0 & 0 & 0 \\ \rho^*\sqrt{\gamma} & 0 & \gamma \end{bmatrix} \tag{109}$$

Conventional backscattering coefficient σ_{hh} and σ_{vv} are plotted as a function of incident angle in Fig. 1.4.2 for the two-layer untilted anisotropic (a) and the isotropic (b) cases. As observed from Fig. 1.4.2, σ_{vv} crosses over σ_{hh} for the anisotropic case whereas, for the isotropic case, σ_{vv} is higher than σ_{hh} over the range of incident angles under consideration. The distinction of the conventional backscattering coefficients, σ_{vv} and σ_{hh}, associated with the two different random media is, however, not as obvious as that of the polarimetric correlation coefficient ρ as indicated in Fig. 1.4.3 where the untilted anisotropic random medium manifests its characteristics in ρ with magnitude and

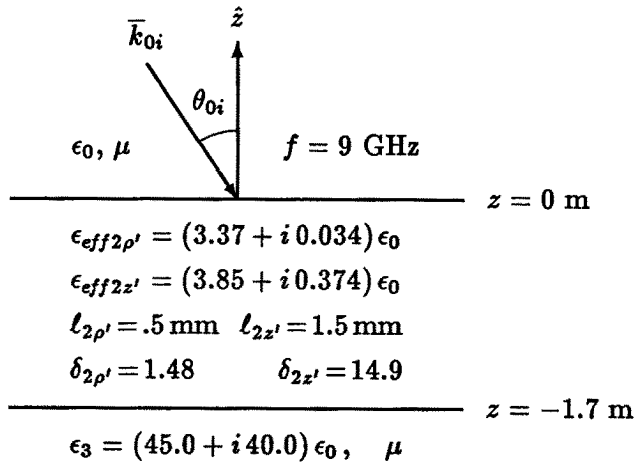

Figure 1.4.1 Parameters for the two-layer configuration.

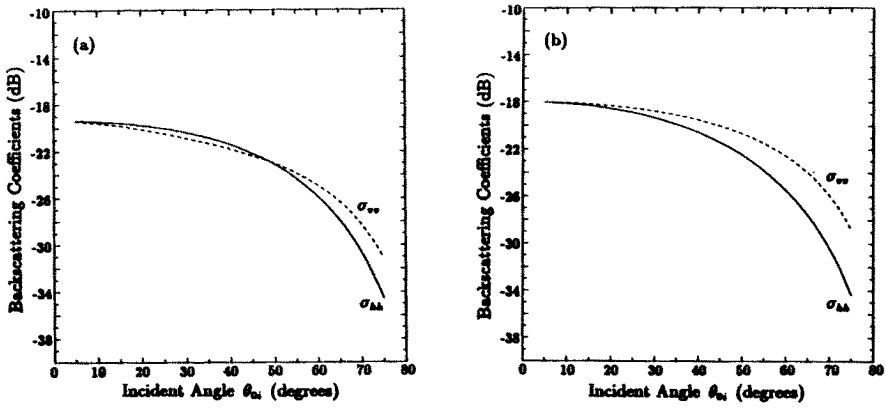

Figure 1.4.2 Conventional backscattering coefficients: (a) untilted anisotropic random medium, (b) isotropic random medium.

phase inversely related to the incident angle while the isotropic random medium ρ simply has the value of approximately 1.0 over the range of incident angles. These results can be explained based on the physical characteristics of the random media. In the anisotropic random medium, the effective complex wave vectors of the ordinary and the extraordinary waves are different; therefore, the h-polarized wave

corresponding to the ordinary wave and the v-polarized wave corresponding to the extraordinary wave have different propagation velocities and attenuation rates which result in the separation of the scattering centers of the two wave types. At normal incident angle, there is no distinction between the h and the v waves for the untilted random medium, the two waves are correlated, and thus the correlation coefficient ρ has the value of unity. As the incident angle is increased, the two waves become increasingly distinctive and less correlated; thus, the correlation coefficient takes on a complex value with decreased magnitude and phase. For the isotropic random medium, the distinction between the h and the v waves is only due to the boundary effect and the good correlation of two wave types leads to the correlation coefficient of value close to unity.

To illustrate the effect of the scatterers tilted in a preferred alignment direction, consider now the anisotropic random medium as described in the previous example but with non-zero tilt angle. For instance, let $\psi = 10°, 20°$ and $\phi_{0i} = 0°$. In this case, the correlation coefficient ρ also contains information about the tilting as shown in Fig. 1.4.3. It is observed that the maximum magnitude of ρ is at normal incidence in the untilted case and moves to a larger incident angle as the tilted angle becomes larger. Also, the phase of ρ does not change sign for the case of $\psi = 0°$ whereas, in the tilted cases, the phase of ρ changes sign at the incident angle where the magnitude of ρ is maximum. Furthermore, it should be noted that the tilting results in non-zero cross terms and the corresponding covariance matrix become fully populated. As shown in this subsection, the covariance matrix describes the fully polarimetric scattering property of the remotely sensed media and thus can be used for the identification and the classification of terrain types.

b. Three-layer Configuration

To identify the effect of the covering top layer on the backscattering from the lower layer, the components of covariance matrices are compared between a two-layer configuration such as the bare sea ice in section 1.4a and a three-layer configuration such as the sea ice with snow cover. In Fig. 1.4.4, the covering dry-snow layer is a low-loss isotropic random medium of thickness $d_1 = 0.1$ m composed of an air background with permittivity $\epsilon_{1b} = \epsilon_0$ and a 20%-volume fraction of ice particles with permittivity $\epsilon_{1s} = (3.15 + i0.002)\epsilon_0$ and correlation

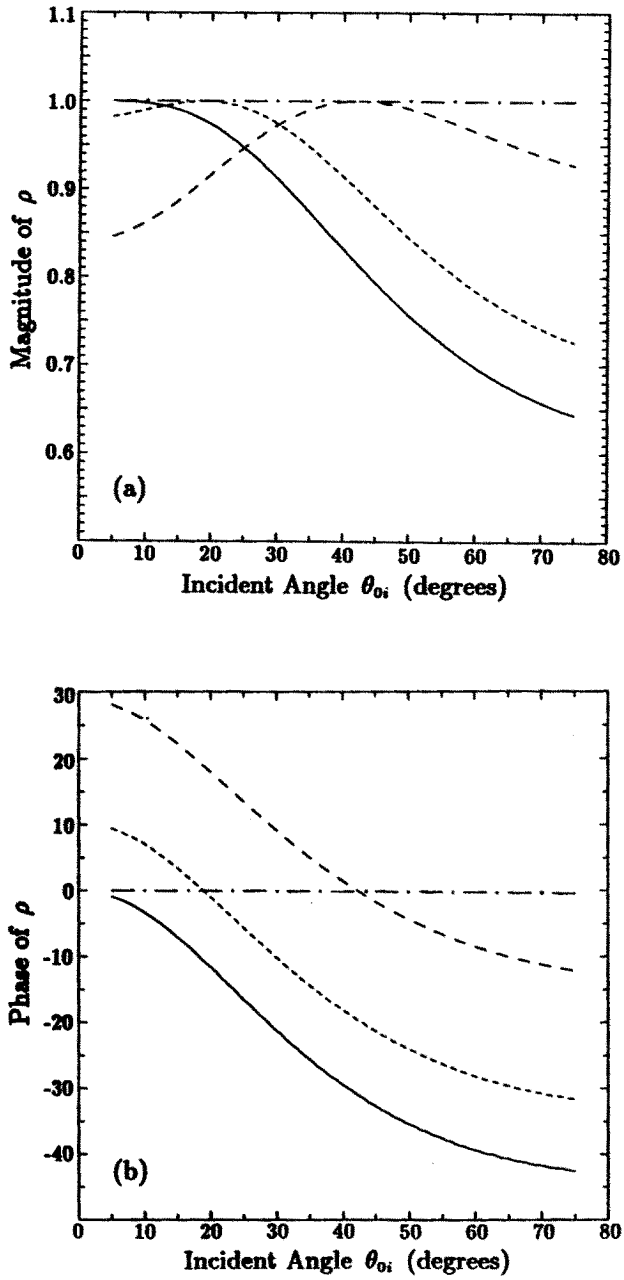

Figure 1.4.3 Correlation coefficients ρ: (a) magnitude, (b) phase. Dash-dot curves are for the isotropic, continuous for the untilted, short-dash for the 10°-tilted, and long-dash for the 20°-tilted random media.

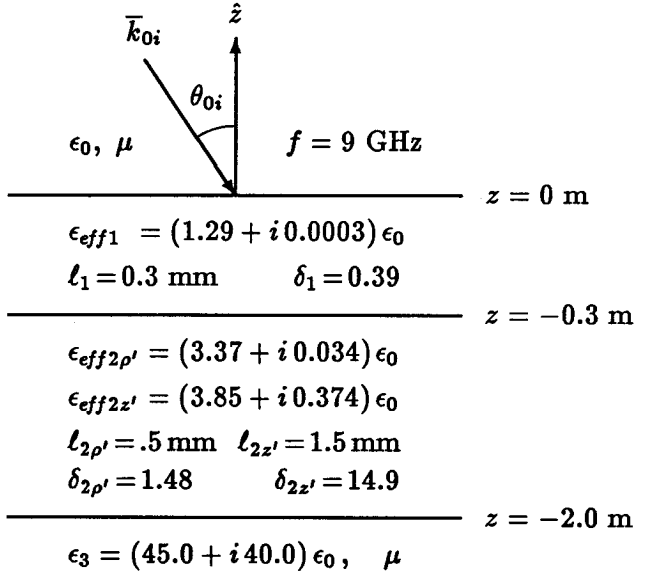

Figure 1.4.4 Parameters for the three-layer configuration.

length $\ell_1 = 0.3$ mm for which the SFT gives the variance of $\delta_1 = 0.39$ and the isotropic effective permittivity of $\epsilon_{eff1} = (1.29 + i0.0003)\epsilon_0$; the middle and the underlying regions are, respectively, the sea ice with vertical brine inclusion over the sea water with the same physical parameters as in the two-layer configuration.

Displayed in Fig. 1.4.5 are the plots of σ_{hh} and σ_{vv} as a function of incident angle for the two-layer and the three-layer configurations. The comparison shows that both σ_{hh} and σ_{vv} are enhanced due to the effect of the dry-snow cover whose ice particles introduce more backscattering. Moreover, the boundary effect is recognized in form of the oscillations on σ_{hh} and σ_{vv}. The oscillations can also be seen clearly on the phase of the correlation coefficient ρ in Fig. 1.4.6b. As compared to the two-layer case, the absolute value of the phase of ρ for the three layer is smaller over the range of incident angle. Physically, this is due to the isotropic covering layer, which characteristically exhibits its isotropy in ρ with a small phase, partially masks the scattering effect of the lower anisotropic random medium. The magnitude of ρ, however, exhibits very weak oscillations while clearly retaining

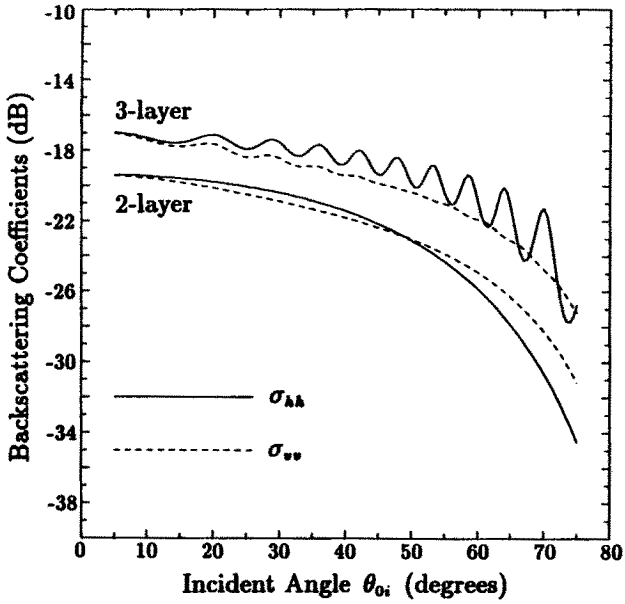

Figure 1.4.5 Conventional backscattering coefficients for the two-layer and three-layer configurations.

the almost same characteristics as observed directly from the two-layer configuration as seen in Fig. 1.4.6b. Thus, the correlation coefficient ρ can carry information from both the covering low-loss isotropic layer and the lower tilted anisotropic layer in a rather distinctive manner. If the top layer is more lossy, both σ_{hh} and σ_{vv} can be diminished and the boundary-effect oscillations can be depressed. As illustrated, the three-layer model can account for the effect of the top scattering layer covering a geophysical medium whose characteristics can be recognized from the polarimetric covariance matrix.

c. Polarization Signatures

For given polarizations of the transmitter and the receiver, (11) can be used to synthesize the scattering coefficient which is similar to the polarization signature defined in [22]. When orientation angle $\alpha_i = \alpha_r = \alpha_c$ and $\beta_i = \beta_r = \beta_c$, the copolarized signature can be displayed with a three-dimensional plot with the vertical axis for the normalized signature and the horizontal plane for α_c and β_c. In

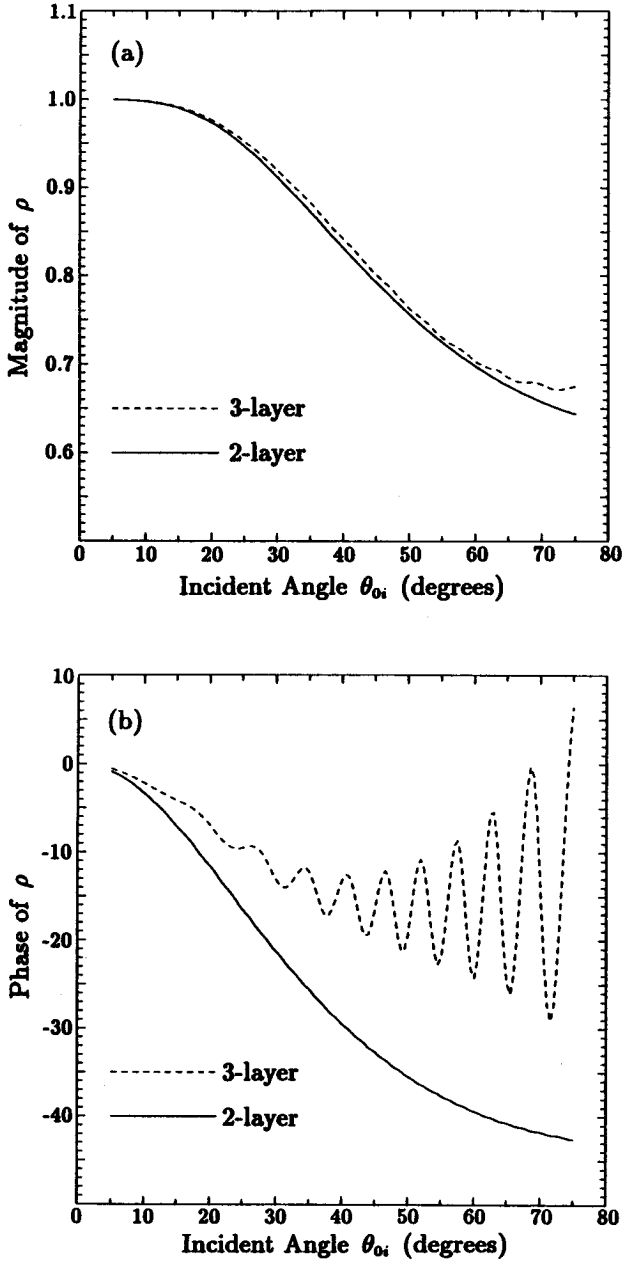

Figure 1.4.6 Correlation coefficients ρ: (a) magnitude, (b) phase. Continuous curves are for the two-layer and dash curves are for the three-layer configurations.

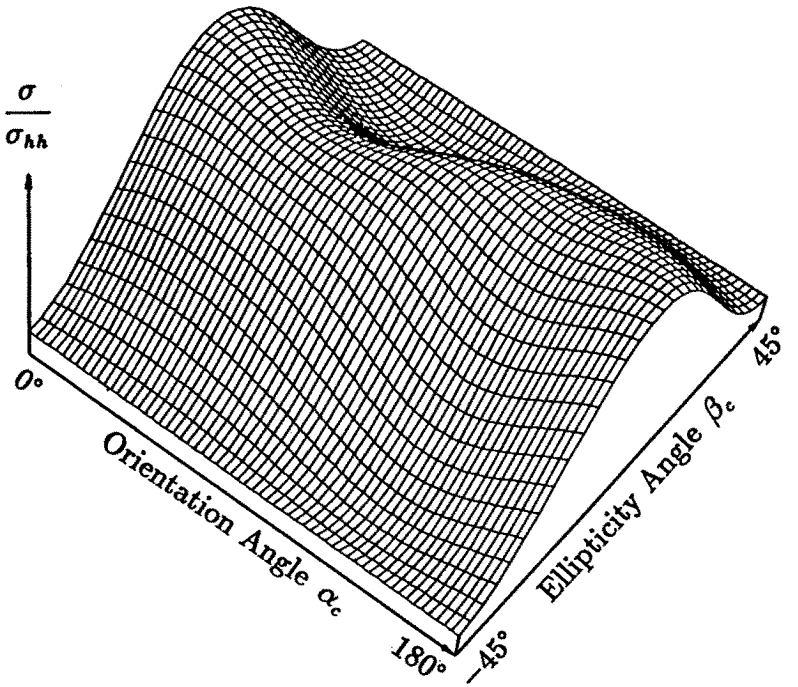

Figure 1.4.7 Copolarized signature normalized to σ_{hh} for the two-layer configuration at $\theta_{0i} = 40°$.

this subsection, the copolarized signature is shown for the bare sea ice and compared with that of the snow-covered sea ice. The forms of the displayed signatures and their relations to the corresponding covariance matrices will be explained.

Consider the 9-GHz wave incident at $\theta_{0i} = 40°$ on the sea ice with vertical brine inclusions. The corresponding covariance matrix is

$$\overline{\overline{C}} = 7.12 \times 10^{-3} \begin{bmatrix} 1 & 0 & (0.83\ \angle -29.5°)\sqrt{\gamma} \\ 0 & 0 & 0 \\ (0.83\ \angle +29.5°)\sqrt{\gamma} & 0 & \gamma = 0.915 \end{bmatrix} \quad (110)$$

The copolarized signature is shown in Fig. 1.4.7 where the variation is seen in both α_c and β_c. To illustrate the variation in α_c, the copolarized signature normalized to σ_{hh} for linear polarization is plotted

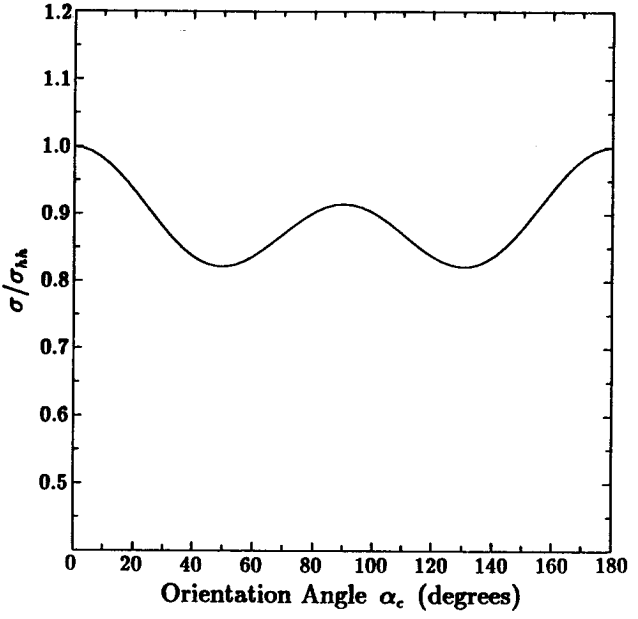

Figure 1.4.8 Linearly copolarized signature normalized to σ_{hh} for the two-layer configuration at $\theta_{0i} = 40°$.

in Fig. 1.4.8 where the normalized signature at $\alpha = 90°$ has the value of 0.915 which is the ratio $\gamma = \sigma_{vv}/\sigma_{hh}$ in covariance matrix (110) and the undulation also depends on the correlation coefficient ρ. For the variation in β_c, the signature at a fixed value of α_c increases to a maximum and then decreases. The variation over the polarization plane (α_c, β_c) makes the signature look like being distorted. To describe this distortion, a "signature distortion track" is defined as the plot of β_c at which the signature is maximum as a function of α_c such that $\partial\sigma(\alpha_c, \beta_c)/\partial\beta_c = 0$. This plot tracks the locations of the local maxima of the copolarized signature over the polarization plane. The result of the signature distortion track for the bare sea ice is shown in Fig. 1.4.9 which indicates that a maximum copolarized scattering coefficient can be obtained with an h $(\alpha_c = 0°, 180°)$ or v $(\alpha_c = 90°)$ polarization and with an elliptical polarization for other orientation angles. To explain the cause of the distortion, the phase of ρ in the covariance matrix (110) is artificially set to zero which consequently gives the signature in Fig. 1.4.10a where the distortion disappears as seen in Fig. 1.4.10b. Thus, the distortion is due to the non-zero phase of ρ which

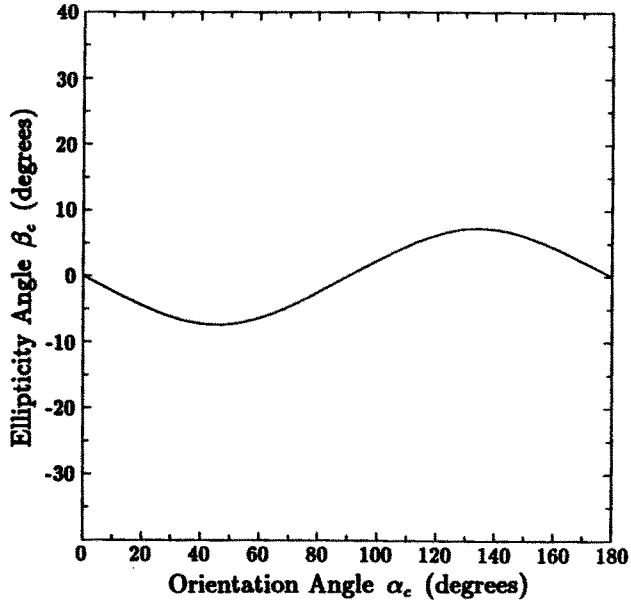

Figure 1.4.9 Signature distortion track of the two-layer configuration.

can come from the anisotropy of the random medium as discussed in subsection 1.4a. Furthermore, the distortion track is symmetric about the v polarization $(\alpha = 90°, \beta = 0°)$ due to the azimuthal symmetry of the untilted anisotropic random medium. Consider an azimuthally symmetric random medium whose polarimetric backscattering properties are characterized with a covariance matrix of the form [45]

$$\overline{\overline{C}} = \sigma_{hh} \begin{bmatrix} 1 & 0 & \rho\sqrt{\gamma} \\ 0 & e & 0 \\ \rho^*\sqrt{\gamma} & 0 & \gamma \end{bmatrix} \tag{111}$$

which is more general than (109). In this case, the distortion track equation is

$$\partial\sigma/\partial\beta_c = \sigma_{hh} \sin 2\beta_c \left[(\gamma - 1)\cos 2\alpha_c - (\gamma + 1 - 4e)\cos^2 2\alpha_c \cos 2\beta_c - 2\sqrt{\gamma}\mathrm{Re}\rho \cos 2\beta_c(1+\sin^2 2\alpha_c)\right] + 2\sigma_{hh}\sqrt{\gamma}\mathrm{Im}\rho \sin 2\alpha_c \cos 4\beta_c = 0 \tag{112}$$

from which the properties of the signature distortion track can be deduced. If $\mathrm{Im}(\rho) = 0$, (112) has solution $\beta_c = 0$ for any given orientation angle α_c and the track is just the straight line at β_c of

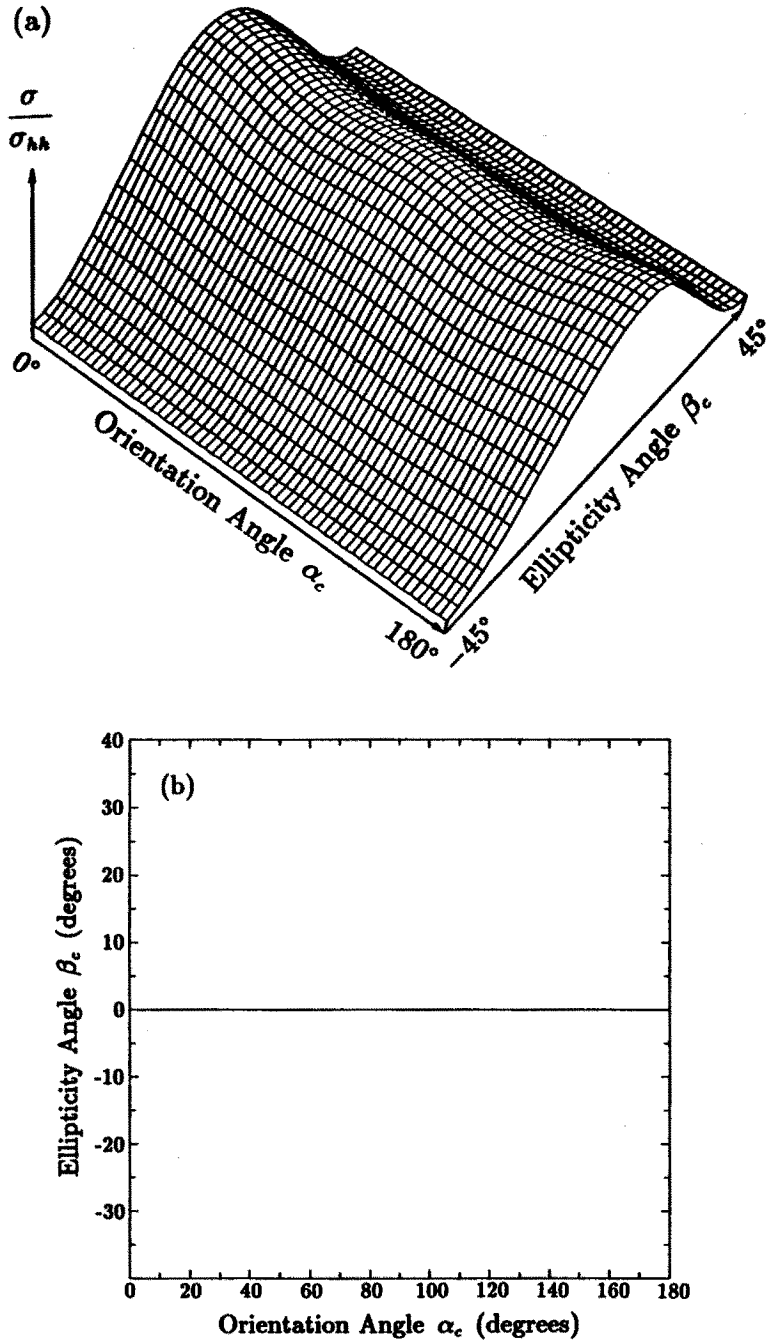

Figure 1.4.10 For the covariance matrix (110) with the phase of ρ set to zero: (a) Copolarized signature normalized to σ_{hh}, (b) Signature distortion track.

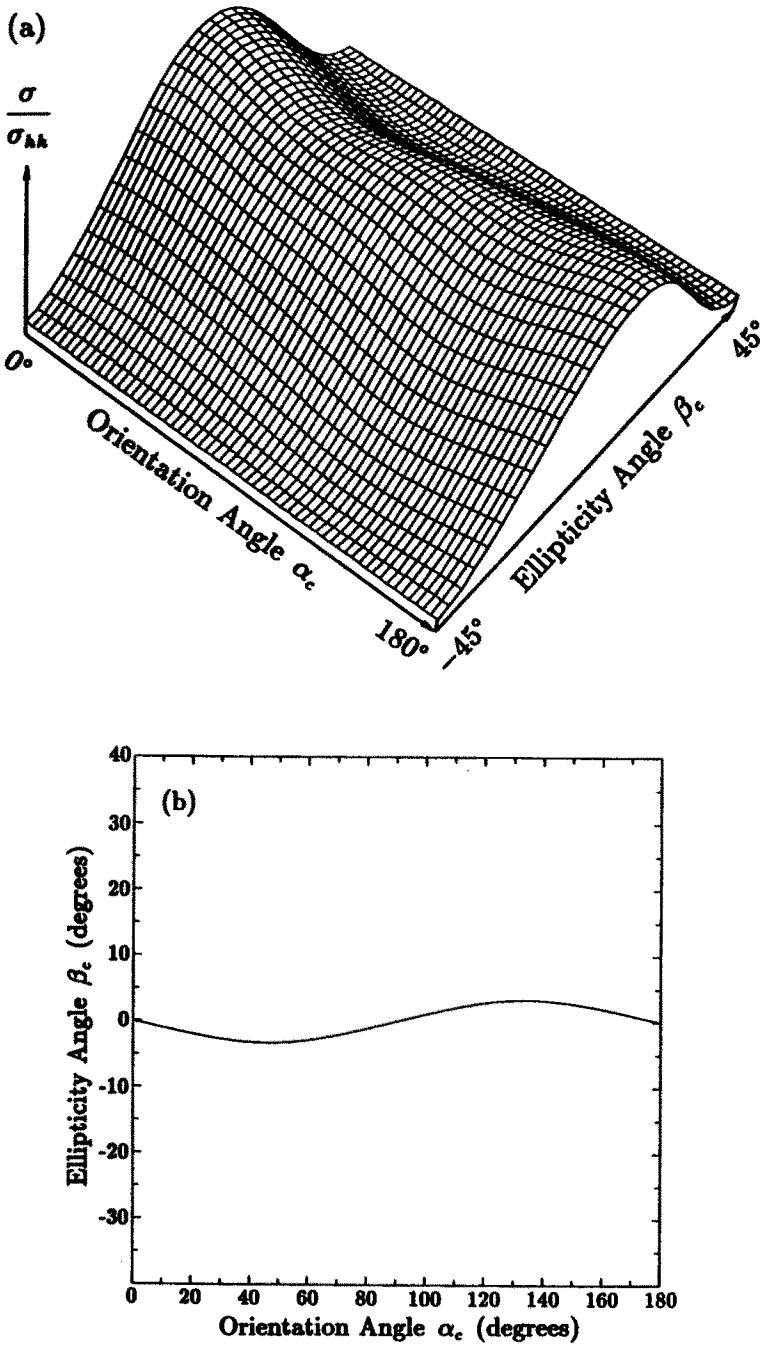

Figure 1.4.11 For the three-layer configuration: (a) Copolarized signature normalized to σ_{hh}, (b) Signature distortion track.

zero value signifying the disappearance of the distortion. Also, the invariance of (112) under the change of α_c and β_c respectively to $(180° - \alpha_c)$ and $-\beta_c$ implies the symmetry about the v polarization $(\alpha_c = 90°, \beta_c = 0°)$. When $e = 0$ as in (109), these properties of the distortion track still remain.

The pedestal is also observed in Fig. 1.4.6. To explain the existence of the pedestal, the pedestal height is calculated from (11) by setting $\beta_c = \pm 45°$ (circular polarizations) for the case of (111)

$$\sigma(\beta_c = \pm 45°)/\sigma_{hh} = e + \frac{1}{4}[(\gamma + 1) - 2\sqrt{\gamma}\mathrm{Re}\rho] \tag{113}$$

Obviously from (113), the pedestal height is composed of two terms: the first term e can come from the depolarization due to multiple scattering [45] and the second term can come from the anisotropy of the random medium. For the untilted anisotropic random medium under consideration, the pedestal height is therefore non-zero even thought the cross term e is not accounted for. In this case, the pedestal is due to the anisotropy and the boundary effects.

For the snow covered sea ice with the three-layer configuration in Fig. 1.4.4, the covariance matrix at the incident angle of $\theta_{0i} = 40°$ is

$$\overline{\overline{C}} = 1.34 \times 10^{-2} \begin{bmatrix} 1 & 0 & (0.84\ \angle -13.2°)\sqrt{\gamma} \\ 0 & 0 & 0 \\ (0.84\ \angle +13.2°)\sqrt{\gamma} & 0 & \gamma = 0.85 \end{bmatrix} \tag{114}$$

The corresponding copolarized signature and the signature distortion track are displayed in Fig. 1.4.11. Compared to the two-layer case, the three-layer signature is less distorted and the pedestal height is lower. This is due to the masking effect of the isotropic covering layer which renders the anisotropic characteristics of the lower scattering layer less pronounced.

The polarization signatures of the two-layer and the three-layer random medium configurations have been shown in this subsection. The forms of the copolarized signatures and the pedestal heights are explained with the components of the covariance matrices from which the polarimetric scattering properties are readily recognized.

1.5 Summary

In this chapter, the fully polarimetric backscattering coefficients have been obtained with the layer random medium model. The top layer is modelled as an isotropic random medium, the middle layer as an anisotropic random medium, and the underlying layer as a homogeneous medium. The strong fluctuation theory is used to calculated the effective permittivities of the scattering layers and the distorted Born approximation is applied to derive the scattered fields. The dyadic Green's functions are used in the calculations and the backscattering processes are explained. The model can be applied to the remote sensing of both bare and covered geophysical media as illustrated for the case of bare and snow covered sea ice. The physical information conveyed in the elements of the covariance matrices are discussed especially for the correlation coefficient ρ. The copolarization signatures for the layer random media are obtained with the Mueller matrices and explained with the scattering coefficients contained in the covariance matrices. Since the fully polarimetric scattering coefficients convey more information about the remotely sensed media as compared to the conventional scattering coefficients, the polarimetry provides a better means for the identification and classification of the geophysical media.

Appendix A: Transmission and Reflection Coefficients

The transmission and reflection coefficients are obtained by matching the boundary conditions at the interfaces where the tangential components of the electric and magnetic fields are continuous. The boundary conditions for the zeroth-order mean fields can be written explicitly as

$$\left.\begin{aligned} \hat{z} \times \langle \overline{F}_0(\overline{r}) \rangle &= \hat{z} \times \langle \overline{F}_1(\overline{r}) \rangle \\ \hat{z} \times \nabla \times \langle \overline{F}_0(\overline{r}) \rangle &= \hat{z} \times \nabla \times \langle \overline{F}_1(\overline{r}) \rangle \end{aligned}\right\} \text{ at } z = 0 \qquad \text{(A.1a)}$$

$$\left.\begin{aligned} \hat{z} \times \langle \overline{F}_1(\overline{r}) \rangle &= \hat{z} \times \langle \overline{F}_2(\overline{r}) \rangle \\ \hat{z} \times \nabla \times \langle \overline{F}_1(\overline{r}) \rangle &= \hat{z} \times \nabla \times \langle \overline{F}_2(\overline{r}) \rangle \end{aligned}\right\} \text{ at } z = -d_1 \qquad \text{(A.1b)}$$

$$\left.\begin{aligned} \hat{z} \times \langle \overline{F}_2(\overline{r}) \rangle &= \hat{z} \times \langle \overline{F}_3(\overline{r}) \rangle \\ \hat{z} \times \nabla \times \langle \overline{F}_2(\overline{r}) \rangle &= \hat{z} \times \nabla \times \langle \overline{F}_3(\overline{r}) \rangle \end{aligned}\right\} \text{ at } z = -d_2 \qquad \text{(A.1c)}$$

The boundary conditions are satisfied by coefficients composed of

half-space Fresnel coefficients and phase factors as expressed in (85). The phase factors in the exponents account for the wave propagation to the boundaries. The Fresnel reflection and transmission coefficients have been derived as shown in [36]. For the coordinate systems defined in this chapter, the Fresnel coefficients are given as follows:

At boundary $z=0$ between the isotropic media of region 0 and region 1

$$R_{01hh} = -R_{10hh} = \frac{k_{0z} - k_{1z}}{k_{0z} + k_{1z}} \tag{A.2a}$$

$$R_{01vv} = -R_{10vv} = \frac{k_1^2 k_{0z} - k_0^2 k_{1z}}{k_1^2 k_{0z} + k_0^2 k_{1z}} \tag{A.2b}$$

$$T_{01hh} = \frac{2k_{0z}}{k_{0z} + k_{1z}}, \quad T_{10hh} = \frac{2k_{1z}}{k_{1z} + k_{0z}} \tag{A.2c}$$

$$T_{01vv} = \frac{2k_0 k_1 k_{0z}}{k_1^2 k_{0z} + k_0^2 k_{1z}}, \quad T_{10vv} = \frac{2k_1 k_0 k_{1z}}{k_0^2 k_{1z} + k_1^2 k_{0z}} \tag{A.2d}$$

At boundary $z=-d_1$ between isotropic region 1 and anisotropic region 2

$$R_{12hh} = -1 + \frac{k_2^2 k_x T_{12he}}{k_\rho U_d} \sin\psi + \frac{T_{12ho}}{k_\rho G_d}\left(k_\rho^2 \cos\psi + k_y k_{2z}^o \sin\psi\right) \tag{A.3a}$$

$$R_{12hv} = \frac{k_1 k_x k_{2z}^o T_{12ho}}{k_\rho k_{1z} G_d} \sin\psi + \frac{k_1 T_{12he}}{k_\rho k_{1z} U_d}\left(k_\rho^2 k_{2z}^{ed} \cos\psi - k_y k_{2z}^{o2} \sin\psi\right) \tag{A.3b}$$

$$R_{12vh} = \frac{k_2^2 k_x T_{12ve}}{k_\rho U_d} \sin\psi + \frac{T_{12vo}}{k_\rho G_d}\left(k_\rho^2 \cos\psi + k_y k_{2z}^o \sin\psi\right) \tag{A.3c}$$

$$R_{12vv} = 1 + \frac{k_1 k_x k_{2z}^o T_{12vo}}{k_\rho k_{1z} G_d} \sin\psi + \frac{k_1 T_{12ve}}{k_\rho k_{1z} U_d}\left(k_\rho^2 k_{2z}^{ed} \cos\psi - k_y k_{2z}^{o2} \sin\psi\right) \tag{A.3d}$$

$$R_{21oo} = \frac{G_d E_e (k_{2z}^o - k_{1z})}{G_u D_d (k_{2z}^o + k_{1z})} \tag{A.3e}$$

$$R_{21oe} = \frac{2k_x k_{2z}^o U_d}{G_u D_e}(k_{1z} - k_{2z}^o) \cdot (k_y \sin\psi - k_{1z}\cos\psi)\sin\psi \tag{A.3f}$$

$$R_{21eo} = \frac{k_2^2 k_x G_d}{U_u D_e}\left(k_{2z}^{ed} - k_{2z}^{eu}\right)(k_{1z} - k_{2z}^o) \cdot (k_y \sin\psi + k_{1z}\cos\psi)\sin\psi \tag{A.3g}$$

$$R_{21ee} = -\frac{U_d I_e}{U_u D_e} \tag{A.3h}$$

$$T_{12ho} = \frac{2k_{1z}G_d}{k_\rho D_e(k_{1z} + k_{2z}^o)}\left[k_\rho^2\left(k_2^2 k_{1z} - k_1^2 k_{2z}^{ed}\right)\cos\psi + k_y\left(k_1^2 k_{2z}^{o2} - k_2^2 k_{1z} k_{2z}^{ed}\right)\sin\psi\right] \tag{A.3i}$$

$$T_{12he} = \frac{2k_x k_{1z} U_d}{k_\rho D_e}\left(k_\rho^2 + k_{1z}k_{2z}^o\right)\sin\psi \tag{A.3j}$$

$$T_{12vo} = -\frac{2k_1 k_2^2 k_x k_{1z} G_d (k_{1z} - k_{2z}^{ed})}{k_\rho D_e(k_{1z} + k_{2z}^o)}\sin\psi \tag{A.3k}$$

$$T_{12ve} = \frac{2k_1 U_d}{k_\rho D_e}\left(k_\rho^2 k_{1z}\cos\psi + k_y k_{1z} k_{2z}^o \sin\psi\right) \tag{A.3l}$$

$$T_{21oh} = \frac{k_2^2 k_x R_{21oe}}{k_\rho U_d}\sin\psi + \frac{1}{k_\rho G_u}\left(k_\rho^2\cos\psi - k_y k_{2z}^o \sin\psi\right) + \frac{R_{21oo}}{k_\rho G_d}\left(k_\rho^2\cos\psi + k_y k_{2z}^o \sin\psi\right) \tag{A.3m}$$

$$T_{21ov} = \frac{k_1 k_x k_{2z}^o R_{21oo}}{k_\rho k_{1z} G_d}\sin\psi - \frac{k_1 k_x k_{2z}^o}{k_\rho k_{1z} G_u}\sin\psi - \frac{k_1 R_{21oe}}{k_\rho k_{1z} U_d}\left(k_y k_{2z}^{o2}\sin\psi - k_\rho^2 k_{2z}^{ed}\cos\psi\right) \tag{A.3n}$$

$$T_{21eh} = \frac{k_2^2 k_x}{k_\rho U_u}\sin\psi + \frac{k_2^2 k_x R_{21ee}}{k_\rho U_d}\sin\psi + \frac{R_{21eo}}{k_\rho G_d}\left(k_\rho^2\cos\psi + k_y k_{2z}^o \sin\psi\right) \tag{A.3o}$$

$$T_{21ev} = \frac{k_1 k_x k_{2z}^o R_{21eo}}{k_\rho k_{1z} G_d}\sin\psi$$

$$- \frac{k_1}{k_\rho k_{1z} U_u} \left(k_y k_{2z}^{o2} \sin\psi - k_\rho^2 k_{2z}^{eu} \cos\psi\right)$$

$$- \frac{k_1 R_{21ee}}{k_\rho k_{1z} U_d} \left(k_y k_{2z}^{o2} \sin\psi - k_\rho^2 k_{2z}^{ed} \cos\psi\right) \tag{A.3p}$$

At boundary $z=-d_2$ between anisotropic region 2 and isotropic region 3

$$R_{23oo} = \frac{G_u G_e (k_{2z}^o - k_{3z})}{G_d F_e (k_{2z}^o + k_{3z})} \tag{A.4a}$$

$$R_{23oe} = \frac{2 k_x k_{2z}^o U_u}{G_d F_e} (k_{2z}^o - k_{3z}) \cdot (k_y \sin\psi + k_{3z} \cos\psi) \sin\psi \tag{A.4b}$$

$$R_{23eo} = \frac{k_2^2 k_x G_u}{U_d F_e} \left(k_{2z}^{ed} - k_{2z}^{eu}\right) (k_{2z}^o - k_{3z}) \cdot (k_y \sin\psi - k_{3z} \cos\psi) \sin\psi \tag{A.4c}$$

$$R_{23ee} = -\frac{U_u H_e}{U_d F_e} \tag{A.4d}$$

$$T_{23oh} = \frac{k_2^2 k_x R_{23oe}}{k_\rho U_u} \sin\psi + \frac{1}{k_\rho G_d} \left(k_\rho^2 \cos\psi + k_y k_{2z}^o \sin\psi\right) + \frac{R_{23oo}}{k_\rho G_u} \left(k_\rho^2 \cos\psi - k_y k_{2z}^o \sin\psi\right) \tag{A.4e}$$

$$T_{23ov} = \frac{k_3 k_x k_{2z}^o R_{23oo}}{k_\rho k_{3z} G_u} \sin\psi - \frac{k_3 k_x k_{2z}^o}{k_\rho k_{3z} G_d} \sin\psi + \frac{k_3 R_{23oe}}{k_\rho k_{3z} U_u} \left(k_y k_{2z}^{o2} \sin\psi - k_\rho^2 k_{2z}^{eu} \cos\psi\right) \tag{A.4f}$$

$$T_{23eh} = \frac{k_2^2 k_x R_{23ee}}{k_\rho U_u} \sin\psi + \frac{k_2^2 k_x}{k_\rho U_d} \sin\psi + \frac{R_{23eo}}{k_\rho G_u} \left(k_\rho^2 \cos\psi - k_y k_{2z}^o \sin\psi\right) \tag{A.4g}$$

$$T_{23ev} = \frac{k_3 k_x k_{2z}^o R_{23eo}}{k_\rho k_{3z} G_u} \sin\psi + \frac{k_3 R_{23ee}}{k_\rho k_{3z} U_u} \left(k_y k_{2z}^{o2} \sin\psi - k_\rho^2 k_{2z}^{eu} \cos\psi\right)$$

$$+\frac{k_3}{k_\rho k_{3z} U_d}\left(k_y k_{2z}^{o2}\sin\psi - k_\rho^2 k_{2z}^{ed}\cos\psi\right) \tag{A.4h}$$

In the above expressions, the following definitions have been used

$$G_d \equiv \sqrt{k_x^2 + \left(k_y\cos\psi + k_{2z}^o\sin\psi\right)^2} \tag{A.5a}$$

$$G_u \equiv \sqrt{k_x^2 + \left(k_y\cos\psi - k_{2z}^o\sin\psi\right)^2} \tag{A.5b}$$

$$U_d \equiv \left\{\frac{\epsilon_{eff2\rho'}}{\epsilon_{eff2\rho'} - \epsilon_{eff2z'}}\left(k_\rho^2 + k_{2z}^{ed2} - k_2^2\right)\left[k_\rho^2 + k_{2z}^{ed2} - k_2^2\left(1 + \frac{\epsilon_{eff2z'}}{\epsilon_{eff2\rho'}}\right)\right]\right\}^{\frac{1}{2}} \tag{A.5c}$$

$$U_u \equiv \left\{\frac{\epsilon_{eff2\rho'}}{\epsilon_{eff2\rho'} - \epsilon_{eff2z'}}\left(k_\rho^2 + k_{2z}^{eu2} - k_2^2\right)\left[k_\rho^2 + k_{2z}^{eu2} - k_2^2\left(1 + \frac{\epsilon_{eff2z'}}{\epsilon_{eff2\rho'}}\right)\right]\right\}^{\frac{1}{2}} \tag{A.5d}$$

$$\begin{aligned} D_e \equiv\ & k_\rho^2\left(k_2^2 k_{1z} - k_1^2 k_{2z}^{ed}\right)\cos^2\psi \\ & + \left[k_2^2\left(k_{1z} - k_{2z}^{ed}\right)\left(k_x^2 + k_{1z}k_{2z}^o\right) + k_y^2 k_{2z}^o\left(k_2^2 - k_1^2\right)\right]\sin^2\psi \\ & + k_y\left(k_{1z} + k_{2z}^o\right)\left(k_{2z}^o - k_{2z}^{ed}\right)\left(k_\rho^2 + k_{1z}k_{2z}^o\right)\cos\psi\sin\psi \end{aligned} \tag{A.5e}$$

$$\begin{aligned} E_e \equiv\ & k_\rho^2\left(k_2^2 k_{1z} - k_1^2 k_{2z}^{ed}\right)\cos^2\psi \\ & + \left[k_2^2\left(k_{1z} - k_{2z}^{ed}\right)\left(k_x^2 - k_{1z}k_{2z}^o\right) - k_y^2 k_{2z}^o\left(k_2^2 - k_1^2\right)\right]\sin^2\psi \\ & - k_y\left(k_{1z} - k_{2z}^o\right)\left(k_{2z}^o + k_{2z}^{ed}\right)\left(k_\rho^2 - k_{1z}k_{2z}^o\right)\cos\psi\sin\psi \end{aligned} \tag{A.5f}$$

$$\begin{aligned} I_e \equiv\ & k_\rho^2\left(k_2^2 k_{1z} - k_1^2 k_{2z}^{eu}\right)\cos^2\psi \\ & + \left[k_2^2\left(k_{1z} - k_{2z}^{eu}\right)\left(k_x^2 + k_{1z}k_{2z}^o\right) + k_y^2 k_{2z}^o\left(k_2^2 - k_1^2\right)\right]\sin^2\psi \\ & + k_y\left(k_{1z} + k_{2z}^o\right)\left(k_{2z}^o - k_{2z}^{eu}\right)\left(k_\rho^2 + k_{1z}k_{2z}^o\right)\cos\psi\sin\psi \end{aligned} \tag{A.5g}$$

$$\begin{aligned} F_e \equiv\ & k_\rho^2\left(k_2^2 k_{3z} + k_3^2 k_{2z}^{eu}\right)\cos^2\psi \\ & + \left[k_2^2\left(k_{3z} + k_{2z}^{eu}\right)\left(k_x^2 + k_{3z}k_{2z}^o\right) + k_y^2 k_{2z}^o\left(k_2^2 - k_3^2\right)\right]\sin^2\psi \\ & - k_y\left(k_{3z} + k_{2z}^o\right)\left(k_{2z}^o + k_{2z}^{eu}\right)\left(k_\rho^2 + k_{3z}k_{2z}^o\right)\cos\psi\sin\psi \end{aligned} \tag{A.5h}$$

$$G_e \equiv k_\rho^2\left(k_2^2 k_{3z} + k_3^2 k_{2z}^{eu}\right)\cos^2\psi$$

$$+ \left[k_2^2\left(k_{3z}+k_{2z}^{eu}\right)\left(k_x^2-k_{3z}k_{2z}^{o}\right)-k_y^2k_{2z}^{o}\left(k_2^2-k_3^2\right)\right]\sin^2\psi$$
$$+ k_y\left(k_{3z}-k_{2z}^{o}\right)\left(k_{2z}^{o}-k_{2z}^{eu}\right)\left(k_\rho^2-k_{3z}k_{2z}^{o}\right)\cos\psi\sin\psi \qquad \text{(A.5i)}$$

$$H_e \equiv k_\rho^2\left(k_2^2k_{3z}+k_3^2k_{2z}^{ed}\right)\cos^2\psi$$
$$+ \left[k_2^2\left(k_{3z}+k_{2z}^{ed}\right)\left(k_x^2+k_{3z}k_{2z}^{o}\right)+k_y^2k_{2z}^{o}\left(k_2^2-k_3^2\right)\right]\sin^2\psi$$
$$- k_y\left(k_{3z}+k_{2z}^{o}\right)\left(k_{2z}^{o}+k_{2z}^{ed}\right)\left(k_\rho^2+k_{3z}k_{2z}^{o}\right)\cos\psi\sin\psi \qquad \text{(A.5j)}$$

Appendix B: Coefficient $\Psi_{1\mu\tau}^{ab}$

The coefficients are derived from (88a) for the DGF, (91a) for the mean field, and (102) for their components which are combined to form $\Psi_{1\mu\tau}^{ab}$ in the manner determined by the first term in (101) and the definition in (104). All the exponential functions have been incorporated into $\mathcal{I}_1^{abcd}$ and $\Psi_{1\mu\tau}^{ab}$ are thus composed of D's, U's, $\hat{h}$'s, and $\hat{v}$'s. For backscattering, D's and U's are evaluated at $\overline{k}_{\rho i}$ and $\hat{h}$'s and $\hat{v}$'s can be expressed in terms of incident polar angle θ_{0i} and incident azimuthal angle ϕ_{0i} as

$$\hat{h}(k_{1z}^u)=\begin{bmatrix}\sin\phi_{0i}\\-\cos\phi_{0i}\\0\end{bmatrix},\quad \hat{v}(k_{1z}^u)=\frac{1}{k_1}\begin{bmatrix}k_{1z}\cos\phi_{0i}\\k_{1z}\sin\phi_{0i}\\k_0\sin\theta_{0i}\end{bmatrix} \qquad \text{(B.1a)}$$

$$\hat{h}(k_{1z}^d)=\begin{bmatrix}\sin\phi_{0i}\\-\cos\phi_{0i}\\0\end{bmatrix},\quad \hat{v}(k_{1z}^d)=\frac{1}{k_1}\begin{bmatrix}-k_{1z}\cos\phi_{0i}\\-k_{1z}\sin\phi_{0i}\\k_0\sin\theta_{0i}\end{bmatrix} \qquad \text{(B.1b)}$$

$$\hat{h}(k_{1zi}^u)=\begin{bmatrix}-\sin\phi_{0i}\\\cos\phi_{0i}\\0\end{bmatrix},\quad \hat{v}(k_{1zi}^u)=\frac{1}{k_1}\begin{bmatrix}-k_{1z}\cos\phi_{0i}\\-k_{1z}\sin\phi_{0i}\\k_0\sin\theta_{0i}\end{bmatrix} \qquad \text{(B.1c)}$$

$$\hat{h}(k_{1zi}^d)=\begin{bmatrix}-\sin\phi_{0i}\\\cos\phi_{0i}\\0\end{bmatrix},\quad \hat{v}(k_{1zi}^d)=\frac{1}{k_1}\begin{bmatrix}k_{1z}\cos\phi_{0i}\\k_{1z}\sin\phi_{0i}\\k_0\sin\theta_{0i}\end{bmatrix} \qquad \text{(B.1d)}$$

The unit vectors of the polarization bases for the upgoing and downgoing waves are shown in Fig. 1.B.1 to help ease the derivation and illustrate the backscattering processes. As seen from the figure, a and b respectively describe scattered and incident wave types which can be upgoing or downgoing wave constituting the four processes depicted in

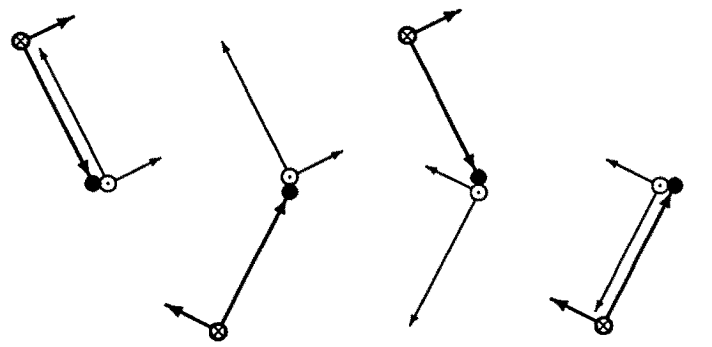

Figure 1.B.1 Polarization bases for incident (thick lines) and scattered (thin lines) waves : $\hat{h}$ = cross or dot circles, $\hat{v}$ = short arrows, $\bar{k}$ = long arrows; black circles are for scatterer.

Fig. 1.3.4. The algebra is straight forward and the results for $\Psi_{1\mu\tau}^{ab}$ can be written as follows:

For h-polarized return due to h-polarized transmission (hh)

$$\Psi_{1hh}^{-1-1} = -D_{1hh}^2(\bar{k}_{\rho i}) - D_{1hv}^2(\bar{k}_{\rho i}) \tag{B.2a}$$

$$\Psi_{1hh}^{-1+1} = -D_{1hh}(\bar{k}_{\rho i})U_{1hh}(\bar{k}_{\rho i}) - k_1^{-2}\left(k_0^2 \sin^2\theta_{0i} - k_{1z}^2\right) D_{1hv}(\bar{k}_{\rho i})U_{1hv}(\bar{k}_{\rho i}) \tag{B.2b}$$

$$\Psi_{1hh}^{+1-1} = -U_{1hh}(\bar{k}_{\rho i})D_{1hh}(\bar{k}_{\rho i}) - k_1^{-2}\left(k_0^2 \sin^2\theta_{0i} - k_{1z}^2\right) U_{1hv}(\bar{k}_{\rho i})D_{1hv}(\bar{k}_{\rho i}) \tag{B.2c}$$

$$\Psi_{1hh}^{+1+1} = -U_{1hh}^2(\bar{k}_{\rho i}) - U_{1hv}^2(\bar{k}_{\rho i}) \tag{B.2d}$$

For h-polarized return due to v-polarized transmission (hv)

$$\Psi_{1hv}^{-1-1} = -D_{1hh}(\bar{k}_{\rho i})D_{1vh}(\bar{k}_{\rho i}) - D_{1hv}(\bar{k}_{\rho i})D_{1vv}(\bar{k}_{\rho i}) \tag{B.3a}$$

$$\Psi_{1hv}^{-1+1} = -D_{1hh}(\bar{k}_{\rho i})U_{1vh}(\bar{k}_{\rho i}) - k_1^{-2}\left(k_0^2 \sin^2\theta_{0i} - k_{1z}^2\right) D_{1hv}(\bar{k}_{\rho i})U_{1vv}(\bar{k}_{\rho i}) \tag{B.3b}$$

$$\Psi_{1hv}^{+1-1} = -U_{1hh}(\bar{k}_{\rho i})D_{1vh}(\bar{k}_{\rho i}) - k_1^{-2}\left(k_0^2 \sin^2\theta_{0i} - k_{1z}^2\right) U_{1hv}(\bar{k}_{\rho i})D_{1vv}(\bar{k}_{\rho i}) \tag{B.3c}$$

$$\Psi_{1hv}^{+1+1} = -U_{1hh}(\bar{k}_{\rho i})U_{1vh}(\bar{k}_{\rho i}) - U_{1hv}(\bar{k}_{\rho i})U_{1vv}(\bar{k}_{\rho i}) \tag{B.3d}$$

For v-polarized return due to h-polarized transmission (vh)

$$\Psi_{1vh}^{-1-1} = D_{1vh}(\overline{k}_{\rho i})D_{1hh}(\overline{k}_{\rho i}) + D_{1vv}(\overline{k}_{\rho i})D_{1hv}(\overline{k}_{\rho i}) \tag{B.4a}$$

$$\Psi_{1vh}^{-1+1} = D_{1vh}(\overline{k}_{\rho i})U_{1hh}(\overline{k}_{\rho i}) + k_1^{-2}\left(k_0^2\sin^2\theta_{0i} - k_{1z}^2\right) D_{1vv}(\overline{k}_{\rho i})U_{1hv}(\overline{k}_{\rho i}) \tag{B.4b}$$

$$\Psi_{1vh}^{+1-1} = U_{1vh}(\overline{k}_{\rho i})D_{1hh}(\overline{k}_{\rho i}) + k_1^{-2}\left(k_0^2\sin^2\theta_{0i} - k_{1z}^2\right) U_{1vv}(\overline{k}_{\rho i})D_{1hv}(\overline{k}_{\rho i}) \tag{B.4c}$$

$$\Psi_{1vh}^{+1+1} = U_{1vh}(\overline{k}_{\rho i})U_{1hh}(\overline{k}_{\rho i}) + U_{1vv}(\overline{k}_{\rho i})U_{1hv}(\overline{k}_{\rho i}) \tag{B.4d}$$

For v-polarized return due to v-polarized transmission (vv)

$$\Psi_{1vv}^{-1-1} = D_{1vh}^2(\overline{k}_{\rho i}) + D_{1vv}^2(\overline{k}_{\rho i}) \tag{B.5a}$$

$$\Psi_{1vv}^{-1+1} = D_{1vh}(\overline{k}_{\rho i})U_{1vh}(\overline{k}_{\rho i}) + k_1^{-2}\left(k_0^2\sin^2\theta_{0i} - k_{1z}^2\right) D_{1vv}(\overline{k}_{\rho i})U_{1vv}(\overline{k}_{\rho i}) \tag{B.5b}$$

$$\Psi_{1vv}^{+1-1} = U_{1vh}(\overline{k}_{\rho i})D_{1vh}(\overline{k}_{\rho i}) + k_1^{-2}\left(k_0^2\sin^2\theta_{0i} - k_{1z}^2\right) U_{1vv}(\overline{k}_{\rho i})D_{1vv}(\overline{k}_{\rho i}) \tag{B.5c}$$

$$\Psi_{1vv}^{+1+1} = U_{1vh}^2(\overline{k}_{\rho i}) + U_{1vv}^2(\overline{k}_{\rho i}) \tag{B.5d}$$

With $k_1^2 = k_0^2\sin^2\theta_{0i} + k_{1z}^2$ and the definitions of $W^{(+1)} = U$ and $W^{(-1)} = D$, all of the above expressions for Ψ's can be summarized as

$$\Psi_{1\mu\tau}^{ab} = \pm W_{\mu h}^{(a)}(\overline{k}_{\rho i})W_{\tau h}^{(b)}(\overline{k}_{\rho i}) \pm k_1^{-2}\left(k_0^2\sin^2\theta_{0i} + abk_{1z}^2\right) W_{\mu v}^{(a)}(\overline{k}_{\rho i})W_{\tau v}^{(b)}(\overline{k}_{\rho i}) \tag{B.6}$$

where the minus signs are for $\mu = h$ and the plus signs are for $\mu = v$.

Appendix C: Coefficients $\Psi_{2\mu\tau,jk}^{pq}$

The coefficients are derived from (102), (88b), and (91b) for the components of the DGF and the mean field which are combined according to the second term in (101) and the definition in (105) to form $\Psi_{2\mu\tau,jk}^{pq}$. The results for the coefficients can be expressed as follows:

For the h-polarized return due to the h-polarized transmission (hh)

$$\Psi_{2hh,jk}^{ou\,ou} = D_{2ho}(-\overline{k}_{\rho})U_{2ho}(\overline{k}_{\rho i})o_j(k_{2z}^{ou})o_k(k_{2zi}^{ou}) \tag{C.1}$$

$$\Psi_{2hh,jk}^{ou\,od} = D_{2ho}(-\overline{k}_{\rho})D_{2ho}(\overline{k}_{\rho i})o_j(k_{2z}^{ou})o_k(k_{2zi}^{od}) \tag{C.2}$$

$$\Psi^{ou\,eu}_{2hh,jk} = D_{2ho}(-\overline{k}_\rho)U_{2he}(\overline{k}_{\rho i})o_j(k^{ou}_{2z})e_k(k^{eu}_{2zi}) \quad \text{(C.3)}$$
$$\Psi^{ou\,ed}_{2hh,jk} = D_{2ho}(-\overline{k}_\rho)D_{2he}(\overline{k}_{\rho i})o_j(k^{ou}_{2z})e_k(k^{ed}_{2zi}) \quad \text{(C.4)}$$

$$\Psi^{od\,ou}_{2hh,jk} = U_{2ho}(-\overline{k}_\rho)U_{2ho}(\overline{k}_{\rho i})o_j(k^{od}_{2z})o_k(k^{ou}_{2zi}) \quad \text{(C.5)}$$
$$\Psi^{od\,od}_{2hh,jk} = U_{2ho}(-\overline{k}_\rho)D_{2ho}(\overline{k}_{\rho i})o_j(k^{od}_{2z})o_k(k^{od}_{2zi}) \quad \text{(C.6)}$$
$$\Psi^{od\,eu}_{2hh,jk} = U_{2ho}(-\overline{k}_\rho)U_{2he}(\overline{k}_{\rho i})o_j(k^{od}_{2z})e_k(k^{eu}_{2zi}) \quad \text{(C.7)}$$
$$\Psi^{od\,ed}_{2hh,jk} = U_{2ho}(-\overline{k}_\rho)D_{2he}(\overline{k}_{\rho i})o_j(k^{od}_{2z})e_k(k^{ed}_{2zi}) \quad \text{(C.8)}$$

$$\Psi^{eu\,ou}_{2hh,jk} = -D_{2he}(-\overline{k}_\rho)U_{2ho}(\overline{k}_{\rho i})e_j(k^{eu}_{2z})o_k(k^{ou}_{2zi}) \quad \text{(C.9)}$$
$$\Psi^{eu\,od}_{2hh,jk} = -D_{2he}(-\overline{k}_\rho)D_{2ho}(\overline{k}_{\rho i})e_j(k^{eu}_{2z})o_k(k^{od}_{2zi}) \quad \text{(C.10)}$$
$$\Psi^{eu\,eu}_{2hh,jk} = -D_{2he}(-\overline{k}_\rho)U_{2he}(\overline{k}_{\rho i})e_j(k^{eu}_{2z})e_k(k^{eu}_{2zi}) \quad \text{(C.11)}$$
$$\Psi^{eu\,ed}_{2hh,jk} = -D_{2he}(-\overline{k}_\rho)D_{2he}(\overline{k}_{\rho i})e_j(k^{eu}_{2z})e_k(k^{ed}_{2zi}) \quad \text{(C.12)}$$

$$\Psi^{ed\,ou}_{2hh,jk} = -U_{2he}(-\overline{k}_\rho)U_{2ho}(\overline{k}_{\rho i})e_j(k^{ed}_{2z})o_k(k^{ou}_{2zi}) \quad \text{(C.13)}$$
$$\Psi^{ed\,od}_{2hh,jk} = -U_{2he}(-\overline{k}_\rho)D_{2ho}(\overline{k}_{\rho i})e_j(k^{ed}_{2z})o_k(k^{od}_{2zi}) \quad \text{(C.14)}$$
$$\Psi^{ed\,eu}_{2hh,jk} = -U_{2he}(-\overline{k}_\rho)U_{2he}(\overline{k}_{\rho i})e_j(k^{ed}_{2z})e_k(k^{eu}_{2zi}) \quad \text{(C.15)}$$
$$\Psi^{ed\,ed}_{2hh,jk} = -U_{2he}(-\overline{k}_\rho)D_{2he}(\overline{k}_{\rho i})e_j(k^{ed}_{2z})e_k(k^{ed}_{2zi}) \quad \text{(C.16)}$$

For the h-polarized return due to the v-polarized transmission (hv)

$$\Psi^{ou\,ou}_{2hv,jk} = D_{2ho}(-\overline{k}_\rho)U_{2vo}(\overline{k}_{\rho i})o_j(k^{ou}_{2z})o_k(k^{ou}_{2zi}) \quad \text{(C.17)}$$
$$\Psi^{ou\,od}_{2hv,jk} = D_{2ho}(-\overline{k}_\rho)D_{2vo}(\overline{k}_{\rho i})o_j(k^{ou}_{2z})o_k(k^{od}_{2zi}) \quad \text{(C.18)}$$
$$\Psi^{ou\,eu}_{2hv,jk} = D_{2ho}(-\overline{k}_\rho)U_{2ve}(\overline{k}_{\rho i})o_j(k^{ou}_{2z})e_k(k^{eu}_{2zi}) \quad \text{(C.19)}$$
$$\Psi^{ou\,ed}_{2hv,jk} = D_{2ho}(-\overline{k}_\rho)D_{2ve}(\overline{k}_{\rho i})o_j(k^{ou}_{2z})e_k(k^{ed}_{2zi}) \quad \text{(C.20)}$$

$$\Psi^{od\,ou}_{2hv,jk} = U_{2ho}(-\overline{k}_\rho)U_{2vo}(\overline{k}_{\rho i})o_j(k^{od}_{2z})o_k(k^{ou}_{2zi}) \quad \text{(C.21)}$$
$$\Psi^{od\,od}_{2hv,jk} = U_{2ho}(-\overline{k}_\rho)D_{2vo}(\overline{k}_{\rho i})o_j(k^{od}_{2z})o_k(k^{od}_{2zi}) \quad \text{(C.22)}$$
$$\Psi^{od\,eu}_{2hv,jk} = U_{2ho}(-\overline{k}_\rho)U_{2ve}(\overline{k}_{\rho i})o_j(k^{od}_{2z})e_k(k^{eu}_{2zi}) \quad \text{(C.23)}$$
$$\Psi^{od\,ed}_{2hv,jk} = U_{2ho}(-\overline{k}_\rho)D_{2ve}(\overline{k}_{\rho i})o_j(k^{od}_{2z})e_k(k^{ed}_{2zi}) \quad \text{(C.24)}$$

$$\Psi^{eu\,ou}_{2hv,jk} = -D_{2he}(-\overline{k}_\rho)U_{2vo}(\overline{k}_{\rho i})e_j(k^{eu}_{2z})o_k(k^{ou}_{2zi}) \quad \text{(C.25)}$$
$$\Psi^{eu\,od}_{2hv,jk} = -D_{2he}(-\overline{k}_\rho)D_{2vo}(\overline{k}_{\rho i})e_j(k^{eu}_{2z})o_k(k^{od}_{2zi}) \quad \text{(C.26)}$$
$$\Psi^{eu\,eu}_{2hv,jk} = -D_{2he}(-\overline{k}_\rho)U_{2ve}(\overline{k}_{\rho i})e_j(k^{eu}_{2z})e_k(k^{eu}_{2zi}) \quad \text{(C.27)}$$

$$\Psi^{eu\,ed}_{2hv,jk} = -D_{2he}(-\overline{k}_\rho)D_{2ve}(\overline{k}_{\rho i})e_j(k^{eu}_{2z})e_k(k^{ed}_{2zi}) \tag{C.28}$$

$$\Psi^{ed\,ou}_{2hv,jk} = -U_{2he}(-\overline{k}_\rho)U_{2vo}(\overline{k}_{\rho i})e_j(k^{ed}_{2z})o_k(k^{ou}_{2zi}) \tag{C.29}$$
$$\Psi^{ed\,od}_{2hv,jk} = -U_{2he}(-\overline{k}_\rho)D_{2vo}(\overline{k}_{\rho i})e_j(k^{ed}_{2z})o_k(k^{od}_{2zi}) \tag{C.30}$$
$$\Psi^{ed\,eu}_{2hv,jk} = -U_{2he}(-\overline{k}_\rho)U_{2ve}(\overline{k}_{\rho i})e_j(k^{ed}_{2z})e_k(k^{eu}_{2zi}) \tag{C.31}$$
$$\Psi^{ed\,ed}_{2hv,jk} = -U_{2he}(-\overline{k}_\rho)D_{2ve}(\overline{k}_{\rho i})e_j(k^{ed}_{2z})e_k(k^{ed}_{2zi}) \tag{C.32}$$

For the v-polarized return due to the h-polarized transmission (vh)

$$\Psi^{ou\,ou}_{2vh,jk} = -D_{2vo}(-\overline{k}_\rho)U_{2ho}(\overline{k}_{\rho i})o_j(k^{ou}_{2z})o_k(k^{ou}_{2zi}) \tag{C.33}$$
$$\Psi^{ou\,od}_{2vh,jk} = -D_{2vo}(-\overline{k}_\rho)D_{2ho}(\overline{k}_{\rho i})o_j(k^{ou}_{2z})o_k(k^{od}_{2zi}) \tag{C.34}$$
$$\Psi^{ou\,eu}_{2vh,jk} = -D_{2vo}(-\overline{k}_\rho)U_{2he}(\overline{k}_{\rho i})o_j(k^{ou}_{2z})e_k(k^{eu}_{2zi}) \tag{C.35}$$
$$\Psi^{ou\,ed}_{2vh,jk} = -D_{2vo}(-\overline{k}_\rho)D_{2he}(\overline{k}_{\rho i})o_j(k^{ou}_{2z})e_k(k^{ed}_{2zi}) \tag{C.36}$$

$$\Psi^{od\,ou}_{2vh,jk} = -U_{2vo}(-\overline{k}_\rho)U_{2ho}(\overline{k}_{\rho i})o_j(k^{od}_{2z})o_k(k^{ou}_{2zi}) \tag{C.37}$$
$$\Psi^{od\,od}_{2vh,jk} = -U_{2vo}(-\overline{k}_\rho)D_{2ho}(\overline{k}_{\rho i})o_j(k^{od}_{2z})o_k(k^{od}_{2zi}) \tag{C.38}$$
$$\Psi^{od\,eu}_{2vh,jk} = -U_{2vo}(-\overline{k}_\rho)U_{2he}(\overline{k}_{\rho i})o_j(k^{od}_{2z})e_k(k^{eu}_{2zi}) \tag{C.39}$$
$$\Psi^{od\,ed}_{2vh,jk} = -U_{2vo}(-\overline{k}_\rho)D_{2he}(\overline{k}_{\rho i})o_j(k^{od}_{2z})e_k(k^{ed}_{2zi}) \tag{C.40}$$

$$\Psi^{eu\,ou}_{2vh,jk} = D_{2ve}(-\overline{k}_\rho)U_{2ho}(\overline{k}_{\rho i})e_j(k^{eu}_{2z})o_k(k^{ou}_{2zi}) \tag{C.41}$$
$$\Psi^{eu\,od}_{2vh,jk} = D_{2ve}(-\overline{k}_\rho)D_{2ho}(\overline{k}_{\rho i})e_j(k^{eu}_{2z})o_k(k^{od}_{2zi}) \tag{C.42}$$
$$\Psi^{eu\,eu}_{2vh,jk} = D_{2ve}(-\overline{k}_\rho)U_{2he}(\overline{k}_{\rho i})e_j(k^{eu}_{2z})e_k(k^{eu}_{2zi}) \tag{C.43}$$
$$\Psi^{eu\,ed}_{2vh,jk} = D_{2ve}(-\overline{k}_\rho)D_{2he}(\overline{k}_{\rho i})e_j(k^{eu}_{2z})e_k(k^{ed}_{2zi}) \tag{C.44}$$

$$\Psi^{ed\,ou}_{2vh,jk} = U_{2ve}(-\overline{k}_\rho)U_{2ho}(\overline{k}_{\rho i})e_j(k^{ed}_{2z})o_k(k^{ou}_{2zi}) \tag{C.45}$$
$$\Psi^{ed\,od}_{2vh,jk} = U_{2ve}(-\overline{k}_\rho)D_{2ho}(\overline{k}_{\rho i})e_j(k^{ed}_{2z})o_k(k^{od}_{2zi}) \tag{C.46}$$
$$\Psi^{ed\,eu}_{2vh,jk} = U_{2ve}(-\overline{k}_\rho)U_{2he}(\overline{k}_{\rho i})e_j(k^{ed}_{2z})e_k(k^{eu}_{2zi}) \tag{C.47}$$
$$\Psi^{ed\,ed}_{2vh,jk} = U_{2ve}(-\overline{k}_\rho)D_{2he}(\overline{k}_{\rho i})e_j(k^{ed}_{2z})e_k(k^{ed}_{2zi}) \tag{C.48}$$

For the v-polarized return due to the v-polarized transmission (vv)

$$\Psi^{ou\,ou}_{2vv,jk} = -D_{2vo}(-\overline{k}_\rho)U_{2vo}(\overline{k}_{\rho i})o_j(k^{ou}_{2z})o_k(k^{ou}_{2zi}) \tag{C.49}$$
$$\Psi^{ou\,od}_{2vv,jk} = -D_{2vo}(-\overline{k}_\rho)D_{2vo}(\overline{k}_{\rho i})o_j(k^{ou}_{2z})o_k(k^{od}_{2zi}) \tag{C.50}$$

$$\Psi_{2vv,jk}^{ou\,eu} = -D_{2vo}(-\overline{k}_\rho)U_{2ve}(\overline{k}_{\rho i})o_j(k_{2z}^{ou})e_k(k_{2zi}^{eu}) \quad \text{(C.51)}$$

$$\Psi_{2vv,jk}^{ou\,ed} = -D_{2vo}(-\overline{k}_\rho)D_{2ve}(\overline{k}_{\rho i})o_j(k_{2z}^{ou})e_k(k_{2zi}^{ed}) \quad \text{(C.52)}$$

$$\Psi_{2vv,jk}^{od\,ou} = -U_{2vo}(-\overline{k}_\rho)U_{2vo}(\overline{k}_{\rho i})o_j(k_{2z}^{od})o_k(k_{2zi}^{ou}) \quad \text{(C.53)}$$

$$\Psi_{2vv,jk}^{od\,od} = -U_{2vo}(-\overline{k}_\rho)D_{2vo}(\overline{k}_{\rho i})o_j(k_{2z}^{od})o_k(k_{2zi}^{od}) \quad \text{(C.54)}$$

$$\Psi_{2vv,jk}^{od\,eu} = -U_{2vo}(-\overline{k}_\rho)U_{2ve}(\overline{k}_{\rho i})o_j(k_{2z}^{od})e_k(k_{2zi}^{eu}) \quad \text{(C.55)}$$

$$\Psi_{2vv,jk}^{od\,ed} = -U_{2vo}(-\overline{k}_\rho)D_{2ve}(\overline{k}_{\rho i})o_j(k_{2z}^{od})e_k(k_{2zi}^{ed}) \quad \text{(C.56)}$$

$$\Psi_{2vv,jk}^{eu\,ou} = D_{2ve}(-\overline{k}_\rho)U_{2vo}(\overline{k}_{\rho i})e_j(k_{2z}^{eu})o_k(k_{2zi}^{ou}) \quad \text{(C.57)}$$

$$\Psi_{2vv,jk}^{eu\,od} = D_{2ve}(-\overline{k}_\rho)D_{2vo}(\overline{k}_{\rho i})e_j(k_{2z}^{eu})o_k(k_{2zi}^{od}) \quad \text{(C.58)}$$

$$\Psi_{2vv,jk}^{eu\,eu} = D_{2ve}(-\overline{k}_\rho)U_{2ve}(\overline{k}_{\rho i})e_j(k_{2z}^{eu})e_k(k_{2zi}^{eu}) \quad \text{(C.59)}$$

$$\Psi_{2vv,jk}^{eu\,ed} = D_{2ve}(-\overline{k}_\rho)D_{2ve}(\overline{k}_{\rho i})e_j(k_{2z}^{eu})e_k(k_{2zi}^{ed}) \quad \text{(C.60)}$$

$$\Psi_{2vv,jk}^{ed\,ou} = U_{2ve}(-\overline{k}_\rho)U_{2vo}(\overline{k}_{\rho i})e_j(k_{2z}^{ed})o_k(k_{2zi}^{ou}) \quad \text{(C.61)}$$

$$\Psi_{2vv,jk}^{ed\,od} = U_{2ve}(-\overline{k}_\rho)D_{2vo}(\overline{k}_{\rho i})e_j(k_{2z}^{ed})o_k(k_{2zi}^{od}) \quad \text{(C.62)}$$

$$\Psi_{2vv,jk}^{ed\,eu} = U_{2ve}(-\overline{k}_\rho)U_{2ve}(\overline{k}_{\rho i})e_j(k_{2z}^{ed})e_k(k_{2zi}^{eu}) \quad \text{(C.63)}$$

$$\Psi_{2vv,jk}^{ed\,ed} = U_{2ve}(-\overline{k}_\rho)D_{2ve}(\overline{k}_{\rho i})e_j(k_{2z}^{ed})e_k(k_{2zi}^{ed}) \quad \text{(C.64)}$$

where o_j (or o_k) and e_j (or e_k) are the $j,k = x,y,z$ components of unit vector $\hat{o}$ and $\hat{e}$ defined in section 1.3c. For backscattering, $\overline{k}_\rho = -\overline{k}_{\rho i}$ and $o_j(k_{2z}^{ou})$, $o_j(k_{2z}^{od})$, $e_j(k_{2z}^{eu})$, and $e_j(k_{2z}^{ed})$ are evaluated for the backscattered waves similarly to the procedure in appendix B.

Appendix D: Integrations of $\mathcal{I}_1^{abcd}$ and $\mathcal{I}_{2jklm}^{pqrs}$

a. Integrations of $\mathcal{I}_1^{abcd}$

The integrations over z_1 and z_1^o in (103a) are carried out to give

$$\mathcal{I}_1^{abcd} = \int_{-\infty}^{\infty} d\beta_z \Phi_1(2\overline{k}_{\rho i}, \beta_z) \cdot \frac{1 - e^{i(\beta_z - \kappa_{ab})d_1}}{\beta_z - \kappa_{ab}} \cdot \frac{1 - e^{-i(\beta_z - \kappa_{cd})d_1}}{\beta_z - \kappa_{cd}} \quad \text{(D.1)}$$

Using (93) and (43b) for the isotropic correlation functions in (D.1) yields

$$\mathcal{I}_1^{abcd} = \delta_1 \ell_1^3 \pi^{-2}(\mathcal{A}_1 + \mathcal{B}_1) \quad \text{(D.2)}$$

where $\mathcal{A}_1$ and $\mathcal{B}_1$ are integrals over β_z defined as

$$\mathcal{A}_1 = \int_{-\infty}^{\infty} d\beta_z \frac{1 - e^{i(\beta_z - \kappa_{ab})d_1} + e^{i(\kappa_{cd} - \kappa_{ab})d_1}}{(\beta_z^2 \ell_1^2 + 1 + 4k_{\rho i}^2 \ell_1^2)^2 (\beta_z - \kappa_{ab})(\beta_z - \kappa_{cd})} \tag{D.3}$$

$$\mathcal{B}_1 = \int_{-\infty}^{\infty} d\beta_z \frac{-e^{-i(\beta_z - \kappa_{cd})d_1}}{(\beta_z^2 \ell_1^2 + 1 + 4k_{\rho i}^2 \ell_1^2)^2 (\beta_z - \kappa_{ab})(\beta_z - \kappa_{cd})} \tag{D.4}$$

The integrations over β_z in (D.3) and (D.4) are carried out with the contour integration method. For $\mathcal{A}_1$, the imaginary part of β_z has to be positive for the integral to converge. Thus, $\mathcal{A}_1$ can be taken as the integral along the positively oriented contour composed of the real β_z axis and the infinite semi-circle on the upper half of the complex β_z plane and centered at origin $\beta_z = 0$. Note that the integral over the semi-circle vanishes on account of Jordan's lemma. The chosen contour encloses simple poles at $\beta_z = \kappa_{ab}, \kappa_{cd}$ (if the imaginary parts of the simple poles are positive) and a double pole at $\beta_z = \kappa_1 = i\ell^{-1}\sqrt{1 + 4k_{\rho i}^2 \ell_1^2}$. Integral $\mathcal{A}_1$ is therefore composed of the residue contribution from the enclosed poles. According to the residue theorem, the result for $\mathcal{A}_1$ is

$$\begin{aligned}
\mathcal{A}_1 = 2\pi i \Bigg\{ & \frac{e^{i(\kappa_{cd} - \kappa_{ab})d_1}}{(\kappa_{ab}^2 \ell_1^2 + 1 + 4k_{\rho i}^2 \ell_1^2)^2 (\kappa_{ab} - \kappa_{cd})} \quad (\text{if } \mathrm{Im}\kappa_{ab} > 0) \\
& + \frac{1}{(\kappa_{cd}^2 \ell_1^2 + 1 + 4k_{\rho i}^2 \ell_1^2)^2 (\kappa_{cd} - \kappa_{ab})} \quad (\text{if } \mathrm{Im}\kappa_{cd} > 0) \\
& - \frac{i d_1 e^{i(\kappa_1 - \kappa_{ab})d_1}}{\ell_1^4 (\kappa_1 - \kappa_1^*)^2 (\kappa_1 - \kappa_{ab})(\kappa_1 - \kappa_{cd})} \\
& - \frac{1 - e^{i(\kappa_1 - \kappa_{ab})d_1} + e^{i(\kappa_{cd} - \kappa_{ab})d_1}}{\ell_1^4 (\kappa_1 - \kappa_1^*)^2 (\kappa_1 - \kappa_{ab})(\kappa_1 - \kappa_{cd})} \\
& \cdot \left[\frac{2}{\kappa_1 - \kappa_1^*} + \frac{1}{\kappa_1 - \kappa_{ab}} + \frac{1}{\kappa_1 - \kappa_{cd}} \right] \Bigg\}
\end{aligned} \tag{D.5}$$

For $\mathcal{B}_1$, the same contour integration method is used except that the infinite semi-circle is in the lower half of the complex β_z plane for convergence of the integral. The integration contour is now negatively oriented along the real β_z axis and the lower semi-circle enclosing simple poles at $\beta_z = \kappa_{ab}, \kappa_{cd}$ (if the imaginary parts of the simple

poles are negative) and a double pole at $\beta_z = \kappa_1^* = -i\ell^{-1}\sqrt{1+4k_{\rho i}^2\ell_1^2}$. The result for $\mathcal{B}_1$ is

$$\begin{aligned}\mathcal{B}_1 = 2\pi i \Bigg\{ & \frac{e^{i(\kappa_{cd}-\kappa_{ab})d_1}}{(\kappa_{ab}^2\ell_1^2+1+4k_{\rho i}^2\ell_1^2)^2(\kappa_{ab}-\kappa_{cd})} \quad (\text{if } \mathrm{Im}\kappa_{ab}<0) \\ & + \frac{1}{(\kappa_{cd}^2\ell_1^2+1+4k_{\rho i}^2\ell_1^2)^2(\kappa_{cd}-\kappa_{ab})} \quad (\text{if } \mathrm{Im}\kappa_{cd}<0) \\ & - \frac{id_1 e^{-i(\kappa_1^*-\kappa_{cd})d_1}}{\ell_1^4(\kappa_1^*-\kappa_1)^2(\kappa_1^*-\kappa_{ab})(\kappa_1^*-\kappa_{cd})} \\ & - \frac{e^{-i(\kappa_1^*-\kappa_{cd})d_1}}{\ell_1^4(\kappa_1^*-\kappa_1)^2(\kappa_1^*-\kappa_{ab})(\kappa_1^*-\kappa_{cd})} \\ & \cdot \left[\frac{2}{\kappa_1^*-\kappa_1}+\frac{1}{\kappa_1^*-\kappa_{ab}}+\frac{1}{\kappa_1^*-\kappa_{cd}}\right]\Bigg\} \end{aligned} \tag{D.6}$$

Substituting (D.6) and (D.5) in (D.4) yields $\mathcal{I}_1^{abcd}$ which is rearranged to obtained the result in (105) for the isotropic random medium.

b. Integrations of $\mathcal{I}_{2jklm}^{pqrs}$

The integrations over z_2 and z_2^o in (103a) are carried out to give

$$\begin{aligned}\mathcal{I}_{2jklm}^{pqrs} = & \int_{-\infty}^{\infty} d\beta_z \Phi_{2jklm}(2\overline{k}_{\rho i},\beta_z) \\ & \cdot \frac{e^{i(\beta_z-\kappa_{pq})d_1}-e^{i(\beta_z-\kappa_{pq})d_2}}{\beta_z-\kappa_{pq}} \cdot \frac{e^{-i(\beta_z-\kappa_{rs})d_1}-e^{-i(\beta_z-\kappa_{rs})d_2}}{\beta_z-\kappa_{rs}} \end{aligned} \tag{D.7}$$

Using (99), (98), and (58b) for the anisotropic correlation functions in (D.7) yields

$$\mathcal{I}_{2jklm}^{pqrs} = \delta_{2jklm}\ell_{2\rho'}^2\ell_{2z'}\pi^{-2}(\mathcal{A}_2+\mathcal{B}_2) \tag{D.8}$$

where integral $\mathcal{A}_2$ and $\mathcal{B}_2$ are defined as

$$\mathcal{A}_2 = \int_{-\infty}^{\infty} d\beta_z \frac{e^{i(\kappa_{rs}-\kappa_{pq})d_1}-e^{i(\kappa_{rs}d_1-\kappa_{pq}d_2)}e^{i(d_2-d_1)\beta_z}+e^{i(\kappa_{rs}-\kappa_{pq})d_2}}{D^2(2\overline{k}_{\rho i},\beta_z)(\beta_z-\kappa_{pq})(\beta_z-\kappa_{rs})} \tag{D.9}$$

$$\mathcal{B}_2 = \int_{-\infty}^{\infty} d\beta_z \frac{-e^{i(\kappa_{rs}d_2-\kappa_{pq}d_1)}e^{-i(d_2-d_1)\beta_z}}{D^2(2\overline{k}_{\rho i},\beta_z)(\beta_z-\kappa_{pq})(\beta_z-\kappa_{rs})} \tag{D.10}$$

In (D.9) and (D.10), $D(2\overline{k}_{\rho i}, \beta_z)$ is a quadratic expression in β_z given by

$$D(2\overline{k}_{\rho i}, \beta_z) = \mathcal{L}_2^2 \beta_z^2 + 2k_{yi}(\ell_{2z'}^2 - \ell_{2\rho'}^2)\sin(2\psi)\beta_z + \left[1 + 4k_{xi}^2 \ell_{2\rho'}^2 + 4k_{yi}^2(\ell_{2\rho'}^2 \cos^2\psi + \ell_{2z'}^2 \sin^2\psi)\right] \qquad \text{(D.11)}$$

with $\mathcal{L}_2^2 = \ell_{2\rho'}^2 \sin^2\psi + \ell_{2z'}^2 \cos^2\psi$. The integrations over β_z in (D.9) and (D.10) are carried out with the contour integration method as in the last section of this appendix. In consideration of the convergence, the contour for $\mathcal{A}_2$ is taken to be positively oriented along the real β_z axis and the upper infinite semi-circle and that for $\mathcal{B}_2$ is negatively oriented along the real β_z axis and the lower infinite semi-circle. Integral $\mathcal{I}_{2jklm}^{pqrs}$ is thus composed of the contribution from the residues of two simple poles at $\beta_z = \kappa_{pq}, \kappa_{rs}$ and two double poles corresponding to the two zeros of quadratic equation $D(2\overline{k}_{\rho i}, \beta_z) = 0$ at $\beta_z = \kappa_2, \kappa_2^*$ for $\kappa_2 = \mathcal{L}_2^{-2}\left[-k_{yi}(\ell_{2z'}^2 - \ell_{2\rho'}^2)\sin(2\psi) + i\sqrt{(1+4k_{xi}^2\ell_{2\rho'}^2)\mathcal{L}_2^2 + 4k_{yi}^2\ell_{2\rho'}^2\ell_{2z'}^2}\right]$. The residue theorem then gives the result in (107) for the anisotropic random medium. Note that the anisotropic result approaches the isotropic result in the limits of $\ell_{2z'} \to \ell_{2\rho'}$ and $d_1 \to 0$.

Acknowledgments

This work was supported by the NASA Contract 958461, the ARO Contract DAAL03-88-J-0057, the ARMY Corp of Engineers Contract DACA39-87-K-0022, the NASA Contract NAGW-1617, and the ONR Contract N00014-89-J-1107.

References

[1] Stokes, G., "On the Composition and Resolution of Streams of Polarized Light from Different Sources," *Proceedings of the Cambridge Philosophical Society*, 1, 140–147, 1852.

[2] Rayleigh, Lord, *Scientific Papers by Lord Rayleigh*, III, Dover Publications, New York, 1964.

[3] Poincaré, H., *Théorie Mathématique de la Lumière*, **2**, Paris, 1892.

[4] Mueller, H., "The Foundation of Optics," *Journal of the Optical Society of America*, **38**, 661, 1948.

[5] Jones, R. C., "A New Calculus for the Treatment of Optical systems–Part I. Description and Discussion of the Calculus," *Journal of the Optical society of America*, **31**, 488–493, 1941.

[6] van de Hulst, H. C., *Light Scattering by Small Particles*, Dover Publications, New York, 1981.

[7] Ishimaru, A., *Wave Propagation in Random Media*, **1–2**, Academic Press, New York, 1978.

[8] Kong, J. A., A. A. Swartz, H. A. Yueh, L. M. Novak, and R. T. Shin, "Identification of Terrain cover Using the Optimum Polarimetric Classifier," *Journal of Electromagnetic Waves and Applications*, **2**, 171–194, 1987.

[9] Born, M., and E. Wolf, *Principle of Optics*, Pergamon Press, New York, 1980.

[10] Chandrasekhar, S., *Radiative Transfer*, Dover Publications, New York, 1960.

[11] Deirmendjian, D., *Electromagnetic Scattering on Spherical Polydispersions*, American Elsevier, New York, 1969.

[12] Kennaugh, E. M., "Effects of the type of polarization on echo characteristics," Report 389-9, Antenna Lab., Ohio State University, 1951.

[13] Rumsey, V. H., "Part I–Transmission between Elliptically Polarized Antennas," *Proc. I.R.E.*, **39**, 535–540, 1951.

[14] Deschamps, G. A., "Part II–Geometrical Representation of the Polarization of a Plane Electromagnetic Wave," *Proc. I.R.E.*, **39**, 540–544, 1951.

[15] Walker, M. J., "Matrix Calculus and the Stokes Parameters of Polarized Radiation," *American Journal of Physics*, **22**, 170–174, 1954.

[16] Deschamps, G. A., and P. E. Mast, "Poincaré Sphere Representation of Partially Polarized Fields," *IEEE Trans. Antennas Propagat.*, **AP–21**, 1973.

[17] Huynen, J. R., "Phenomenological Theory of Radar Targets," in *Electromagnetic Scattering*, edited by P. L. E. Uslenghi, Academic Press, New York, 1978.

[18] Hauge, P. S., "Mueller Matric Ellipsometry with Imperfect Compensator," *Journal of the Optical Society of America*, **68**, 1519–1528, 1978.

[19] Ioannidis, G. A., and D. E. Hammers, "Optimum Antenna Polarizations for Target Discrimination in Clutter," *IEEE Trans. Antennas Propagat.*, **AP–27**, 357–363, 1979.

[20] Kostinski, A. B., and W.-M. Boerner, "On Foundations of Radar Polarimetry," *IEEE Trans. Antennas Propagat,*, **AP–34**, 1986.

[21] Kim, K., L. Mandel, and E. Wolf, "Relationship between Jones and Mueller Matrices for Random Media," *Journal of the Optical Society of America A*, **4**, 433–437, 1987.

[22] van Zyl, J. J., H. A. Zebker, and C. Elachi, "Imaging Radar Polarization Signatures: Theory and Observation," *Radio Science*, **22**, 529–543, 1987.

[23] Kong, J. A., *Electromagnetic Wave Theory*, Wiley-Interscience, New York, 1986.

[24] Tsang, L., J. A. Kong, and R. T. Shin, *Theory of Microwave Remote Sensing*, Wiley-Interscience, New York, 1985.

[25] Tatarskii, V. I., *Wave Propagation in a Turbulent Medium*, McGraw-Hill, New York, 1961.

[26] Tatarskii, V. I., *The Effects of Turbulent Atmosphere on Wave Propagation*, U.S. Department of Commerce, National Technical Information Service, Springfield, Virginia, 1971.

[27] Keller, J. B., "Wave Propagation in Random Media," *Proceedings of Symposia in Applied Mathematics, American Mathematical Society*, **13**, 227–246, 1962.

[28] Frisch, U., "Wave Propagation in Random Medium," in *Probabilistic Methods in Applied Mathematics*, edited by A. T. Bharucha-Reid, **1**, 75–198, Academic, New York, 1968.

[29] Stogryn, A., "Electromagnetic Scattering by Random Dielectric Constant Fluctuations in a Bounded Medium," *Radio Science*, **9**, 509–518, 1974.

[30] Tsang, L., and J. A. Kong, "Microwave Remote Sensing of a Two-Layer Random Medium," *IEEE Trans. Antennas Propagat.*, **AP–24**, 283–287, 1976.

[31] Fung, A. K., and H. S. Fung, "Application of First Order Renormalization Method to Scattering from a Vegetation-like Half Space," *IEEE Transactions on Geoscience Electronics*, **GE–15**, 189–195, 1977.

[32] Zuniga, M. A., T. M. Habashy, and J. A. Kong, "Active Remote Sensing of Layered Random Media," *IEEE Transactions on Geoscience Electronics*, **GE–17**, 296–302, 1979.

[33] Zuniga, M. A., J. A. Kong, and L. Tsang, "Depolarization Effects in the Active Remote Sensing of Random Media," *Journal of Applied Physics*, **51**, 2315–2325, 1980.

[34] Vallese, F., and J. A. Kong, "Correlation Function Studies for Snow and Ice," *Journal of Applied Physics*, **52**, 4921–4925, 1981.

[35] Lang, R. H., "Electromagnetic Backscattering from a Sparse Distribution of Lossy Dielectric Scatterers," *Radio Science*, **16**, 25–30, 1981.

[36] Lee, J. K., and J. A. Kong, "Dyadic Greens' Functions for Layered Anisotropic Medium," *Electromagnetics*, **3**, 111-130, 1983.

[37] Lee, J. K., and J. A. Kong, "Active Microwave Remote Sensing of an Anisotropic Random Medium Layer," *IEEE Transactions on Geoscience and Remote Sensing*, **GE–23**, 910–923, 1985.

[38] Lee, J. K., and J. A. Kong, "Passive Microwave Remote Sensing of an Anisotropic Random Medium Layer," *IEEE Transactions on Geoscience and Remote Sensing*, **GE–23**, 924–932, 1985.

[49] Tsang, L., and J. A. Kong, "Application of Strong Fluctuation Random Medium Theory to Scattering from Vegetation-like Half Space," *IEEE Transactions on Geoscience and Remote Sensing*, **GE–19**, 62–69, 1981.

[40] Tsang, L., and J. A. Kong, "Scattering of Electromagnetic Waves from Random Media with Strong Permittivity Fluctuations," *Radio Science*, **16**, 303–320, 1981.

[41] Tsang, L., J. A. Kong, and R. W. Newton, "Application of Strong Fluctuation Random Medium Theory to Scattering of Electro-

magnetic Waves from a Half-Space of Dielectric Mixture," *IEEE Trans. Antennas Propagat.*, **AP–30**, 292–302, 1982.

[42] Stogryn, A., "A Note on the Singular Part of the Dyadic Green's Function in Strong Fluctuation Theory," *Radio Science*, **18**, 1283–1286, 1983.

[43] Borgeaud, M., R. T. Shin, and J. A. Kong, "Theoretical Models for Polarimetric Radar Clutter," *Journal of Electromagnetics Waves and Applications*, **1**, 73–89, 1987.

[44] Borgeaud, M., S. V. Nghiem, R. T. Shin, and J. A. Kong, "Theoretical Models for Polarimetric Microwave Remote Sensing of Earth Terrain," *Journal of Electromagnetic Waves and Applications*, **3**, 61–81, 1989.

[45] Borgeaud, M., J. A. Kong, R. T. Shin, and S. V. Nghiem, "Theoretical Models for Polarimetric Microwave Remote Sensing of Earth Terrain," *Proceedings of the 1988 NATO Advanced Research Workshop*, Nuremberg, F. R. Germany, September, 1988.